

Houston
Lighting
& Power
Company

Electric Tower
P.O. Box 1700
Houston, Texas 77001

August 8, 1979
ST-HL-AE-367
SFN: V-0100

Mr. Dominic B. Vassallo
Assistant Director
Division of Project Management
United States Nuclear Regulatory Commission
1717 H. Street
Washington, D.C. 20555

Dear Mr. Vassallo:

South Texas Project
Units 1 & 2
Docket Nos. STN 50-498, 50-499
Transmittal of Technical Publications
Related to Soil Structure Interaction

The attached technical publications discussing analytical methods related to soil-structure interaction were requested by Mr. E. Licitra of your office in a telephone conversation between Houston Lighting and Power, Mr. Raja Gupta and Mr. Licitra of the Nuclear Regulatory Commission. The articles provide a detailed discussion of the analytical methods proposed to be used in performing soil-structure interaction studies as required by NRC question SEB 130.12.

Mr. Gupta was provided a copy of the attachments by Federal Express courier on August 7, 1979. Should additional information be required, please contact Mr. L. R. Jacobi at (713) 676-7953.

Very truly yours,

E. A. Turner
Vice President
Power Plant Construction
& Technical Services

LRJ:bf

Attachments (4)

CC: Without Attachments

Director, NRC Office of Inspection & Enforcement
M. D. Schwarz (Baker & Botts)
R. Gordon Gooch (Baker & Botts)
J. R. Newman (Lowenstein, Newman, Reis, Axelrad & Toll)
D. G. Barker
A. J. Granger
R. A. Frazar

BOO
DS
171

649 239 7908140 668 18

James P. Lee
Brown & Root

JOURNAL OF THE SOIL MECHANICS AND FOUNDATIONS DIVISION

Vertical Vibration of Embedded Footings

By Milos Novak¹ and Youpele O. Beredugo²

INTRODUCTION

Most of the existing theoretical solutions treat the footing as a rigid body attached to the surface of an elastic half-space. However, real footings are usually partially embedded, and experiments indicate that embedment can considerably affect the dynamic response of footings (7,14).

No rigorous analytical solution of embedded footings is available because of the obvious mathematical difficulties. The most promising way of approaching this problem seems to be the finite element analyses as used by Lysmer and Kuhlemeyer (13), and by Kaldjian (9) for static stiffness. Nevertheless, there is a need for alternative approximate solutions that would be able to predict the motion in more degrees-of-freedom and to yield the stiffness and damping characteristics of embedded footings readily applicable in dynamic analyses of various structures.

An approximate analytical approach was formulated by Baranov (1), who assumed that the soil underlying the footing base is an elastic half-space and that the overlying soil is an independent elastic layer composed of a series of infinitesimally thin independent elastic layers. The compatibility condition between the elastic half-space and the overlying elastic layer was satisfied only at the body and very far from it. Nevertheless, the solution seems to yield reasonable results in closed forms, and is very versatile and easily applicable to any vibration mode (3,16). For these reasons, this solution is further extended in this paper and compared with finite element solutions and with experiments in order to verify its applicability. Embedment into a stratum is also investigated.

Note.—Discussion open until May 1, 1973. To extend the closing date one month, a written request must be filed with the Editor of Technical Publications, ASCE. This paper is part of the copyrighted Journal of the Soil Mechanics and Foundations Division, Proceedings of the American Society of Civil Engineers, Vol. 98, No. SM12, December, 1972. Manuscript was submitted for review for possible publication on April 21, 1971.

¹Prof., Faculty of Engrg. Sci., Univ. of Western Ontario, London, Ontario, Canada.

²Shell-BP Nigeria Ltd., Lagos, Nigeria.

SI CONVERSION FACTORS

In 1970 action of the ASCE Board of Direction, which Society should list all measurements in both customary (SI) units, the list below contains conversion factors for SI unit values of measurements. A complete guide to SI units from the American Society for Testing & Materials, Inc. (1910) at a price of \$1.25 per copy (minimum single copy) for civil engineering is available from ASCE headquarters. We are being asked to prepare their papers in this dual-unit system. The majority of papers published, we will continue to

To	Multiply by
millimeters (mm)	25.40
centimeters (cm)	2.540
meters (m)	0.0254
inches (in)	0.305
kilometers (km)	1.61
meters (m)	0.91
square centimeters (cm ²)	6.45
square meters (m ²)	0.093
square meters (m ²)	0.836
square meters (m ²)	4047.
square kilometers (km ²)	2.59
cubic centimeters (cm ³)	16.4
cubic meters (m ³)	0.028
cubic meters (m ³)	0.765
kilograms (kg)	0.453
kilograms (kg)	907.2
newtons (N)	4.45
newtons (N)	9.81
newtons per square meter (N/m ²)	47.9
kilonewtons per square meter (kN/m ²)	6.9
cubic meters (m ³)	0.0038
liter (dm ³)	3.8
cubic meters (m ³)	1233.
cubic meters/minute (m ³ /min)	0.0038
pascals (Pa)	1.00

649 240

Special attention is devoted to the vertical motion because this is the fundamental vibration mode for checking the theory. A brief consideration of all vibration modes is given in Ref. 16. Coupled horizontal and rocking motion is analyzed in detail in Ref. 3.

EQUATION OF MOTION

Fig. 1 shows a model of the embedded footing-soil system, and the forces acting on the footing. The basic differential equation of motion is

$$m\ddot{w}(t) = P(t) - R_z(t) - N_z(t) \dots \dots \dots (1)$$

in which: m = mass of footing; w = vertical displacement of footing; $P(t)$ = time dependent vertical excitation force; $R_z(t)$ = dynamic vertical reaction at base of footing; and $N_z(t)$ = dynamic vertical reaction along the side surface of footing.

In order to solve Eq. 1, the following assumptions are made:

1. The footing is a rigid cylindrical body with radius r_0 .
2. Linear elasticity is assumed.
3. The dynamic reaction, $R_z(t)$, is independent of the depth of embedment.
4. There is a perfect bond between the sides of the footing and the soil.
5. The excitation force, $P(t)$, is harmonic and acts along the vertical axis.

Under these assumptions, the dynamic reaction at the base can be expressed using elastic half-space solutions. The relation between footing base displacement $w(t)$ and elastic half-space reaction $R_z(t)$ can be written as

$$R_z(t) = Gr_0(C_1 + iC_2)w(t) \dots \dots \dots (2)$$

$$\text{in which: } C_1 = \frac{-f_1}{f_1^2 + f_2^2}, C_2 = \frac{f_2}{f_1^2 + f_2^2} \dots \dots \dots (3)$$

Herein, $f_{1,2}$ = functions of dimensionless frequency $a_0 = \omega r_0 \sqrt{\rho/G}$, Poisson's ratio and stress distribution in the base, G = shear modulus of half space, and r_0 = radius of footing. (Functions $f_{1,2}$ were introduced by Reissner and can be taken from later solutions, e.g., Refs. 4, 12, 18.)

The dynamic reaction, $N_z(t)$, acting on the vertical sides of the footing is a complex function of the embedment depth, l , the dimensionless frequency a_0 , the shear modulus, G_1 , and density ρ_1 , of the adjacent soil layer and also of the quality of the contact between the soil and the footing. If s = the dynamic reaction per unit depth of embedment, then:

$$N_z(t) = \int_0^l s(z,t) dz \dots \dots \dots (4)$$

If the approximate assumption is accepted that s is independent of z , then $s = s(t)$ and Baranov's solution (1), of which the basic assumptions are outlined in the Introduction, can be used. According to Ref. 1, the unit reaction:

$$i = G_1(S_1 + iS_2)w(t) \dots \dots \dots (5)$$

$$s(t) = G_1(S_1 + iS_2)w(t)$$

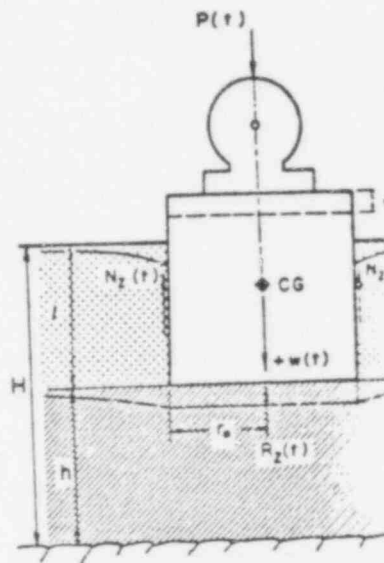


Fig. 1.—Embedded Footing Excited

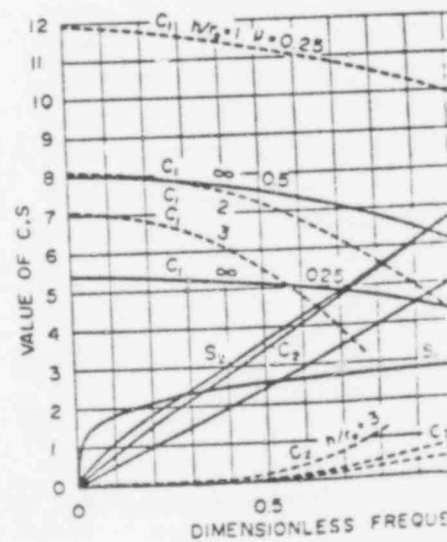


Fig. 2.—Stiffness Parameters C_1, S_1 and Damping Parameters S_1, S_2 (Dashed Lines) and Side Layer

to the vertical motion because this is the fundamental theory. A brief consideration of all vibration coupled horizontal and rocking motion is analyzed

the embedded footing-soil system, and the forces associated differential equation of motion is

$$(1)$$

where: w = vertical displacement of footing; $P(t)$ = excitation force; $R_z(t)$ = dynamic vertical reaction; $R_s(t)$ = dynamic vertical reaction along the side surface

The following assumptions are made:

- 1. Cylindrical body with radius r_0 .
- 2. $R_z(t)$ is independent of the depth of embedment.
- 3. $R_s(t)$ is independent between the sides of the footing and the soil.
- 4. $P(t)$ is harmonic and acts along the vertical axis.

The dynamic reaction at the base can be expressed as follows. The relation between footing base displacement $w(t)$ and $R_z(t)$ can be written as

$$(2)$$

$$(3)$$

where dimensionless frequency $a_0 = \omega r_0 \sqrt{\rho_s / G}$, G = shear modulus of half space, ρ_s = density of soil. (Functions $f_{1,2}$ were introduced by Reissner and others, e.g., Refs. 4, 12, 18.)

$R_s(t)$, acting on the vertical sides of the footing is independent of embedment depth, l , the dimensionless frequency a_0 and density ρ_s of the adjacent soil layer and also independent between the soil and the footing. If s = the dynamic reaction, then:

$$(4)$$

It is assumed that s is independent of z , then $R_s(t)$ is independent of z , of which the basic assumptions are outlined above. According to Ref. 1, the unit reaction:

$$(5)$$

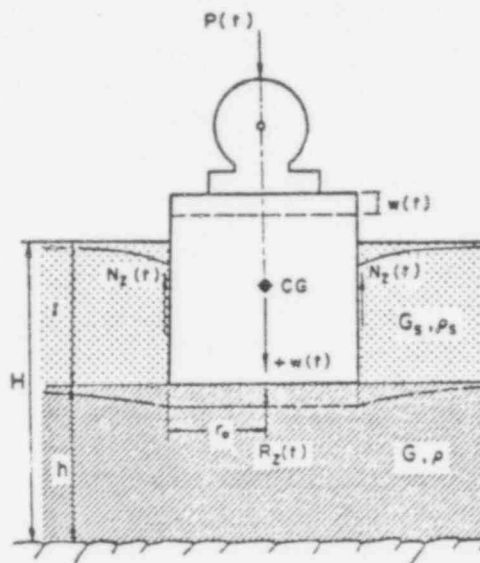


Fig. 1.—Embedded Footing Excited Vertically

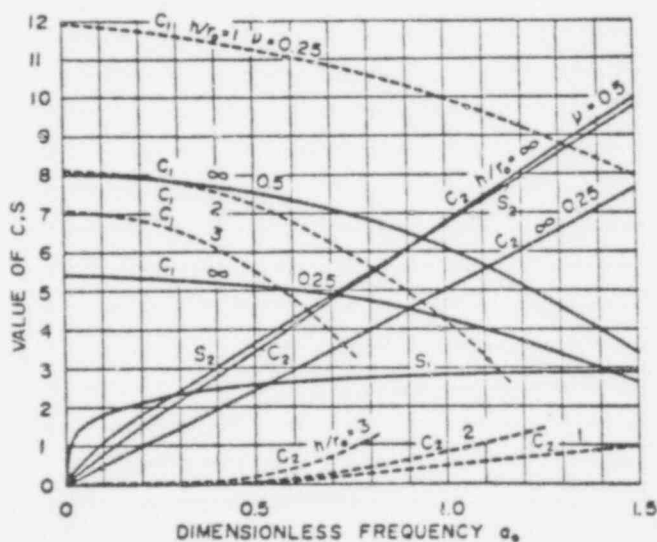


Fig. 2.—Stiffness Parameters C_1, S_1 and Damping Parameters C_2, S_2 for Half-Space Stratum (Dashed Lines) and Side Layer

649 242

in which $S_1 = 2\pi a_0 \frac{J_1(a_0)J_0(a_0) + Y_1(a_0)Y_0(a_0)}{J_0^2(a_0) + Y_0^2(a_0)}$ (6)

$S_2 = \frac{4}{J_0^2(a_0) + Y_0^2(a_0)}$ (7)

Herein $J_0(a_0)$, $J_1(a_0)$ = Bessel functions of the first kind of order zero and one, respectively, and $Y_0(a_0)$, $Y_1(a_0)$ = Bessel functions of the second kind of order zero and one. Then the total side reaction is, from Eqs. 4 and 5:

$N_s(t) = \int_0^l G_s(S_1 + iS_2)w(t) dz = G_s l(S_1 + iS_2)w(t)$ (8)

Substitution of Eqs. 2 and 8 into Eq. 1 yields the equation of vertical vibrations:

$m\ddot{w}(t) + Gr_0 \left[C_1 + iC_2 + \frac{G_s l}{G r_0} (S_1 + iS_2) \right] w(t) = P(t)$ (9)

With complex excitation:

$P(t) = P_0 \exp(i\omega t) = P_0(\cos \omega t + i \sin \omega t)$ (10)

the steady-state response is

$w(t) = w \exp(i\omega t)$ (11)

in which P_0 = real force amplitude and w = complex response amplitude. Note the frequency dependent stiffness (spring) constant:

$k = Gr_0 \left(C_1 + \frac{G_s l}{G r_0} S_1 \right)$ (12)

and the frequency dependent damping constant:

$c = \frac{Gr_0}{\omega} \left(C_2 + \frac{G_s l}{G r_0} S_2 \right)$ (13)

Then the real part of the vibration is

$w(t) = w_0 \cos(\omega t + \phi)$ (14)

in which real amplitude

$w_0 = \frac{P_0}{\sqrt{(k - m\omega^2)^2 + (c\omega)^2}} = \frac{P_0}{k} \frac{1}{\sqrt{\left[1 - \left(\frac{\omega}{\omega_0}\right)^2\right]^2 + 4D^2 \left(\frac{\omega}{\omega_0}\right)^2}}$ (15)

phase shift $\phi = -\text{atan} \frac{c\omega}{k - m\omega^2}$ (16)

damping ratio $D = \frac{c}{2m\omega_0}$ (17)

and natural undamped frequency of an embedded footing

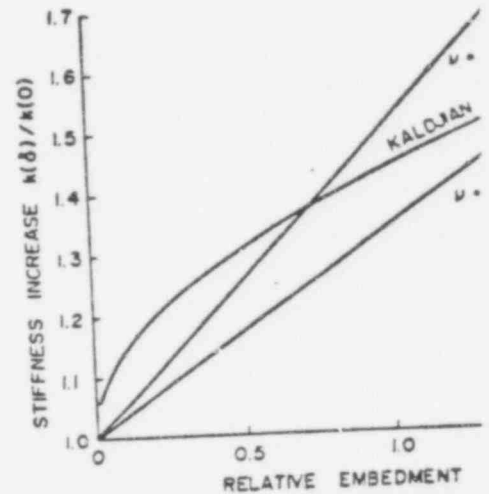


Fig. 3.—Comparison of Stiffness Increase with

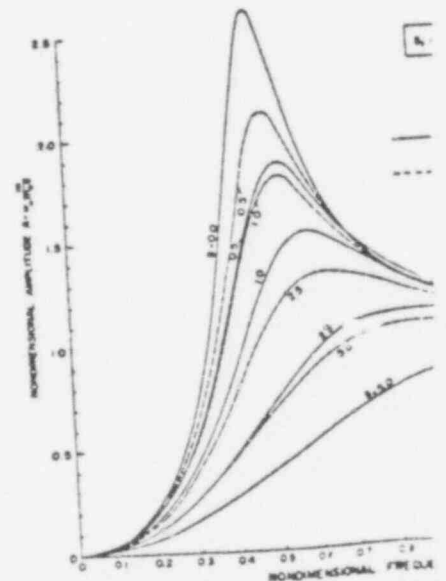


Fig. 4.—Theoretical Response Curves of Footings (E Lines) and Side Fill (Dashed Lines) (Rigid Base Str)

$$\frac{J_0(a_0)Y_1(a_0) + Y_1(a_0)Y_0(a_0)}{J_0^2(a_0) + Y_0^2(a_0)} \dots (6)$$

$$\dots (7)$$

essel functions of the first kind of order zero and
 $Y_1(a_0)$ = Bessel functions of the second kind
 the total side reaction is, from Eqs. 4 and 5:

$$P(t) dz = G_1 l (S_1 + iS_2) w(t) \dots (8)$$

Eq. 1 yields the equation of vertical vibrations:

$$\left[\frac{G_1 l}{G r_0} (S_1 + iS_2) \right] w(t) = P(t) \dots (9)$$

$$P(t) = P_0 e^{i\omega t} \dots (10)$$

$$\dots (11)$$

amplitude and w = complex response amplitude.
 constant stiffness (spring) constant:

$$\dots (12)$$

damping constant:

$$\dots (13)$$

ibration is

$$\dots (14)$$

$$\frac{P_0}{k} \frac{1}{\sqrt{\left[1 - \left(\frac{\omega}{\omega_0}\right)^2\right]^2 + 4D^2 \left(\frac{\omega}{\omega_0}\right)^2}} \dots (15)$$

$$\frac{c\omega}{m\omega^2} \dots (16)$$

$$\dots (17)$$

ncy of an embedded footing

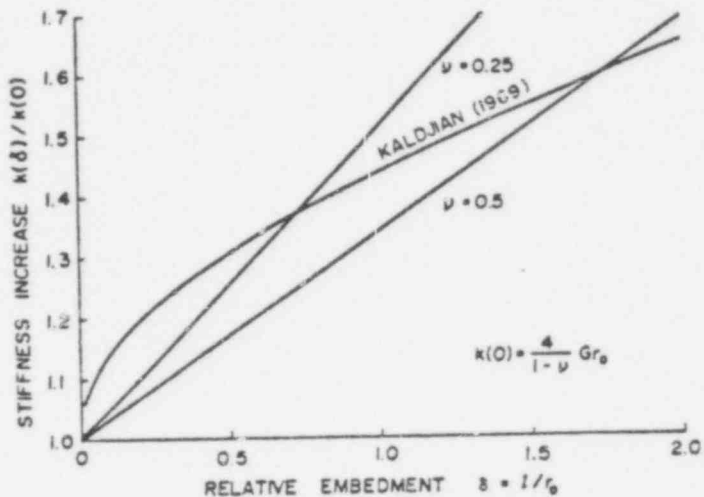


Fig. 3.—Comparison of Stiffness Increase with Finite Element Solution

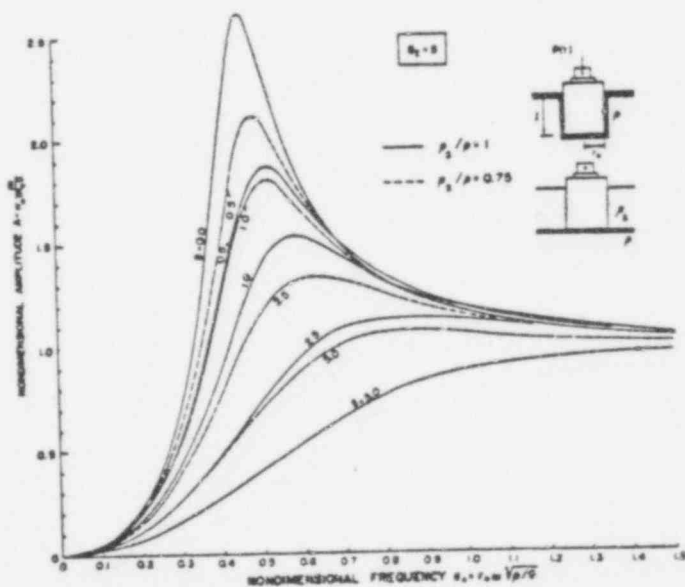


Fig. 4.—Theoretical Response Curves of Footings Embedded in Undisturbed Soil (Full Lines, and Side Fill (Dashed Lines) (Rigid Base Stress Distribution, $B_1 = 5$)

$$\omega_0 = \sqrt{\frac{k}{m}} = \sqrt{\frac{Gr_0}{m} \left(C_1 + \frac{G_2 l}{G r_0} S_1 \right)} \dots (18)$$

(The natural undamped frequency must be determined from Eq. 18 by trial and error approach because it appears in both C_1 and S_1 .)

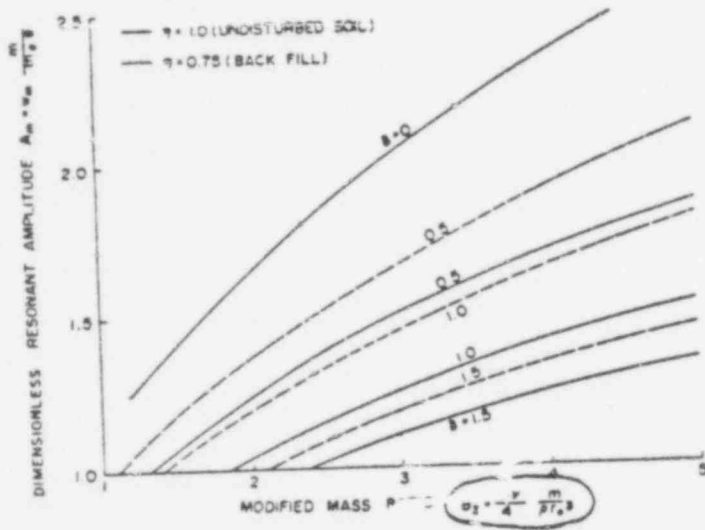


Fig. 5.—Dimensionless Resonant Amplitudes Versus Mass Ratio for Various Embedments $\delta = l/r_0$ (Undisturbed Soil and Side Fill with $\eta = \rho_s/\rho = 0.75$)

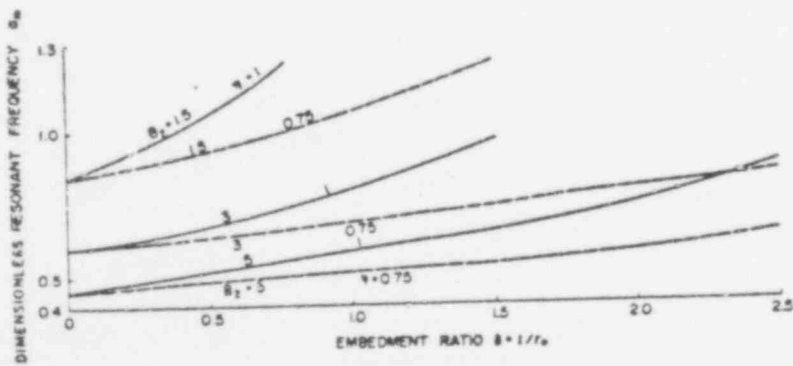


Fig. 6.—Dimensionless Resonant Frequencies Versus Relative Embedment for Various Mass Ratios $B_2 (\eta = \rho_s/\rho)$

In most practical problems, the excitation force, $P(t)$, is caused by rotation of an unbalanced mass, m_e , and in Eq. 15 the exciting force amplitude is:

$$P_0 = m_e e \omega^2 \dots (19)$$

in which e = eccentricity of rotating mass; it is so introduce the dimensionless amplitude, $A = w_m / (g \cdot \tau_0)$

EXAMPLES OF NUMERICAL RESULTS

From Eq. 15 the response curves of embedded with various assumptions concerning both the pertinent stiffness parameters C_1 and S_1 , and data are shown in Fig. 2 and given in a polynomial

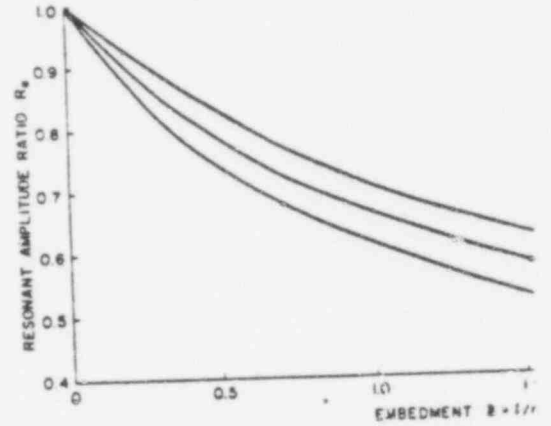


Fig. 7.—Resonant Amplitude Ratio Versus Embedment Mass Ratio, Undisturbed Soil $\eta = 1$, Side Fill $\eta = 0.7$

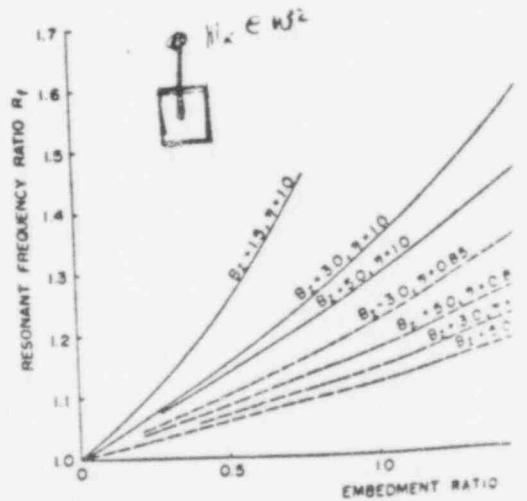
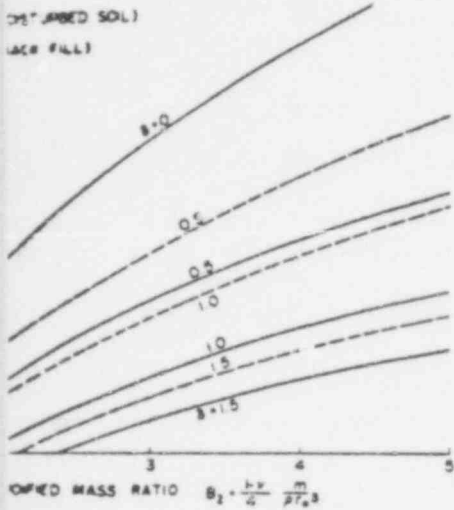


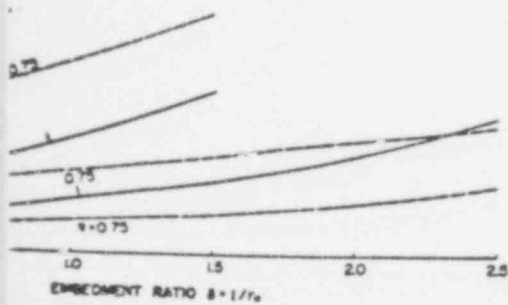
Fig. 8.—Resonant Frequency Ratio Versus Embedment Side Fill

$$\frac{G_s I}{G r_s S_1} \dots \dots \dots (18)$$

Frequency must be determined from Eq. 18 by trial and error (since ω appears in both C_1 and S_1 .)



Resonant Amplitude Ratio Versus Mass Ratio for Various Embedment Ratios and Side Fill with $\eta = \rho_s/\rho = 0.75$



Resonant Frequency Ratio Versus Relative Embedment for Various Mass Ratios and Side Fill with $\eta = \rho_s/\rho = 0.75$

When the excitation force, $P(t)$, is caused by rotation of the mass, in Eq. 15 the excitation force amplitude is:

$$P_0 = \frac{w_0 m (m_1 e)}{m_1} \dots \dots \dots (19)$$

in which e = eccentricity of rotating mass; it is sometimes convenient to also introduce the dimensionless amplitude, $A = w_0 m / (m_1 e)$.

EXAMPLES OF NUMERICAL RESULTS

From Eq. 15 the response curves of embedded footings can be computed with various assumptions concerning both the base and side reactions. The pertinent stiffness parameters C_1 and S_1 , and damping parameters C_2 and S_2 are shown in Fig. 2 and given in a polynomial form in Tables 1 and 2 to

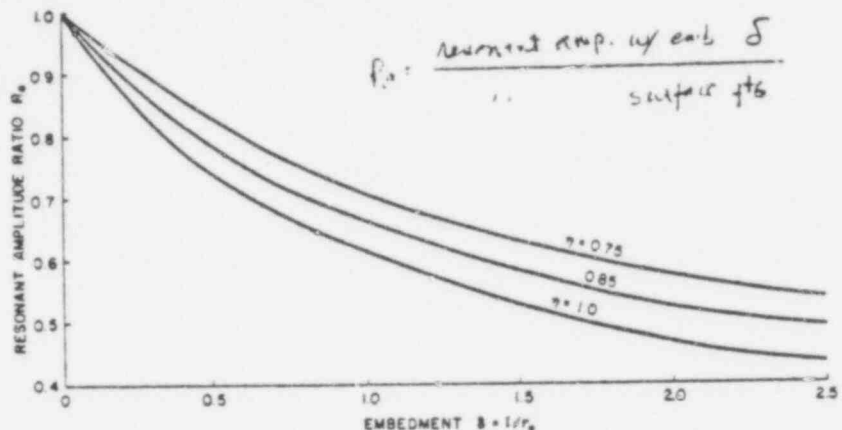


Fig. 7.—Resonant Amplitude Ratio Versus Embedment (Approximately Valid for any Mass Ratio; Undisturbed Soil $\eta = 1$, Side Fill $\eta = 0.75, 0.85$)

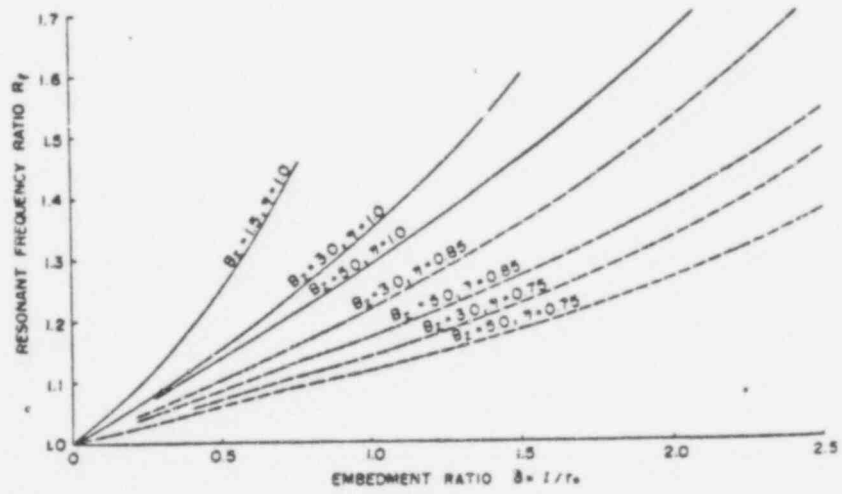


Fig. 8.—Resonant Frequency Ratio Versus Embedment (— Undisturbed Soil, - - Side Fill)

facilitate the computation. Curves concerning strata were calculated with $\nu = 0.25$ from Warbarton (20) and are shown in Fig. 2 in dashed lines. Curves

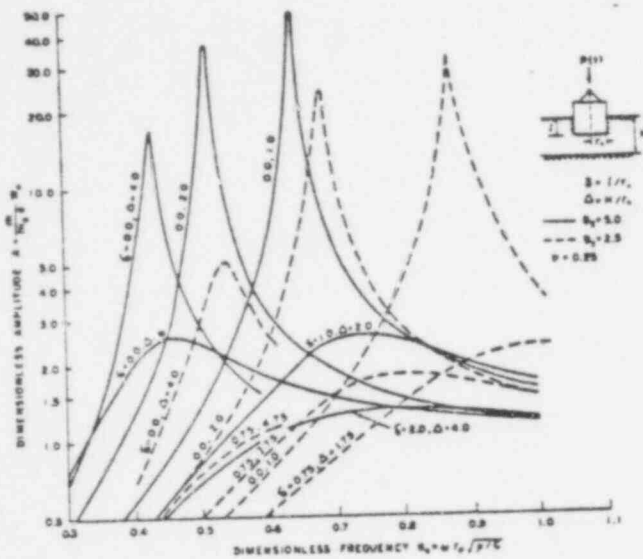


Fig. 9.—Theoretical Response Curves for Vertical Vibration of Footings Embedded in Elastic Stratum (Undisturbed Soil, Various Embedments, and Various Thicknesses of Elastic Stratum)

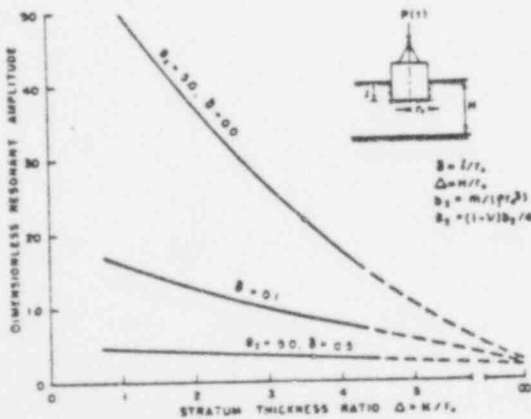


Fig. 10.—Variation of Theoretical Resonant Amplitudes of Vertical Vibration of Footing Embedded in Elastic Stratum with Thickness of Stratum (Undisturbed Soil, Various Embedments)

concerning half-space were computed from Bycroft (4). It will be noticed that $S_1 = 0$ for $a_0 \rightarrow 0$ which results from the assumption that the base overlying

layer is independent of the underlying half-space and in Fig. 3 the static stiffness increase found by k stiffness increases obtained from Eq. 12 with C for a rather representative frequency $a_0 = 0.8$. embedment, δ , $k(0) =$ stiffness for surface footing element method and thus, Fig. 3 yields an idea about of the approximate analytical approach. It may tend to overestimate the rigidity increase with s shown later herein.

Embedment in Half-Space.—In Fig. 4, the the given for a rigid base stress distribution. The curve a situation where the footing is embedded in an are in reasonable agreement with the finite element method and thus, Fig. 3 yields an idea about of the approximate analytical approach. It may tend to overestimate the rigidity increase with s shown later herein.

The curves shown in Fig. 4 were computed for the effect of embedment very distinctly. The variation with embedment for other mass ratios can be seen amplitude ratio $R_0 =$ resonant amplitude with embedment of surface footing, was found practically independent of δ . 7 can be used for any footing embedded in a half-space amplitude reduction.

The natural frequency (ω_0) variations appear ratio too. However, the resonant frequency (frequency ratio $R_1 =$ resonant frequency with embedment δ of footing, highly depends on mass ratio (Fig. 8).

Embedment in Stratum.—With equal ease, the in a stratum can be analyzed using the proper stiffness and damping parameters $C_{1,2}$. Side the same as before.

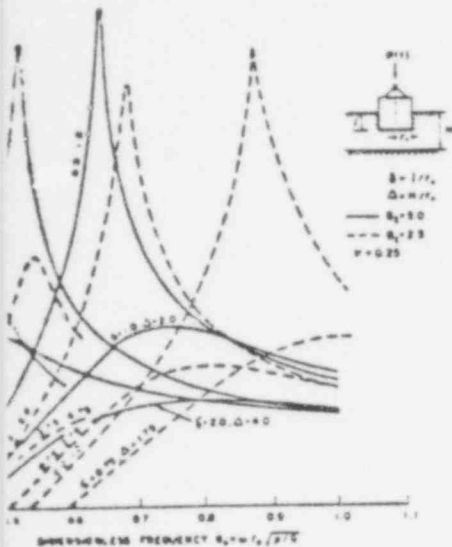
Examples of theoretical response curves are shown of relative embedment δ and two values of m of embedment, as well as a strong variability of the involved, are obvious. The variations of resonant frequency and stratum thickness are plotted in Fig. 10. embedment considerably reduces the dependence graphs shown do not apply for other mass ratios trends to be expected. Any particular situation can as long as the base reactions are available.

It can be seen that the omission of embedment overestimation of amplitudes in the case of a omission of layering can lead to substantial underestimation

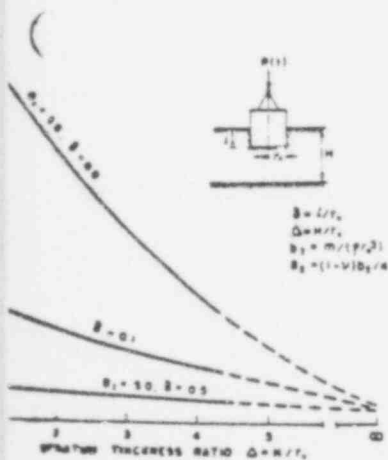
SIMPLIFIED DESIGN ANALYSIS

Calculation of amplitudes and resonant frequency defined if stiffness parameters C_1 and S_1 are taken as f

curves concerning strata were calculated with $\nu = 0.25$ and are shown in Fig. 2 in dashed lines. Curves



Curves for Vertical Vibration of Footings Embedded in Soil, Various Embedments, and Various Thicknesses



Resonant Amplitudes of Vertical Vibration of Footing with Thickness of Stratum (Undisturbed Soil, Various

computed from Bycroft (4). It will be noticed that results from the assumption that the base overlying

layer is independent of the underlying half-space and has an infinite span.

In Fig. 3 the static stiffness increase found by Kaldjian (9) is compared with stiffness increases obtained from Eq. 12 with $C_1 = 4/1 \nu$ and S_1 computed for a rather representative frequency $\omega_0 = 0.8$. [$k(\delta) =$ stiffness with the embedment, δ , $k(0) =$ stiffness for surface footing.] Kaldjian used the finite element method and thus, Fig. 3 yields an idea about the accuracy and limitations of the approximate analytical approach. It may be noted that all the theories tend to overestimate the rigidity increase with small embedments as will be shown later herein.

Embedment in Half-Space.—In Fig. 4, the theoretical response curves are given for a rigid base stress distribution. The curves shown in full lines describe a situation where the footing is embedded in an undisturbed soil. The curves are in reasonable agreement with the finite element solution by Lysmer and Kuhlemeyer (13). The dashed lines show a different case in which the footing is surrounded by a side fill whose density $\rho_1 = 0.75 \rho$. [In this example it was assumed that $G_1/G = (\rho_1/\rho)^3$.]

The curves shown in Fig. 4 were computed for a high mass ratio to show the effect of embedment very distinctly. The variations of resonant amplitudes with embedment for other mass ratios can be seen in Figs. 5, 6, and 7. Resonant amplitude ratio $R_0 =$ resonant amplitude with embedment δ /resonant amplitude of surface footing, was found practically independent of mass ratio. Thus Fig. 7 can be used for any footing embedded in a half-space to estimate the resonant amplitude reduction.

The natural frequency (ω_0) variations appear highly independent of mass ratio too. However, the resonant frequency (frequency at maximum amplitude) ratio $R_f =$ resonant frequency with embedment δ /resonant frequency of surface footing, highly depends on mass ratio (Fig. 8).

Embedment in Stratum.—With equal ease, the response of footings embedded in a stratum can be analyzed using the proper functions f_1 and f_2 to compute the stiffness and damping parameters $C_{1,2}$. Side reaction parameters $S_{1,2}$ are the same as before.

Examples of theoretical response curves are shown in Fig. 9 for several values of relative embedment δ and two values of mass ratio. The essential effect of embedment, as well as a strong variability of the response with all the parameters involved, are obvious. The variations of resonant amplitudes with embedment and stratum thickness are plotted in Fig. 10. With higher embedments, the embedment considerably reduces the dependence on the stratum thickness. The graphs shown do not apply for other mass ratios; however, they indicate the trends to be expected. Any particular situation can be analyzed without difficulty as long as the base reactions are available.

It can be seen that the omission of embedment can result in unrealistic overestimation of amplitudes in the case of a stratum. And, contrarily, the omission of layering can lead to substantial underestimation of amplitudes.

SIMPLIFIED DESIGN ANALYSIS

Calculation of amplitudes and resonant frequencies can be considerably simplified if stiffness parameters C_1 and S_1 are taken as frequency independent (constant).

Table 1.—Stiffness and Damping Parameters for Half Space and Side Layers

ν (1)	Values (2)	Constant parameters (3)	Validity range (4)
(a) Half Space			
0.0	$C_1 = 4.00 - 0.08356 a_0 + 0.6346 a_0^2 - 2.600 a_0^3 + 1.801 a_0^4 - 0.3646 a_0^5$	$\bar{C}_1 = 3.90$	$0 \leq a_0 \leq 1.5$
	$C_2 = 3.438 a_0 + 0.5742 a_0^2 - 1.154 a_0^3 + 0.7433 a_0^4$	$\bar{C}_2 = 3.50$	
0.25	$C_1 = 5.37 + 0.364 a_0 - 1.41 a_0^2$	$\bar{C}_1 = 5.20$	
	$C_2 = 5.06 a_0$	$\bar{C}_2 = 5.00$	
0.5	$C_1 = 8.00 + 2.180 a_0 - 12.63 a_0^2 + 20.73 a_0^3 - 16.47 a_0^4 + 4.458 a_0^5$	$\bar{C}_1 = 7.50$	
	$C_2 = 7.414 a_0 - 2.986 a_0^2 + 4.324 a_0^3 - 1.782 a_0^4$	$\bar{C}_2 = 6.80$	
(b) Side Layer			
any value	$S_1 = 0.2153 a_0 + 2.760 a_0 / a_0 + 0.06084$	$\bar{S}_1 = 2.70$	$0 \leq a_0 \leq 2.00$
	$S_2 = 6.059 a_0 + 0.7022 a_0 / a_0 + 0.01616$	$\bar{S}_2 = 6.70$	

Empirical values for circular footings

Table 2.—Stiffness and Damping Parameters for Stratum

h/r_0 (1)	Stratum $\nu = 0.25$ (2)	Constant parameters (3)	Validity range (4)
1.0	$C_1 = 12.23 - 1.178 a_0 - 0.3056 a_0^2 - 1.177 a_0^3 + 0.4160 a_0^4$	$\bar{C}_1 = 10.0$	$0 \leq a_0 \leq 1.50$
	$C_2 = 0.2395 a_0^2 + 0.5646 a_0^3 + 0.0227 a_0^4 - 0.3403 a_0^5 + 0.203 a_0^6$	$\bar{C}_2 = 0.30$	
2.0	$C_1 = 8.13 + 0.8516 a_0 - 3.664 a_0^2 - 8.289 a_0^3 + 11.18 a_0^4 - 3.978 a_0^5$	$\bar{C}_1 = 7.00$	$0 \leq a_0 \leq 1.25$
	$C_2 = 0.004044 a_0 - 0.7386 a_0^2 + 13.27 a_0^3 - 39.61 a_0^4 + 49.8 a_0^5 - 26.95 a_0^6 + 5.069 a_0^7$	$\bar{C}_2 = 0.45$	
		$\bar{C}_1 = 5.5$	$0 \leq a_0 \leq 0.81$

0.0	$C_1 = 4.00 - 0.08356 a_0 + 0.6346 a_0^2 - 2.600 a_0^3 + 0.01 a_0^4 - 0.3646 a_0^5$ $C_2 = 3.438 a_0 + 0.5742 a_0^2 - 1.154 a_0^3 + 0.7433 a_0^4$	$\hat{C}_1 = 3.90$ $\hat{C}_2 = 3.50$	$0 \leq a_0 \leq 1.5$
0.25	$C_1 = 5.37 + 0.366 a_0 - 1.41 a_0^2$ $C_2 = 5.06 a_0$	$\hat{C}_1 = 5.20$ $\hat{C}_2 = 5.00$	
0.5	$C_1 = 8.00 + 2.180 a_0 - 12.63 a_0^2 + 20.73 a_0^3 - 16.47 a_0^4 + 4.458 a_0^5$ $C_2 = 7.414 a_0 - 2.986 a_0^2 + 4.324 a_0^3 - 1.782 a_0^4$	$\hat{C}_1 = 7.50$ $\hat{C}_2 = 6.80$	
(b) Side Layer			
any value	$S_1 = 0.2153 a_0 + 2.760 a_0/a_0 + 0.06084$ $S_2 = 6.059 a_0 + 0.7022 a_0/a_0 + 0.01616$	$\hat{S}_1 = 2.70$ $\hat{S}_2 = 6.70$	$0 \leq a_0 \leq 2.00$

Table 2.—Stiffness and Damping Parameters for Stratum

h/r_0 (1)	Stratum $\nu = 0.25$ (2)	Constant parameters (3)	Validity range (4)
1.0	$C_1 = 12.23 - 1.178 a_0 - 0.3056 a_0^2 - 1.177 a_0^3 + 0.4160 a_0^4$ $C_2 = 0.2395 a_0^2 + 0.5646 a_0^3 + 0.0227 a_0^4 - 0.3403 a_0^5 + 0.203 a_0^6$	$\hat{C}_1 = 10.0$ $\hat{C}_2 = 0.30$	$0 \leq a_0 \leq 1.50$
2.0	$C_1 = 8.13 + 0.8516 a_0 - 3.664 a_0^2 - 8.289 a_0^3 + 11.18 a_0^4 - 3.978 a_0^5$ $C_2 = 0.004044 a_0 - 0.7386 a_0^2 + 13.27 a_0^3 - 39.61 a_0^4 + 49.8 a_0^5 - 26.95 a_0^6 + 5.069 a_0^7$	$\hat{C}_1 = 7.00$ $\hat{C}_2 = 0.45$	$0 \leq a_0 \leq 1.25$
3.0	$C_1 = 7.04 + 0.4659 a_0 - 6.989 a_0^2$ $C_2 = 0.7361 a_0^2 - 1.462 a_0^3 + 3.573 a_0^4$	$\hat{C}_1 = 5.5$ $\hat{C}_2 = 0.65$	$0 \leq a_0 \leq 0.81$
4.0	$C_1 = 6.579 - 0.2422 a_0 - 0.3889 a_0^2 - 29.69 a_0^3 + 7.711 a_0^4 + 76.44 a_0^5 - 77.42 a_0^6$ $C_2 = 0.02804 a_0 + 3.02 a_0^2 + 7.458 a_0^3 - 184.2 a_0^4 + 655.7 a_0^5 - 804.9 a_0^6 + 314.2 a_0^7$	$\hat{C}_1 = 4.30$ $\hat{C}_2 = 1.00$	$0 \leq a_0 \leq 0.62$

649 250

and damping parameters C_2 and S_2 as proportional to dimensionless frequency, a_0 (Fig. 2). These assumptions seem well justified for the embedment parameters S_1 and S_2 if $a_0 \gg 0.1$, as they do for C_2 for a half space; C_2 for a stratum is less linear but very small, thus adding little to the total damping. The constancy of C_1 may be generally questioned (see Ref. 12); nevertheless, it seems acceptable in the shown frequency range. Altogether, the simplifying assumptions are consistent with the generally accepted practice in design analysis of surface footings (17).

Therefore, assume that $C_1 = \bar{C}_1$ and $S_1 = \bar{S}_1$ and that:

$$C_2 = \bar{C}_2 a_0, S_2 = \bar{S}_2 a_0 \dots \dots \dots (20)$$

in which $\bar{C}_{1,2}$ and $\bar{S}_{1,2}$ = constants whose values can be readily established

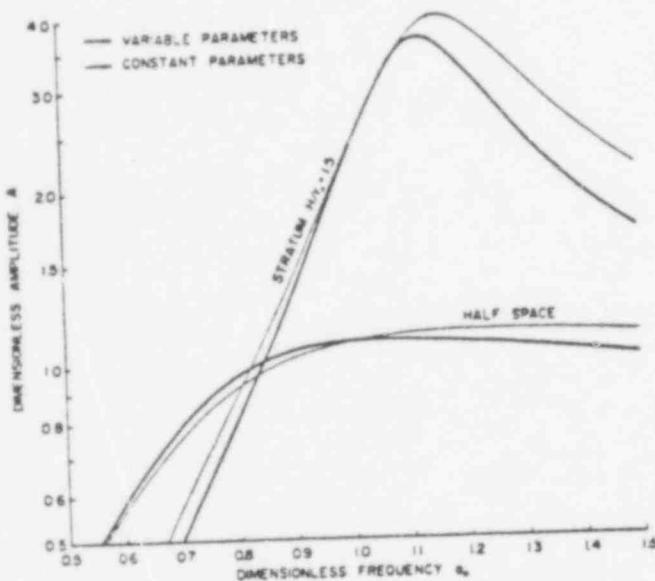


Fig. 11.—Comparison of Response Curves Computed with Variable and Constant Parameters ($l/r_0 = 0.5$, $b_0 = 8.1$, $\rho/\rho_s = 0.75$ and $G_s/G = 0.5$)

from Fig. 2, Tables 1 and 2 or any other suitable formulae for $f_{1,2}$. Several suitable values of $\bar{C}_{1,2}$ and $\bar{S}_{1,2}$ are given in Tables 1 and 2.

With constant stiffness parameters, \bar{C}_1 and \bar{S}_1 substituted in Eq. 12 in place of C_1 and S_1 , the frequency independent stiffness constant is obtained, and with it, the natural undamped frequency ω_0 directly follows from Eq. 18.

Substitution of Eqs. 20 into Eq. 13 yields the frequency independent damping constant for embedded footings

$$c = r_0^2 \sqrt{\rho G} \left(\bar{C}_2 + \bar{S}_2 \frac{l}{r_0} \sqrt{\frac{\rho_s G_s}{\rho G}} \right) \dots \dots \dots (21)$$

or the damping ratio

$$D = \frac{1}{2\sqrt{b_0}} \frac{\left(\bar{C}_2 + \bar{S}_2 \frac{l}{r_0} \sqrt{\frac{\rho_s G_s}{\rho G}} \right)}{\sqrt{\bar{C}_1 + \frac{G_s l}{G r_0} \bar{S}_1}} \dots \dots \dots$$

in which mass ratio $b_0 = m/\rho r_0^3$. Then, the vertical amplitude is obtained from E interest.

The amplitude at natural frequency ω_0 (slightly amplitude) is simply:

$$w_0(\omega_0) = \frac{P_0 l}{k 2D} \dots \dots \dots$$

or with frequency variable excitation (Eq. 19):

$$w_0(\omega_0) = \frac{m_s e l}{m 2D} \dots \dots \dots$$

as in any one degree-of-freedom system (Voigt model). Values of G can be determined by tests, or from Eq. 17.

In Fig. 11, example of response curves computed with constant parameters are shown for embedment in a stratum. The differences decrease with increasing embedment depth and appear to yield an accuracy sufficient for practical design.

COMPARISON WITH EXPERIMENTS

In order to assess the practical applicability of the solution, the theoretical results have been compared with laboratory experiments (5), and with a series of field experiments at the University of Western Ontario by the second writer.

In the latter tests, two concrete blocks were used: (1) $27 \text{ in.} \times 48 \text{ in.}$ ($0.686 \text{ m} \times 0.686 \text{ m} \times 1.22 \text{ m}$); (2) $38 \text{ in.} \times 48 \text{ in.}$ ($0.483 \text{ m} \times 0.966 \text{ m} \times 1.22 \text{ m}$). The concrete block was cast directly in the foundation. The test apparatus consisted of a mechanical oscillator LAZAN and a Kopp Variator.

Different embedments were obtained by cutting the footing sides to the appropriate depth. The material at the test site are: (1) Density of undisturbed soil = 1.8 g/cm^3 ; (2) Poisson's ratio = 0.36; (3) shear modulus = 1.5 kg/cm^2 ; (4) equivalent radius of footing = 1.22 m; (5) depth of footing = 15.48 m; and (6) Lysmer's modified modulus = 1.5 kg/cm^2 .

The experiments are described in more detail in Ref. 5. The response curves in rocking modes are also shown in Fig. 12.

and S_2 as proportional to dimensionless frequency, seem well justified for the embedment parameters they do for C_2 for a half space; C_2 for a stratum thus adding little to the total damping. The constancy noted (see Ref. 12); nevertheless, it seems acceptable. Altogether, the simplifying assumptions are accepted practice in design analysis of surface

$C_1 = \bar{C}_1$ and $S_1 = \bar{S}_1$, and that: (20)

constants whose values can be readily established



Response Curves Computed with Variable and Constant Parameters, $\rho_s/\rho = 0.75$ and $G_s/G = 0.5$

or any other suitable formulae for $f_{1,2}$. Several parameters, \bar{C}_1 and \bar{S}_1 substituted in Eq. 12 in place of independent stiffness constant is obtained, and frequency ω_0 directly follows from Eq. 18. Eq. 13 yields the frequency independent damping

$$\frac{\rho_s G_s}{\rho G} \dots \dots \dots (21)$$

or the damping ratio

$$D = \frac{1}{2\sqrt{b_0}} \frac{\left(\bar{C}_2 + \bar{S}_2 \frac{l}{r_0} \sqrt{\frac{\rho_s G_s}{\rho G}} \right)}{\sqrt{\bar{C}_1 + \frac{G_s l}{G r_0} \bar{S}_1}} \dots \dots \dots (22)$$

in which mass ratio $b_0 = m/\rho r_0^3$.

Then, the vertical amplitude is obtained from Eq. 15 for any frequency of interest.

The amplitude at natural frequency ω_0 (slightly smaller than the maximum amplitude) is simply:

$$w_0(\omega_0) = \frac{P_0}{k} \frac{1}{2D} \dots \dots \dots (23)$$

or with frequency variable excitation (Eq. 19):

$$w_0(\omega_0) = \frac{m_s e}{m} \frac{1}{2D} \dots \dots \dots (24)$$

as in any one degree-of-freedom system (Voigt model).

Values of G can be determined by tests, or found in literature, e.g., Ref. 17.

In Fig. 11, examples of response curves computed with both variable and constant parameters are shown for embedment in a stratum and in a half space. The differences decrease with increasing embedment. The constant parameters appear to yield an accuracy sufficient for practical purposes.

COMPARISON WITH EXPERIMENTS

In order to assess the practical applicability of the approximate analytical solution, the theoretical results have been compared with earlier field tests (14), laboratory experiments (5), and with a series of field tests carried out at the University of Western Ontario by the second writer.

In the latter tests, two concrete blocks were used with dimensions 27 in. x 27 in. x 48 in. (0.686 m x 0.686 m x 1.22 m) (square base) and 19 in. x 38 in. x 48 in. (0.483 m x 0.966 m x 1.22 m) (rectangular base). Each concrete block was cast directly in the foundation pit. The excitation equipment consisted of a mechanical oscillator LAZAN and a 220 v. three-phase motor coupled with a Kopp Variator.

Different embedments were obtained by carefully removing the soil around the footing sides to the appropriate depth. The major soil and footing properties at the test site are: (1) Density of undisturbed soil = 103.0 lb/ft³ (1,650 kg/m³); (2) Poisson's ratio = 0.38; (3) shear modulus = 6.6 lb/ft² x 10³ lb/ft² (320 kg/cm²); (4) equivalent radius of footing = 1.26 ft (0.344 m); (5) mass ratio of footing = 15.48; and (6) Lysmer's modified mass factor = 2.40.

The experiments are described in more detail in Refs. 2 and 16, in which the response curves in rocking modes are also given.

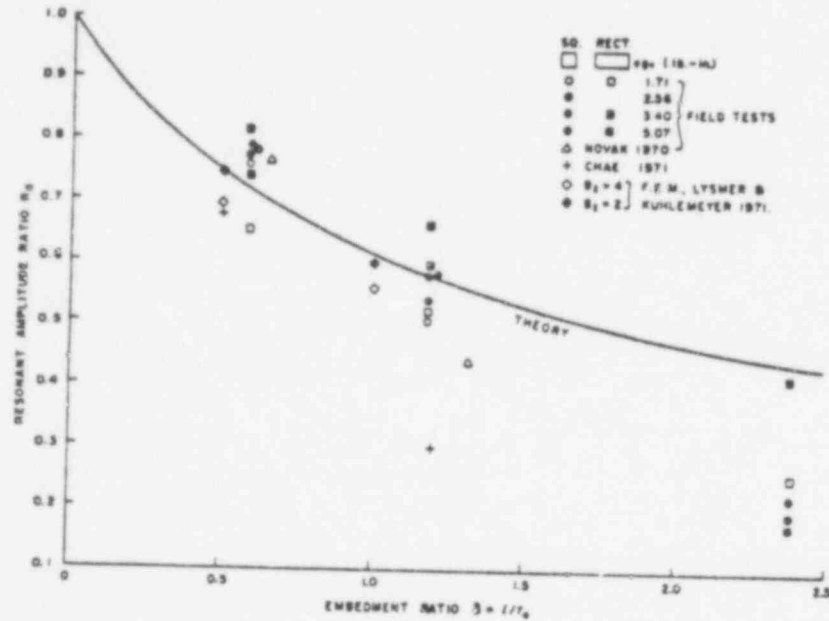


Fig. 12.—Comparison of Theoretical and Experimental Resonant Amplitude Ratio Variations with Embedment in Undisturbed Soil (Theoretical Curve Approximately Applies for all Mass Ratios)

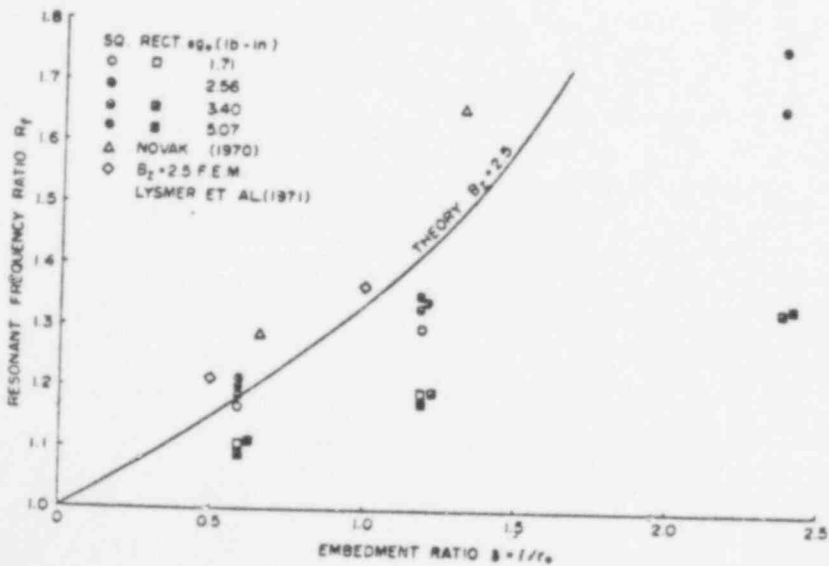


Fig. 13.—Comparison of Theoretical and Experimental Resonant Frequency Ratio Variations with Embedment in Undisturbed Soil

The comparison of the theory with the experimental results shows a significant nonlinearity which makes the nondimensional resonant frequency dependent upon the intensity of excitation. This nonlinearity can be analyzed using a procedure given in Ref. 14. The inevitable scatter in the comparison of experiment

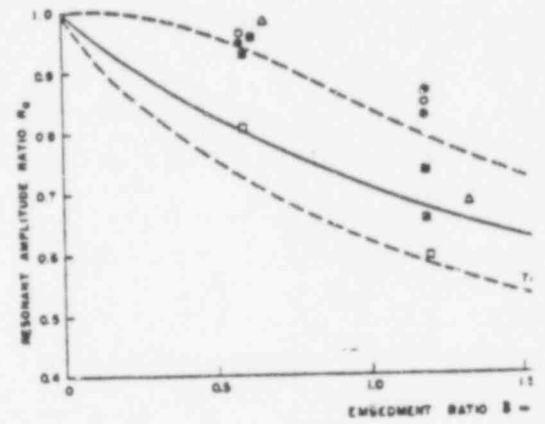


Fig. 14.—Comparison of Theoretical Resonant Amplitude Ratio of Footings Embedded in Back Fill Having Density Ratio $R = \rho_f / \rho_s$

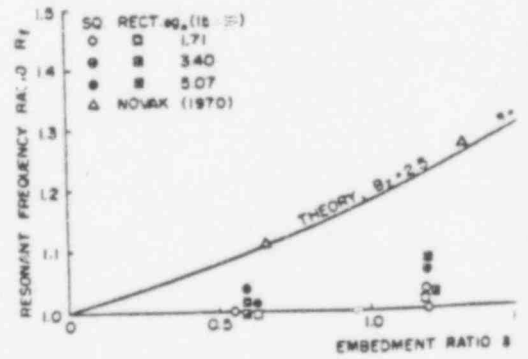
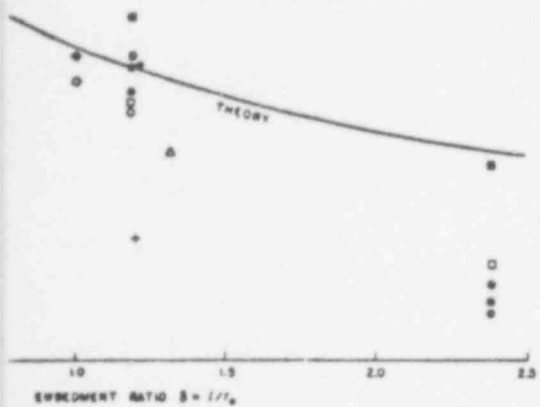


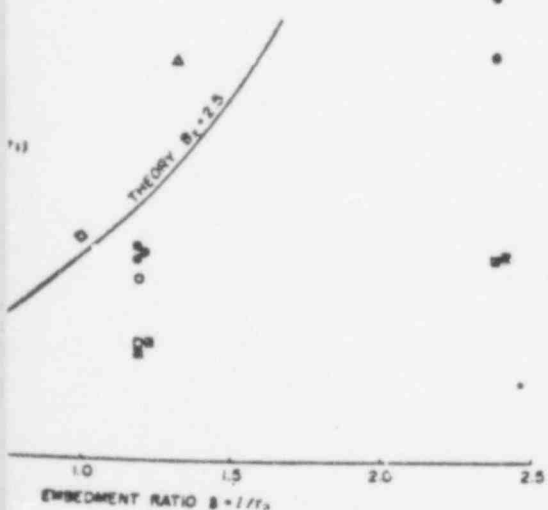
Fig. 15.—Comparison of Theoretical Resonant Frequency Ratio of Footing Embedded in Back Fill Having Density Ratio $R = \rho_f / \rho_s$

A second difficulty is due to the fact that the experimental results for the surface footing are consistently found to be greater than the theoretical values. [This was also noted in Ref. (14).] This difference may be caused by the presence of soil layer interfaces and fissures, variations in the soil properties at the base, and partly by the shape of the footing base. However, as far as the effect of embedment

SO. RECT. ρ_s (lb-in)
 □ 1.71
 ○ 2.56
 ● 3.40
 ■ 5.07 } FIELD TESTS
 △ NOVAK 1970
 + CHAE 1971
 ○ $B_1 = 4$ F.E.M. LYSMER &
 ● $B_2 = 2$ KUHLEMEYER 1971



Theoretical and Experimental Resonant Amplitude Ratio of Footings Embedded in Undisturbed Soil (Theoretical Curve Approximately $\eta = \rho_s/\rho = 0.765$)



Theoretical and Experimental Resonant Frequency Ratio of Footings Embedded in Undisturbed Soil

The comparison of the theory with the experiments is complicated due to nonlinearity which makes the nondimensional resonant amplitudes and frequencies dependent upon the intensity of excitation. (Nonlinear response curves can be analyzed using a procedure given in Ref. 15.) Nonlinearity causes an inevitable scatter in the comparison of experimental results with a linear theory.

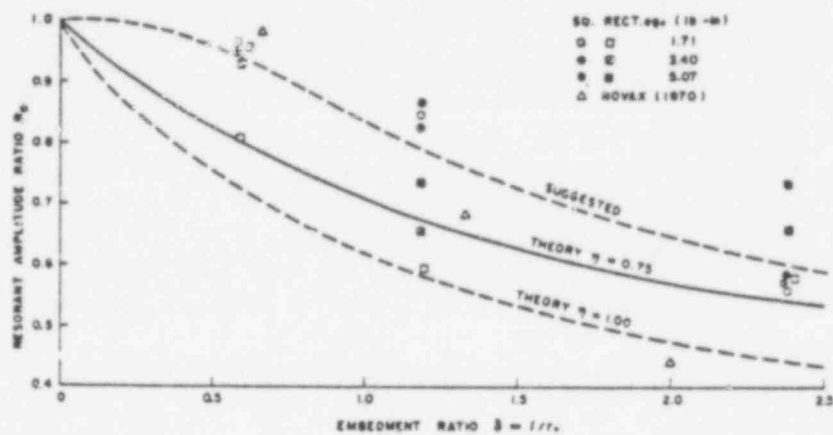


Fig. 14.—Comparison of Theoretical Resonant Amplitude Reduction with Field Tests of Footings Embedded in Back Fill Having Density Ratio $\eta = \rho_s/\rho = 0.765$

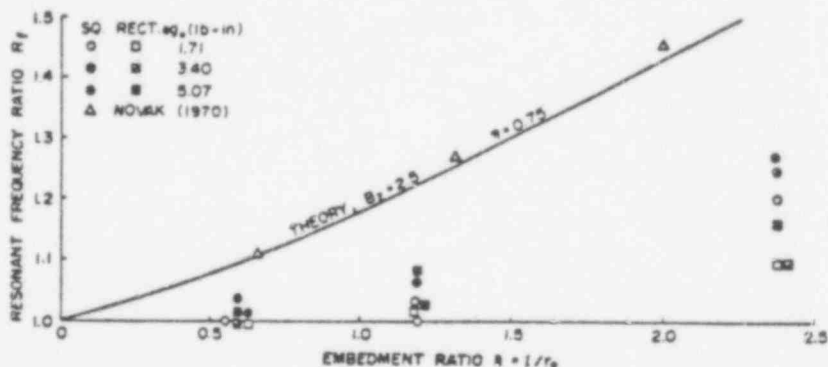


Fig. 15.—Comparison of Theoretical Resonant Frequency Ratio with Field Tests of Footings Embedded in Back Fill Having Density Ratio $\eta = \rho_s/\rho = 0.765$

A second difficulty is due to the fact that the measured resonant amplitudes of the surface footing are consistently found to be two times to three times greater than the theoretical values. [This was also found in previous experiments (14).] This difference may be caused by the reflection of elastic waves from layer interfaces and fissures, variations in the stress distribution in the footing base, and partly by the shape of the footing base.

However, as far as the effect of embedment is concerned, the differences

in absolute values of amplitudes can become less substantial if the relative variations are compared. These relative variations in resonant amplitudes and frequencies are plotted in Figs. 12 to 15.

In Fig. 12, the relative variations in resonant (maximum) amplitudes are shown versus relative embedment depth for undisturbed soil. Experiments with both square and rectangular bases are presented. Lysmer and Kuhlemeyer's results of their finite element solution are plotted also. They indicate a good agreement with the approximate analytical solution. The field experiments are also in good agreement with the theory except for the highest embedment at which most experiments exhibit greater amplitude reduction. Also, the strong effect of nonlinearity is visible. Usually greater strength of the upper cohesive soil layer may contribute to a greater amplitude reduction at full embedment. Chae's laboratory experiments feature a much stronger amplitude reduction than both theory and field tests, probably due to the conditions of laboratory tests.

In Fig. 13 resonant frequency ratio is plotted against embedment. In most experiments the frequency increase was considerably smaller than the theory predicts, particularly with the rectangular base. The reason for this may have been that the bond between the soil and the footing was not perfect, as the theory assumes.

Figs. 14 and 15 present an analogous comparison for a footing surrounded by a backfill. According to Fig. 14, the theory tends to overestimate the effect of embedment, especially for small embedments. This seems to indicate that there is a lack of bond between the footing and the backfill. Perfect force transmission is assumed in the theory, which can hardly be satisfied with shallow embedments where the horizontal soil pressure and the frictional bond are very low. These conclusions are further substantiated by Fig. 15. In this figure previous experiments (14) agree with the theory very well. The backfill (loess loam) was compacted very heavily and possibly a better bond between the fill and the footing was achieved. Because the bond depends also on the roughness of the footing sides, this seems to be a further factor affecting the quality of the force transmission between footing and the backfill.

From Figs. 14 and 15, the conclusion can be drawn that for backfill the effects of embedment upon both the resonant frequencies and amplitudes can be considerably reduced. This reduction depends on the soil used, i.e., on its compaction and roughness of the footing sides. Therefore, with footings cast into forms, an even smaller effect of embedment can be expected than that observed in the experiments described. The reduced effect of the backfill can be accounted for in the theory by considering $p_s < p$ and $G_s < G$.

SUMMARY AND CONCLUSIONS

The effect of embedment upon vertical forced vibration of a rigid footing was investigated both theoretically and experimentally in the field. The conclusions can be summarized as follows:

1. The approximate analytical solution compares favorably with the finite element solution and can easily be applied to the analysis of footings and structures supported by embedded foundations.

2. The real effect of embedment depends on the difference between undisturbed soil and backfill important in the case of a stratum.

3. The theory and experiments agree qualitatively in resonant amplitudes and an increase in resonant embedment depth and increasing density of the soil.

4. The experimental resonant amplitudes are in good agreement with theoretical values computed with a rigid base of two to three in the described case.

5. There is a reasonable agreement between the relative variations of the resonant amplitudes with the embedment in the case of the undisturbed soil. The increase in resonant frequencies is much smaller than the resonant amplitudes are in better agreement.

6. The resonant (maximum) amplitude reduction is smaller, while the corresponding frequency increase is larger.

ACKNOWLEDGMENT

This study was supported by a grant-in-aid from the Research Council of Canada to the senior author and a Commonwealth Scholarship by the Canadian Government to the writer.

APPENDIX I.—STIFFNESS AND DAMPING PARAMETERS

Stiffness and damping parameters presented in Eqs. 3, 6, and 7 by curve fitting to facilitate comparison are sufficient. Functions $f_{1,2}$ were taken from the reactions and from Warburton (Ref. 20) for comparison. (The sign convention of these functions in this paper.) Some of the parameters are also given for stratum reactions can be found in Refs. 10 and 11. They can be adjusted according to the frequency range.

APPENDIX II.—REFERENCES

1. Baranov, V. A., "On the Calculation of Excited Vibrations," (in Russian) *Voprosy Dynamiki i Prochnosti* of Riga, 1967, pp. 195-209.
2. Beredugo, Y. O., "Vibrations of Embedded Structures," Ph.D. thesis, University of Western Ontario, at London, 1967, for the requirements for the degree of Doctor of Philosophy.
3. Beredugo, Y. O. and Novak, M., "Coupled Horizontal Vibrations of Embedded Footings," *Canadian Geotechnical Journal*, Vol. 10, No. 1, 1973, pp. 1-12.
4. Bycroft, G. N., "Forced Vibrations of a Rigid Circle on a Half-Space and on an Elastic Stratum," *Philosophical Magazine*, Series A, Vol. 248, No. 948, 1956, pp. 3-12.
5. Chae, Y. S., "Dynamic Behavior of Embedded Foundations," *Research Record*, No. 323, 1971, pp. 49-50.

amplitudes can become less substantial if the relative
These relative variations in resonant amplitudes and
Figs. 12 to 15.

variations in resonant (maximum) amplitudes are shown
of depth for undisturbed soil. Experiments with both
cases are presented. Lysmer and Kuhlemeyer's results
ation are plotted also. They indicate a good agreement
physical solution. The field experiments are also in good
ry except for the highest embedment at which most
ster amplitude reduction. Also, the strong effect of
ually greater strength of the upper cohesive soil layer
ater amplitude reduction at full embedment. Chae's
ature a much stronger amplitude reduction than both
ably due to the conditions of laboratory tests.

frequency ratio is plotted against embedment. In most
y increase was considerably smaller than the theory
h the rectangular base. The reason for this may have
een the soil and the footing was not perfect, as the

at an analogous comparison for a footing surrounded
to Fig. 14, the theory tends to overestimate the effect
y for small embedments. This seems to indicate that
between the footing and the backfill. Perfect force
n the theory, which can hardly be satisfied with shallow
horizontal soil pressure and the frictional bond are very
e further substantiated by Fig. 15. In this figure previous
vi the theory very well. The backfill (loess loam)
ily and possibly a better bond between the fill and
f. Because the bond depends also on the roughness
s seems to be a further factor affecting the quality
between footing and the backfill.

the conclusion can be drawn that for backfill the
on both the resonant frequencies and amplitudes can
This reduction depends on the soil used, i.e., on its
s of the footing sides. Therefore, with footings cast
lter effect of embedment can be expected than that
nts described. The reduced effect of the backfill can
eory by considering $\rho_s < \rho$ and $G_s < G$.

DISCUSSION

ent upon vertical forced vibration of a rigid footing
oretically and experimentally in the field. The conclu-
as follows:

ysical solution compares favorably with the finite
ily be applied to the analysis of footings and structures
undations.

2. The real effect of embedment depends on embedment depth, with a marked
difference between undisturbed soil and backfill, and becomes particularly
important in the case of a stratum.

3. The theory and experiments agree qualitatively that there is a decrease
in resonant amplitudes and an increase in resonant frequencies with increasing
embedment depth and increasing density of the backfill.

4. The experimental resonant amplitudes are consistently higher than the
theoretical values computed with a rigid base stress distribution by a factor
of two to three in the described case.

5. There is a reasonable agreement between the theoretical and experimental
relative variations of the resonant amplitudes and of the resonant frequencies
with the embedment in the case of the undisturbed soil. With the backfill the
increase in resonant frequencies is much smaller than predicted. The variations
of resonant amplitudes are in better agreement.

6. The resonant (maximum) amplitude reduction is essentially independent
of the mass, while the corresponding frequency ratio is mass dependent.

ACKNOWLEDGMENT

This study was supported by a grant-in-aid of research from the National
Research Council of Canada to the senior writer and by the award of a
Commonwealth Scholarship by the Canadian Federal Government to the junior
writer.

APPENDIX I.—STIFFNESS AND DAMPING PARAMETERS

Stiffness and damping parameters presented in Tables 1 and 2 were obtained
from Eqs. 3, 6, and 7 by curve fitting to facilitate the calculations. Their accuracy
is sufficient. Functions $f_{1,2}$ were taken from Bycroft (Ref. 4) for half-space
reactions and from Warburton (Ref. 20) for stratum reactions by mechanical
reproduction. (The sign convention of these writers have been maintained in
this paper.) Some of the parameters are also plotted in Fig. 2. More data on
stratum reactions can be found in Refs. 10 and 11. The constant parameters
can be adjusted according to the frequency range of interest.

APPENDIX II.—REFERENCES

1. Baranov, V. A., "On the Calculation of Excited Vibrations of an Embedded Founda-
tion," (in Russian) *Voprosy Dynamiki i Prochnosti*, No. 14, Polytechnical Institute
of Riga, 1967, pp. 195-209.
2. Beredugo, Y. O., "Vibrations of Embedded Symmetric Footings," thesis presented
to the University of Western Ontario, at London, Canada, in 1971, in partial fulfillment
of the requirements for the degree of Doctor of Philosophy.
3. Beredugo, Y. O. and Novak, M., "Coupled Horizontal and Rocking Vibration of
Embedded Footings," *Canadian Geotechnical Journal*, Nov., 1972.
4. Bycroft, G. N., "Forced Vibrations of a Rigid Circular Plate on a Semi-infinite Elastic
Half-Space and on an Elastic Stratum," *Philosophical Transactions of the Royal Society*,
London, Series A, Vol. 248, No. 948, 1956, pp. 327-268.
5. Chae, Y. S., "Dynamic Behavior of Embedded Foundation—Soil Systems," *Highway
Research Record*, No. 323, 1971, pp. 49-59.

6. Elorduy, J., Nieto, J. A., and Szekely, E. M., "Dynamic Response of Bases of Arbitrary Shape Subjected to Periodic Vertical Loading," *Properties of Earth Materials*, Albuquerque, N.M., Aug., 1967.
7. Fry, Z. B., "Development and Evaluation of Soil Bearing Capacity, Foundation of Structures," *WES Tech. Report No. 3-632, Report 1*, 1963.
8. Gupta, B. N., "Effect of Foundation Embedment on the Dynamic Behaviour of the Foundation-Soil System," *Geotechnique* 22, London, England, No. 1, Mar., 1972, pp. 129-137.
9. Kaldjian, M. J., discussion of "Design Procedures for Dynamically Loaded Foundations," by R. V. Whitman and F. E. Richard, Jr., *Journal of Soil Mechanics and Foundations Division, ASCE*, Vol. 95, No. SM1, Proc. Paper 6324, Jan. 1969, pp. 364-366.
10. Kobori, T., and Suzuki, T., "Foundation Vibrations on a Visco-elastic Multi-layered Medium," *Proceedings, Third Japan Earthquake Engineering Symposium—1970*, Tokyo, Japan, Nov., 1970, pp. 493-499.
11. Kobori, T., Minai, R., and Suzuki, T., "The Dynamical Ground Compliance of a Rectangular Foundation on a Viscoelastic Stratum," *Bulletin of the Disaster Prevention Research Institute, Kyoto Univ.*, Vol. 20, Mar., 1971, pp. 289-329.
12. Luco, Y. E., and Westmann, R. A., "Dynamic Response of Circular Footings," *Journal of the Engineering Mechanics Division, ASCE*, Vol. 97, No. EM5, Proc. Paper 8416, Oct., 1971, pp. 1381-1395.
13. Lysmer, J., and Kuhlemeyer, R. L., "Finite Dynamic Model for Infinite Media," *Journal of the Engineering Mechanics Division, ASCE*, Vol. 95, No. EM4, Proc. Paper 6719, Aug. 1969, pp. 859-877; Closure, Vol. 97, No. EM1, Proc. Paper 7862, Feb., 1971, pp. 129-131.
14. Novak, M., "Prediction of Footing Vibrations," *Journal of the Soil Mechanics and Foundations Division, ASCE*, Vol. 96, No. SM3, Proc. Paper 7268, May, 1970, pp. 836-861.
15. Novak, M., "Data Reduction from Nonlinear Response Curves," *Journal of the Engineering Mechanics Division, ASCE*, Vol. 97, No. EM1, Proc. Paper 8300, August, 1971, pp. 1187-1204.
16. Novak, M., and Beredugo, Y. O., "Effect of Embedment on Footing Vibration," *Proceedings of 1st Canadian Conference on Earthquake Engineering*, Univ. of British Columbia, Vancouver, Canada, May, 1971, pp. 111-125.
17. Richart, F. E., Hall, J. R., and Woods, R. D., *Vibrations of Soils and Foundations*, Prentice-Hall, Inc., Englewood Cliffs, N. J., 1970.
18. Sung, T. Y., "Vibrations in Semi-Infinite Solids due to Periodic Surface Loading," *American Society for Testing and Materials Special Technical Publication No. 156*, Symposium on Dynamic Testing of Soils, 1953, pp. 35-64.
19. Thomson, W. T., and Kobori, T., "Dynamical Compliance of Rectangular Foundations on an Elastic Half Space," *Journal of Applied Mechanics, Transactions, American Society of Mechanical Engineers*, Dec., 1963, pp. 579-584.
20. Warburton, G. B., "Forced Vibration of a Body on an Elastic Stratum," *Journal of Applied Mechanics*, Mar., 1957, pp. 55-58.

APPENDIX III.—NOTATION

The following symbols are used in this paper:

- $A = w_0 m / (m_e e)$ = nondimensional displacement amplitude;
 A_m = nondimensional resonant (maximum) amplitude of displacement of embedded footing;
 a_m = nondimensional frequency at resonant (maximum) amplitude of embedded footing;
 $a_0 = r_0 \omega \sqrt{\rho / G}$ = nondimensional frequency;
 $B_1 = 1 - \nu / 4 b_0$ = Lysmer's modified mass ratio;

- $b_0 = m / \rho r_0^3$ = dimensionless mass ratio;
 C_1 = half-space (stratum) stiffness;
 \bar{C}_1 = frequency independent half meter;
 C_2 = half-space (stratum) damping;
 \bar{C}_2 = constant related to C_2 ;
 c = damping constant for embed
 D = damping ratio;
 e = eccentricity of unbalanced rot
 f_1, f_2 = components of Reissner's di
vibration;
 G = shear modulus of soil beneath
 G_s = shear modulus of backfill (si
 δ_0 = weight of unbalanced rotatin
 H = total thickness of stratum;
 h = thickness of stratum under fo
 $i = \sqrt{-1}$ = imaginary unit;
 k = stiffness (spring) constant fo
 $k(\delta)$ = stiffness with embedment δ ;
 l = depth of embedment of footi
 m = mass of footing;
 m_e = unbalanced rotating mass;
 $N_z(t)$ = vertical dynamic reaction alo
 $\dot{P}(t)$ = excitation force;
 P_0 = excitation force amplitude;
 R_a = resonant (maximum) amplitu
with embedment δ /resonant
 R_f = resonant frequency ratio = r
ment δ /resonant frequency c
 $R_z(t)$ = vertical dynamic reaction at
 r_0 = radius of cylindrical footing;
or rectangular footing (see R
 S_1, S_2 = frequency dependent stiffnes
to embedment;
 \bar{S}_1 = frequency independent (cons
embedment;
 \bar{S}_2 = constant related to S_2 ;
 $s(t)$ = vertical side dynamic reactio
 t = time;
 $w(t)$ = vertical displacement of rigid
 w = complex amplitude of vertica
 w_m = real resonant (maximum) am;
 w_0 = real amplitude of vibration;
 z = vertical coordinate;
 $\Delta = H / r_0$ = relative thickness of stratum;
 $\delta = l / r_0$ = embedment ratio;
 $\eta = \rho_s / \rho$ = density ratio;
 ν = Poisson's ratio;

and Szekely, E. M., "Dynamic Response of Bases of Periodic Vertical Loading," *Properties of Earth Materials*, 1963.

and Evaluation of Soil Bearing Capacity, Foundation of Report No. 3-632, Report I, 1963.

Foundation Embedment on the Dynamic Behaviour of Soil," *Geotechnique* 22, London, England, No. 1, Mar., 1972.

of "Design Procedures for Dynamically Loaded Foundations and F. E. Richard, Jr., *Journal of Soil Mechanics and Foundations*, Vol. 95, No. SM1, Proc. Paper 6324, Jan., 1969, pp. 6324-6330.

"Foundation Vibrations on a Visco-elastic Multi-layered Soil," *Third Japan Earthquake Engineering Symposium—1970*, pp. 493-499.

and Suzuki, T., "The Dynamical Ground Compliance of a Viscoelastic Stratum," *Bulletin of the Disaster Prevention Research Institute*, Vol. 20, Mar., 1971, pp. 289-329.

and R. A., "Dynamic Response of Circular Footings," *Journal of Mechanical Division, ASCE*, Vol. 97, No. EM5, Proc. Paper 1381-1395.

and R. L., "Finite Dynamic Model for Infinite Media," *Journal of Mechanical Division, ASCE*, Vol. 95, No. EM4, Proc. Paper 859-877; Closure, Vol. 97, No. EM1, Proc. Paper 7862.

of Footing Vibrations," *Journal of the Soil Mechanics and Foundations*, Vol. 96, No. SM3, Proc. Paper 7268, May, 1970, pp. 7268-7274.

from Nonlinear Response Curves," *Journal of the Mechanical Division, ASCE*, Vol. 97, No. EM1, Proc. Paper 8300, August, 1970.

and Y. O., "Effect of Embedment on Footing Vibration," *Canadian Conference on Earthquake Engineering*, Univ. of British Columbia, May, 1971, pp. 111-125.

R., and Woods, R. D., *Vibrations of Soils and Foundations*, McGraw-Hill, New York, N. J., 1970.

in Semi-Infinite Solids due to Periodic Surface Loading," *Testing and Materials Special Technical Publication No. 156*, American Institute of Steel Construction, Inc., Chicago, Ill., 1953, pp. 35-64.

and Mori, T., "Dynamical Compliance of Rectangular Foundations," *Journal of Applied Mechanics, Transactions, American Society of Mechanical Engineers*, Dec., 1963, pp. 579-584.

of Free Vibration of a Body on an Elastic Stratum," *Journal of Applied Mechanics*, 1957, pp. 55-58.

NOTATION

are used in this paper:

dimensional displacement amplitude;
 dimensional resonant (maximum) amplitude of displacement of embedded footing;
 dimensional frequency at resonant (maximum) amplitude of embedded footing;
 dimensional frequency;
 dimensionless modified mass ratio;

$b_0 = m/\rho r_0^3$ = dimensionless mass ratio;
 C_1 = half-space (stratum) stiffness parameter;
 \bar{C}_1 = frequency independent half-space (stratum) stiffness parameter;
 C_2 = half-space (stratum) damping parameter;
 \bar{C}_2 = constant related to C_2 ;
 c = damping constant for embedded footing;
 D = damping ratio;
 e = eccentricity of unbalanced rotating masses;
 f_1, f_2 = components of Reissner's displacement function for vertical vibration;
 G = shear modulus of soil beneath footing;
 G_s = shear modulus of backfill (side layer);
 g_0 = weight of unbalanced rotating mass m_s ;
 H = total thickness of stratum;
 h = thickness of stratum under footing base;
 $i = \sqrt{-1}$ = imaginary unit;
 k = stiffness (spring) constant for embedded footing;
 $k(\delta)$ = stiffness with embedment δ ;
 l = depth of embedment of footing;
 m = mass of footing;
 m_s = unbalanced rotating mass;
 $N_z(t)$ = vertical dynamic reaction along embedded footing sides;
 $\dot{P}(t)$ = excitation force;
 P_0 = excitation force amplitude;
 R_s = resonant (maximum) amplitude ratio = resonant amplitude with embedment δ /resonant amplitude of surface footing;
 R_f = resonant frequency ratio = resonant frequency with embedment δ /resonant frequency of surface footing;
 $R_z(t)$ = vertical dynamic reaction at base of footing;
 r_0 = radius of cylindrical footing; also equivalent radius of square or rectangular footing (see Ref. 17, p. 347);
 S_1, S_2 = frequency dependent stiffness and damping parameters due to embedment;
 \bar{S}_1 = frequency independent (constant) stiffness parameter due to embedment;
 \bar{S}_2 = constant related to S_2 ;
 $s(t)$ = vertical side dynamic reaction per unit depth of embedment;
 t = time;
 $w(t)$ = vertical displacement of rigid footing at time t ;
 w = complex amplitude of vertical displacement;
 w_m = real resonant (maximum) amplitude;
 w_0 = real amplitude of vibration;
 z = vertical coordinate;
 $\Delta = H/r_0$ = relative thickness of stratum;
 $\delta = l/r_0$ = embedment ratio;
 $\eta = \rho_s/\rho$ = density ratio;
 ν = Poisson's ratio;

- ρ = mass density of elastic half-space (soil);
 ρ_s = mass density of side layer (backfill);
 ϕ = phase angle;
 ω = circular frequency of excitation;
 ω_n = resonant circular frequency (at maximum amplitudes); and
 ω_0 = natural circular frequency.

JOURNAL SOIL MECHANICS FOUNDATION

Bearing Capacity Theory from Experiments

By A. Verghese Chummar

INTRODUCTION

The plastic equilibrium theories on bearing capacity on failure surfaces either assumed or derived from the failure surfaces observed in the experiments on soils by Selig and McKee (10), Verghese (12) and the shape of the failure surfaces adopted in the theories given in Fig. 1 between some of the observed and theoretical failure surfaces reveals a marked discrepancy. The existing theories on bearing capacity fairly accurately until it was established that for long footings, the plane strain conditions prevail and the value of ϕ under plane strain is about 1.1 times the value of ϕ in the soil. Fig. 2 gives the experimental values of the bearing capacity against plane-strain values of ϕ and the N_c values given by the existing theories. The comparison clearly indicates that the existing theories do not accurately determine the bearing capacity of long footings. It is herein to determine the actual shape of the failure surface and to develop a bearing capacity theory based on that surface. In the present study, the data, the present study is restricted to the case of cohesionless soils.

FAILURE SURFACE

The shape of the failure surface is determined from the failure surfaces observed by different research workers by deducing a pattern from the observed ones.

Note.—Discussion open until May 1, 1973. To extend the closing date one month, a written request must be filed with the Editor of the Journal. This paper is part of the copyrighted Journal of the Soil Mechanics and Foundations Division, Proceedings of the American Society of Civil Engineers, Vol. 99, No. 12, December, 1972. Manuscript was submitted for review for possible publication on August 1, 1972. Lect., Dept. of Civ. Engrg., Indian Inst. of Tech., Kanpur.

J. P. Lee
BROWN & ROOT

K 2/6

DYNAMIC ANALYSIS OF EMBEDDED STRUCTURES

E. KAUSEL

*Stone & Webster Engineering Corporation,
P.O. Box 2325, Boston, Massachusetts 02107, U.S.A.*

R. V. WHITMAN

*Department of Civil Engineering, Massachusetts Institute of Technology,
Cambridge, Massachusetts 02139, U.S.A.*

F. ELSABEE

Stone & Webster Engineering Corporation, Cherry Hill, New Jersey, U.S.A.

J. P. MORRAY

EDS Nuclear Inc., 220 Montgomery Street, San Francisco, California 94104, U.S.A.

SUMMARY

The paper presents simplified rules to account for embedment and soil layering in the soil-structure interaction problem, to be used in dynamic analyses. The relationship between the spring method, and a direct solution (in which both soil and structure are modeled with finite elements and linear members) is first presented. It is shown that for consistency of the results with the two solution methods the spring method should be performed in the following three steps:

1. Determination of the motion of the massless foundation (having the same shape as the actual one) when subjected to the same input motion as the direct solution. For an embedded foundation it will yield, in general, both translations and rotations.
2. Determination of the frequency dependent subgrade stiffness for the relevant degrees of freedom. This step yields the so-called "soil springs".
3. Computations of the response of the real structure supported on frequency dependent soil springs and subjected at the base of these springs to the motion computed in step 1.

The first two steps require, in general, finite element methods, which would make the procedure not attractive. It is shown in the paper, however, that excellent approximations can be obtained, on the basis of 1-dimensional wave propagation theory for the solution of step 1, and correction factors modifying for embedment the corresponding springs of a surface footing on a layered stratum, for the solution of step 2. Use of these rules not only provides remarkable agreement with the results obtained from a full finite element analysis, but results in substantial savings of computer execution and storage requirements. This frees the engineer to perform extensive studies, varying the input properties over a wide range to account for uncertainties, in particular with respect to the soil properties.

SMIRT Conference

San Francisco August 1977

649 260

1. Introduction

Significant efforts have been directed in recent years to formulate engineering solutions to the problems of vibration of foundations and seismic response of buildings. The problem is of special interest in the seismic analysis and design of massive buildings such as nuclear containment structures.

Building foundations, and nuclear reactors in particular, are usually buried to some extent beneath the surface of the ground. This embedment has in many cases considerable effect on the dynamic response of the structure, both in terms of relative frequency contents and amplitude of the resulting motions. Because of the complicated boundary conditions that must be satisfied in a theoretical formulation, rigorous analytical solutions for embedded foundations are nonexistent at present. Hence, numerical (finite element), experimental and approximate analytical techniques are currently being used to provide a solution to the problem at hand for these complicated geometries. An awareness of the effects associated with embedment, coupled with the availability of numerical solutions and the lack of rigorous solutions, has been the basis in recent times for discrediting the spring method as a tool for analyses, particularly in the nuclear power industry. The detracting of the spring method has been argued by some researchers on the basis of comparisons between the classical half space method, and more involved finite element solutions. Many of these comparisons are not meaningful, since they were based on inappropriate values for both the "spring constant" and the "support motion." In fact, the spring method and finite element solutions can be shown to be mathematically equivalent; if they are classified as different, it is because of inconsistencies in their implementation.

It is the purpose of this paper to show the relationship between a more general spring method, and the solutions provided by direct finite element procedures, and to present practical rules for use in dynamic analysis.

2. The basic superposition theorem

Referring to Fig. 1, assume that the general equations of motion of a structure-foundation system are given by the matrix equation

$$M\ddot{U} + C\dot{Y} + KY = 0 \tag{1}$$

where M, C, K, are the system mass, damping and stiffness matrices; U and Y are the absolute and relative displacements with respect to some general ground reference system. The solution of this equation is equivalent to the solution of the two matrix equations

$$M_1 \ddot{U}_1 + C\dot{Y}_1 + KY_1 = 0 \tag{2}$$

$$M \ddot{Y}_2 + C\dot{Y}_2 + KY_2 = -M_2 \ddot{U}_1 \tag{3}$$

where $U_1 = Y_1 + U_g$, $U = U_1 + Y_2$, and $M = M_1 + M_2$. M_1 excludes the mass of the structure, while M_2 excludes the mass of the soil. U_g is some generalized ground motion vector. The equivalence of 2) with 1) is demonstrated by simple addition. In Eq. 2, the response of the massless structure is found first, and will be referred to as the kinematic interaction. The results of this step are then used in Eq. 3) which shall define the inertial interaction, and which is solved by application of fictitious inertia forces applied to the structure alone.

In the solution of the second step, it is irrelevant whether the soil is modeled with finite elements, or equivalently, with a (far-coupled) matrix of stiffness functions modelling the subgrade, and defined at the soil-structure interface. These stiffness functions can be

regarded as
(a frequency

For the
becomes legiti
cious, rock
dashpots." I
linearly depe
the foundatio
pletely defic
rigid body.
foundation, a

Also, a
as a vector o
tions and roc

Provided
break the sol

1. deter
- same
- embed
2. deter
- degre
3. compu
- soil

Notice th
of the structu
should be iden
consistent def

The super
damping of the
occurs as a re
Thus, the soil
the structure
account for the

The first
that the 3-step
interaction tes
the basis of or
tion factors m
layered stratur
agreement with
substantial sav
to perform exte
uncertainties.

regarded as resulting from a dynamic condensation of all the degrees of freedom in the soil (a frequency domain solution is implied).

For the particular situation where the combination foundation-structure is very rigid, it becomes legitimate to replace the matrix of stiffness functions by the overall vertical, torsional, rocking and swaying stiffness functions, i.e., by frequency dependent "springs" and dashpots." For this case, the nodal displacements at the foundation-soil interface are linearly dependent and, at most, six degrees of freedom are needed to describe the motion of the foundation. It also follows that the solution of the kinematic interaction phase is completely defined by the rotations and translations of the massless structure, which moves as a rigid body. Hence, one can replace the massless structure in Eq. 2) by a rigid massless foundation, subjected to the same ground excitation as the original system.

Also, a more careful examination of Eq. 3 will show that the solution Υ_2 can be regarded as a vector of displacements relative to a fictitious support, while the rigid body translations and rotations of the massless foundation in Eq. 2 are the equivalent support motion.

Provided that the assumption of rigid foundation is pertinent, it is, therefore, valid to break the solution into three steps: (also see Fig. 2)

1. determination of the motion of the massless rigid foundation, when subjected to the same input motion as the total solution. This is the solution of Eq. 2). For an embedded foundation, it will yield, in general, both translations and rotations.
2. determination of the frequency dependent subgrade stiffnesses for the relevant degrees of freedom. This step yields the so-called soil "springs."
3. computation of the response of the real structure supported on frequency dependent soil springs, and subjected at the base of these springs to the motion computed in a).

Notice that the only approximation involved in this approach concerns the deformability of the structural foundation. If this foundation were rigid, the solution of this procedure should be identical to that of the direct (or one-pass) approach (assuming, of course, consistent definitions of the motion and the same numerical procedures).

The superposition principle is valid only for a linear system. While the modulus and damping of the soil are strain-dependent, studies (6) have shown that most of the nonlinearity occurs as a result of the earthquake motion, and not as a result of soil-structure interaction. Thus, the soil properties consistent with the levels of strain in the free field (i.e., before the structure has been built) may be used in steps 1 and 2 without further modification to account for the additional strains imposed by the structure.

The first two steps require, in general, finite element methods, and thus it might appear that the 3-step method has no advantage as compared to considering both kinematic and inertial interaction together in a single step. However, reasonable approximations can be obtained on the basis of one-dimensional wave propagation theory for the solution of step 1, and correction factors modifying for embedment the corresponding springs of a surface footing on a layered stratum for the solution of step 2. Use of these rules not only provides remarkable agreement with the results obtained from a full finite element analysis, but results in substantial savings of computer execution and storage requirements. This frees the engineer to perform extensive studies, varying the input properties over a wide range to account for uncertainties, in particular with respect to the soil properties. Also, deviations from axial

symmetry may be introduced into the model of the structure in step 3 (which means that a torsional "spring" and "dashpot" must be evaluated in step 2) and the effect of changes in the mass and stiffness of the structure be evaluated without having to rerun an entire analysis.

3. Approximate Solution for Circular, Embedded Foundations

The solutions presented in the following sections have been obtained with a three-dimensional axisymmetric finite element formulation. A fundamental feature of the program used is the exact representation of the model boundary which separates the finite element region from the semi-infinite continuum (the free field). This consistent energy transmitting boundary was developed for the plane strain case by Waas and Lysmer (11), (7), and was extended to the three-dimensional case by the first author (2), (3), (5). In essence, it can be regarded as a virtual extension of the finite element mesh to infinity, and can be placed without loss of accuracy immediately next to the foundation.

In the following section, it will be assumed that the motion which the ground experiences before any structure (or hypothetical massless foundation) has been built, can be described by means of one-dimensional wave propagation theory. The control motion, i.e., the specified earthquake record, will be assumed to take place at the free surface in the "free field." Motions at other points in the free field can be obtained by the so-called "deconvolution" process, which makes use of one-dimensional wave propagation theory.

3.1 Approximations to the Kinematic Interaction

The third author investigated the kinematic interaction problem in a parametric study (8), using a wide range of embedment ratios E/R and stratum ratios R/R, covering a range of values typically found in nuclear reactor design, and proposed rules to approximate the kinematic interaction.

Referring to Fig. 3, a unit harmonic displacement was specified at the free surface, and deconvolved to bedrock. Using the finite element program, frequency dependent transfer functions u_B and ϕ_B for the displacement and rotation of the massless foundation, relative to the motion at the free surface, were determined. Similarly, the frequency dependent transfer functions for the displacement in the free field at the elevation of the foundation, and for the pseudorotation of the free field

$$\phi_B(\Omega) = \frac{u_A - u_B}{R} \approx \frac{1 - u_B}{E}$$

were computed. Typical results are found in Fig. 4. The transfer functions u and u_B , ϕ and ϕ_B were then compared for a range of embedment and stratum depth values, and rules to approximate these functions were suggested (8). A simplified version of these rules is given below.

Let $F(\Omega)$ be the Fourier transform of the acceleration at the free surface in the free field (in most cases, the design earthquake). The translation and rotation of the massless, rigid foundation are then given approximately by

$$u = \text{IFT} \begin{cases} F(\Omega) \cdot \left[\cos\left(\frac{\pi}{2}\right) \cdot \frac{f}{f_n} \right] & \text{if } f < 0.7 f_n \\ F(\Omega) \cdot [0.453] & \text{if } f > 0.7 f_n \end{cases}$$

$$\delta = \text{IFT} \begin{cases} F(\Omega) \cdot [0.257 (1 - \cos \frac{\pi}{2} \cdot f/f_n)/R] & \text{if } f \leq f_n \\ F(\Omega) \cdot [0.257/R] & \text{if } f > f_n \end{cases}$$

(δ is positive clockwise)

where IFT stands for Inverse Fourier Transformation; f_n is the fundamental shear beam frequency of the embedment region (for uniform soil properties in the embedment region, this value is given by $f_n = C_s/4E$ with C_s being the shear wave velocity, and E the depth of embedment. The expression in square brackets describes an approximation to the transfer functions for the translation and rotation of the massless foundation. For surface footings, $E = 0$, $f_n = \infty$, $\cos 0 = 1$; it follows that no kinematic interaction takes place for this case.

The procedure described yields satisfactory results for a wide range of embedment ratios, see for instance Fig. 5. It should be noted, however, that the rotational component is sensitive to the lateral soil conditions, and particularly to the flexibility of the lateral walls. For flexible sidewalls, the actual rotation is significantly smaller, and in the extreme case of no sidewalls, the rotation even changes sign! Nevertheless, the contribution of the rotational component to the response of the structure is in most cases not very significant. For nuclear containment structures, the effect of the rotational component on the structural response is of the order of 15-20 percent.

3.2 Approximations for the Stiffness Functions

As with the kinematic interaction, the values of the subgrade stiffness functions (impedance functions) depend only on the geometric configuration of the foundation and on the properties of the founding soil. These functions can be evaluated using analytical, experimental, or numerical methods.

The results presented in this paper are based on parametric studies performed by the fourth writer to determine approximate expressions for stiffness functions of circular, embedded foundations (1). For each particular geometry, the static values were evaluated with two or three meshes (a fine, a standard, and a coarse mesh), and the results were corrected for mesh size error in a manner similar to that described in Ref. 4. The study was limited to the coupled horizontal translation and rotation (rocking-swaying) of the rigid, circular, embedded foundation in a homogenous stratum. For this particular case, the force displacement relationship can be written

$$\begin{Bmatrix} F \\ M \end{Bmatrix} = \begin{Bmatrix} K_{xx} & K_{x\phi} \\ K_{\phi x} & K_{\phi\phi} \end{Bmatrix} \begin{Bmatrix} u \\ \phi \end{Bmatrix}$$

where F = the horizontal force; M = the rocking moment; and u , ϕ , are the corresponding displacements (rotations). The elements K_{xx} , $K_{x\phi}$, $K_{\phi\phi}$ of the stiffness matrix depend on the frequency of excitation Ω of the forces (moments). Since these forces and the resulting displacements are generally not in phase with each other, these elements are complex functions of frequency. Each stiffness function is of the form $K^0 (1 + 2i\beta) (k + ia_0c)$, where K^0 is the static stiffness, β a measure of the internal damping in the soil (of a hysteretic nature), $i = \sqrt{-1}$, and a_0 is the dimensionless frequency $\Omega R/C_s$. (Ω is the circular frequency of the motion and excitation, R the radius of the foundation slab, and C_s a reference shear wave velocity.)

k and c are frequency dependent coefficients normalized with respect to the static stiffness. The coefficient c is related to the energy loss by radiation.

Using the program described earlier, the dynamic stiffness functions were computed for a range of embedment and stratum depth ratios, and written as described above as:

$$K_{xx} = K_{xx}^0 (k_{11} + ia_0 \cdot c_{11}) (1 + 2i\delta)$$

$$K_{x\phi} = K_{x\phi}^0 (k_{12} + ia_0 \cdot c_{12}) (1 + 2i\delta)$$

$$K_{\phi\phi} = K_{\phi\phi}^0 (k_{22} + ia_0 \cdot c_{22}) (1 + 2i\delta)$$

Analysis of the results obtained provided then the following approximations to the static values K_{xx}^0 , $K_{x\phi}^0$, $K_{\phi\phi}^0$, and to the dynamic stiffness coefficients k_{11} , k_{12} , c_{11} , c_{12} , c_{22} :

Static Values:

$$K_{xx}^0 = \frac{8GR}{2-\nu} \left(1 + \frac{1}{2} \frac{R}{H}\right) \left(1 + \frac{2}{3} \frac{R}{H}\right) \left(1 + \frac{3}{4} \frac{R}{H}\right)$$

$$K_{x\phi}^0 = K_{xx}^0 \left(\frac{2}{3} \frac{R}{H} - 0.03\right) \quad (\phi \text{ is positive clockwise})$$

$$K_{\phi\phi}^0 = \frac{8GR^3}{3(1-\nu)} \left(1 + \frac{1}{6} \frac{R}{H}\right) \left(1 + \frac{2}{3} \frac{R}{H}\right) \left(1 + 0.71 \frac{R}{H}\right)$$

In these formulas, G = the shear modulus of soil underneath the mat; R = the radius of the foundation, E = the depth of embedment, H = the depth to bedrock, and ν = Poisson's ratio.

Dynamic Stiffness Coefficients:

k_{11} , k_{22} half space solution (i.e., Ref. 10)

$$c_{11} = \begin{cases} 0.88 \frac{a_0}{a_{01}} & \text{for } a_0 < \frac{1}{2} \frac{R}{H} = a_{01} \\ \text{Half space solution for } a_0 > a_{01} \end{cases}$$

$$c_{22} = \begin{cases} 0.58 \frac{a_0}{a_{02}} & \text{for } a_0 < \frac{1}{2} \frac{R}{H} \frac{C_p}{C_s} = a_{02} \\ \text{Half space solution for } a_0 > a_{02} \end{cases}$$

$$k_{12} = k_{11}, \quad c_{12} = c_{11}$$

where δ is the internal (hysteretic) damping in the soil; C_p and C_s are the dilatational wave velocities in the subgrade; a_{01} and a_{02} are the (nondimensional) fundamental shear beam and dilatation frequencies of the stratum, as defined above.

Except for the stiffness coefficient k_{11} , which displays a somewhat wavy nature, the suggested approximation for the stiffness and damping coefficients provide reasonable substitutes for the true functions. It can be observed that the radiation damping coefficients c_1 , c_2 are larger for the embedded case than for the surface footing; therefore, the suggested procedure should give conservative results for an embedded structure.

4. Soil-Structure

Once the in simple dynamic terms can be added frequency domain simpler physical stiffness and damping modes.

A number of the static stiffness that the increased lateral soil, which properties and its selection of the conditions within the analysis is clear.

The spring used for the lines and the accuracy possibility in this meets these requirements coupling between practical standpoint specified by a brief. If the direct approximations with depth rotating waves) may be conditions, it may vicinity of the structure.

spect to the static stiffness.

functions were computed for a
described above as:

(8)

(8)

(8)

approximations to the static
terms k_{11} , k_{12} , c_{11} , c_{12} , c_{22}

$$\frac{5}{4} \frac{E}{H}$$

a positive clockwise)

$$1 + 0.71 \frac{E}{H}$$

α mat; R = the radius of the
ck, and ν = Poisson's ratio.

Ref. 10)

α_{o1}

α_2

α_{o2}

and C_p are the dilatational wave
1) fundamental shear beam end

a somewhat wavy nature, the
ents provide reasonable sub-
radiation damping coefficients
ooting; therefore, the suggested
ecture.

4. Soil-Structure Interaction Problem

Once the input motion and the base impedances are known, the last step is reduced to a simple dynamic analysis of a multidegree of freedom system. The "stiffness" and "damping" terms can be added directly to the corresponding terms for the structure in a solution in the frequency domain. A time domain solution, and a modal solution in particular (9), offer a simpler physical interpretation of the results. They require, however, frequency independent stiffness and damping coefficients, and for the latter, in addition the existence of normal modes.

A number of comparative studies indicate that it is more important to reproduce correctly the static stiffnesses than their complete frequency variation. It is also worth noticing that the increase in stiffness due to embedment is very sensitive to the properties of the lateral soil, which may be disturbed. Considering, in addition, the uncertainties in the soil properties and its nonlinear behavior, it is clear that engineering judgment is needed in the selection of the most appropriate model, and that parametric studies, varying the assumed conditions within reasonable limits, are advisable. This, of course, is equally true whether the analysis is carried out in a single step (one-pass method) or in three steps as suggested here.

The spring method has the advantage of being less time-consuming when approximations are used for the kinematic interaction problem. It allows, therefore, more parametric studies, and the accuracy of each step is subject to better control. Of particular importance is the possibility in this method to make use of symmetry or cylindrical conditions if the foundation meets these requirements even if the structure does not (which is a frequent situation). The coupling between the corresponding terms will come in naturally in the third step. From a practical standpoint, the procedure has an additional advantage when the design motion is specified by a broad band response spectrum not tailored to the soil conditions at the site. If the direct approach is applied to such a case, deamplification of certain frequency components with depth resulting from the use of one single wave pattern (i.e., vertically propagating waves) may lead to unconservative estimates for the motions of the structure. Under such conditions, it may be better to regard the design motion as an "average" motion in the vicinity of the structure, and to use it directly as input to Step 3.

References

- [1] ELSABER, F., "Static Stiffness Coefficients for Circular Foundations Embedded in an Elastic Medium," M. S. thesis, Mass. Inst. of Tech., Cambridge, Massachusetts, 1975.
- [2] KAUSEL, E., "Forced Vibrations of Circular Foundations on Layered Media," MIT Research Report R74-11, Soils publication No. 336, Structures publication No. 384, January, 1974.
- [3] KAUSEL, E., ROESSET, J. M., WAAS, G., "Dynamic Analysis of Footings on Layered Media," Journ. Eng. Mech. Div., ASCE, October, 1975.
- [4] KAUSEL, E., ROESSET, J. M., "Dynamic Stiffness of Circular Foundations," Journ. Eng. Mech. Div., ASCE, December, 1975.
- [5] KAUSEL, E., ROESSET, J. M., "Semianalytic Hyperelement for Layered Strata," paper accepted for publication in the Journ. Eng. Mech. Div., ASCE, 1977.
- [6] KAUSEL, E., ROESSET, J. M., CHRISTIAN, J. T., "Nonlinear Behavior in Soil-Structure Interaction," Journ. of the Geotech. Eng. Div., ASCE, November, 1976.
- [7] LYSMER, T., WAAS, G., "Shear Waves in Plane Infinite Structures," Journ. Eng. Mech. Div., ASCE, Vol. 98, February, 1972.
- [8] MORRAY, J. P., "The Kinematic Interaction Problem of Embedded Circular Foundations," M. S. Thesis, Mass. Inst. of Tech., Cambridge, Massachusetts, 1975.
- [9] ROESSET, J.M., WHITMAN, R. V., DOBRY, R., "Modal Analysis for Structures with Foundation Interaction," Journ. Struct. Div., ASCE, Vol. 99, March, 1973.
- [10] VELETOS, A., WEI, Y., "Lateral and Rocking Vibration of Footings," Journ. Eng. Soil Mech. and Foundation Div., ASCE, Vol. 97, September, 1971.
- [11] WAAS, G., "Linear Two-dimensional Analysis of Soil Dynamics Problems in Semi-infinite Layered Media," Ph.D. Thesis, University of California, Berkeley, 1972.

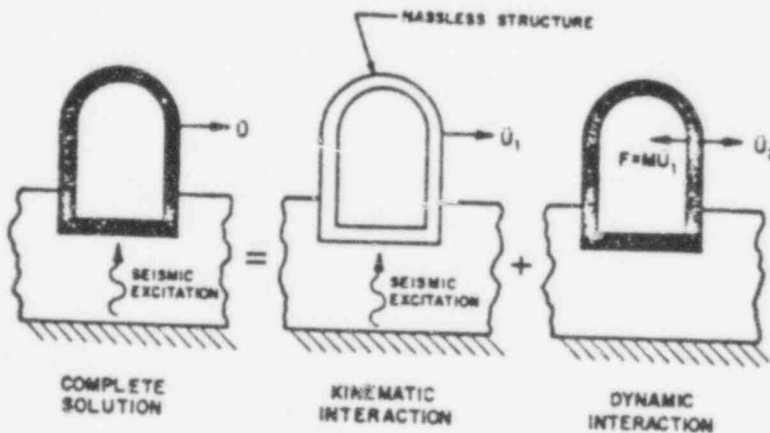


FIGURE 1
SUPERPOSITION THEOREM

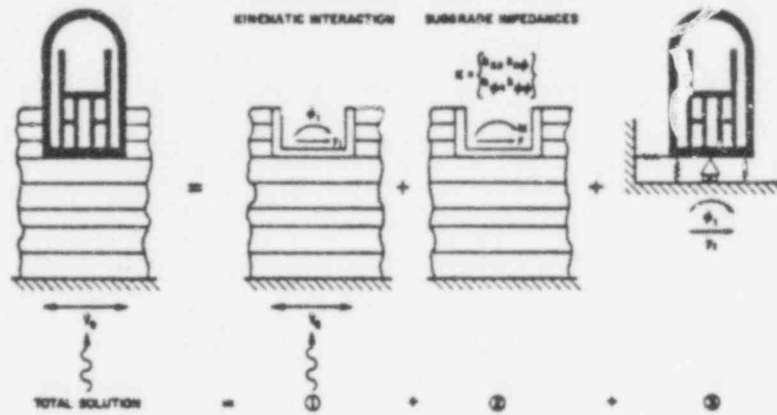


FIGURE 2
THE 3-STEP SOLUTION

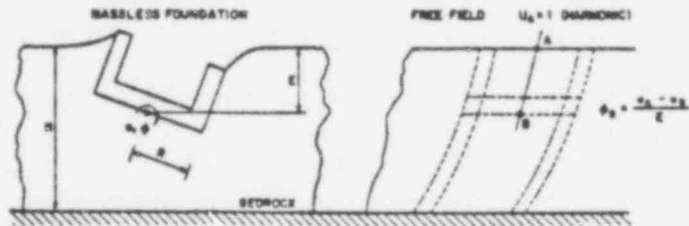
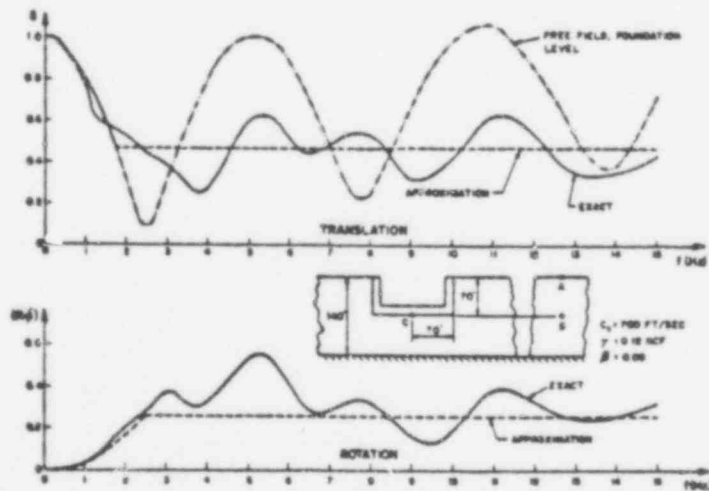


FIGURE 3
KINEMATIC INTERACTION PROBLEM



649 268

er Foundations Embedded in an
Cambridge, Massachusetts, 1975.

on Layered Media," MIT Research
publication No. 384, January,

is of Footings on Layered Media,"

ular Foundations," Journ. Eng.

t for Layered Strata," paper
., ASCE, 1977.

er Behavior in Soil-Structure
November, 1976.

Structures," Journ. Eng. Mech.

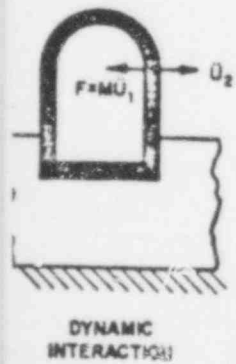
Embedded Circular Foundations,"
1975.

is for Structures with
1. 99, March, 1973.

of Footings," Journ. Eng. Soil
1971.

anics Problems in Semi-infinite
Berkeley, 1972.

FIGURE



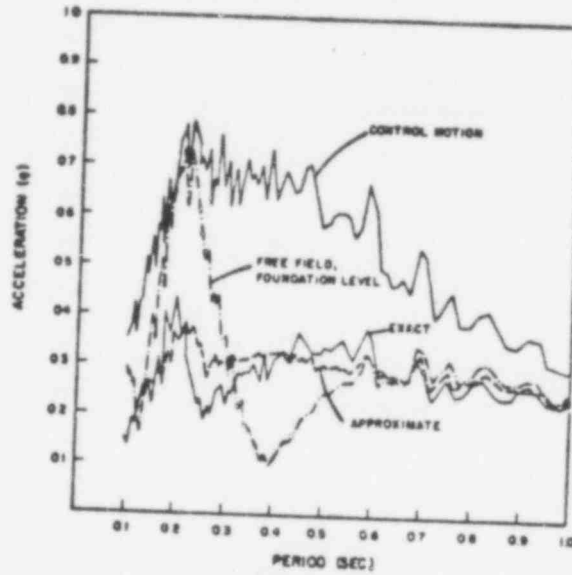


FIG. 5
MOTION OF MASSLESS FOUNDATION, RESPONSE SPECTRA
1% OSCILLATOR DAMPING
 $H/R = 2, E/R = 1$

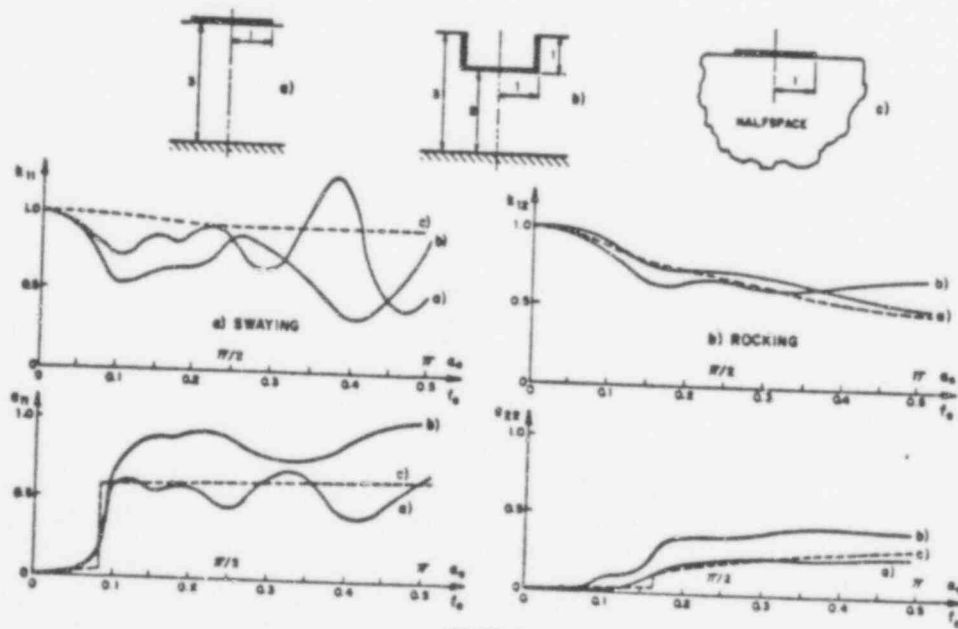


FIGURE 6
DYNAMIC STIFFNESS COEFFICIENTS, $\nu = 1/3, \beta = 0.05$

649 269

Soil, (height) der. The force displ (18 c) char these clude earth, indric. In identi bution unifor. At diff perim of FE reson were. As bedded damp ing m ing m

TORSIONAL AND COUPLED VIBRATIONS OF EMBEDDED FOOTINGS

M. NOVAK*

Faculty of Engineering Science, The University of Western Ontario, London, Ontario, Canada

AND

K. SACHS

AEG-Telefunken, Frankfurt, Germany

SUMMARY

An approximate analytical solution is presented for torsional vibrations of footings partially embedded into a semi-infinite medium or a stratum. Simple formulas derived for pure torsional motion make it possible to apply a correction for the effect of embedment to the known solutions of surface footings. The solution completes an approach to the analysis of all modes of footing vibrations, including the coupled modes. The approach to coupled modes is illustrated by the solution of coupled response involving horizontal translation, rocking and torsion. Formulas are presented for stiffness and damping coefficients that can be used in the analysis of embedded footings or structures supported by such footings.

Field experiments were conducted with concrete footings featuring circular, square and rectangular bases and variable embedment depths. The experimental results were compared with theoretical predictions of pure torsional vibrations.

INTRODUCTION

This paper complements an approach to the analysis of embedded footing vibration which related to pure vertical, horizontal and rocking modes^{13,14} and coupled horizontal and rocking modes.⁴ Pure torsional response is treated herein as well as response in a coupled mode involving torsional, horizontal and rocking components.

There is experimental evidence that the dynamic response of footings can be considerably affected by their partial embedment beneath the surface of the soil.^{12,13,22} However, a rigorous analytical solution of this effect is very difficult and finite element solutions appear the most promising approach to this problem.^{11,20}

The approximate analytical solution presented in this paper offers advantages of simplicity, the possibility to solve any number of degrees of freedom, and great versatility, thereby making it possible to consider layering and to introduce the dynamic soil reactions into the analysis of structures resting on embedded footings.

The solution assumes a rigid cylindrical footing, linear isotropic elasticity and a perfect bond between the footing and the soil. The total dynamic reaction of soil is composed of a reaction acting in the footing base and on the footing vertical sides. The base reaction is derived from an elastic half-space which is assumed to model the soil under the footing base. The side reaction is derived as a reaction of an independent layer overlying the half-space. As well, this overlying layer is considered to be composed of a series of infinitesimally thin independent layers which facilitates the analysis of more complicated vibration modes involving non-uniform displacements of footing sides. Such assumptions were first adopted by Baranov;² however, he did not consider the torsional modes analyzed herein.

* Professor.

Received 24 August 1972
Revised 18 December 1972

The assumptions are approximate, primarily because the compatibility condition between the soil under the base and the overlying layer is satisfied only at the footing and very far from it. Nevertheless, the same theoretical approach to embedment yielded a reasonable agreement with the finite element solution for vertical vibration¹⁴ and considerably improved the agreement between the theory and experiments for coupled horizontal and rocking vibration.⁴ Thus, it appears useful to obtain some information on the torsional response of embedded footings too because large differences were observed between the strict elastic theory and experiments with surface footings.²¹ Finally, the approach presented offers a way of applying an approximate correction for embedment to the already numerous solutions for surface footings.^{1, 6, 7, 9, 10, 18, 21}

SIDE REACTIONS OF THE LAYER

Firstly, dynamic reactions will be determined acting on the footing sides if the cylindrical body performs harmonic torsional oscillations with frequency ω around its vertical axis.

With the omission of body forces and with the notation according to Love, the equations of motion of elastic media in cylindrical co-ordinates, are

$$\left. \begin{aligned} (\lambda + 2G) \frac{\partial \Delta}{\partial r} - \frac{2G}{r} \frac{\partial \omega_\theta}{\partial \theta} + 2G \frac{\partial \omega_z}{\partial z} &= \rho \frac{\partial^2 u}{\partial t^2} \\ (\lambda + 2G) \frac{\partial \Delta}{r \partial \theta} - 2G \frac{\partial \omega_r}{\partial z} + 2G \frac{\partial \omega_\theta}{\partial r} &= \rho \frac{\partial^2 v}{\partial t^2} \\ (\lambda + 2G) \frac{\partial \Delta}{\partial z} - \frac{2G}{r} \frac{\partial}{\partial r} (r \omega_\theta) + \frac{2G}{r} \frac{\partial \omega_r}{\partial \theta} &= \rho \frac{\partial^2 w}{\partial t^2} \end{aligned} \right\} \quad (1)$$

in which relative volume change:

$$\Delta = \frac{1}{r} \frac{\partial}{\partial r} (ru) + \frac{1}{r} \frac{\partial v}{\partial \theta} + \frac{\partial w}{\partial z}$$

and components of rotational vector,

$$\left. \begin{aligned} \omega_r &= \frac{1}{2} \left(\frac{1}{r} \frac{\partial w}{\partial \theta} - \frac{\partial v}{\partial z} \right) \\ \omega_\theta &= \frac{1}{2} \left(\frac{\partial u}{\partial z} - \frac{\partial w}{\partial r} \right) \\ \omega_z &= \frac{1}{2} \left(\frac{1}{r} \frac{\partial (rv)}{\partial r} - \frac{1}{r} \frac{\partial u}{\partial \theta} \right) \end{aligned} \right\} \quad (3)$$

With pure torsional vibration of the layer around the vertical axis, both vertical and radial components of the motion vanish, i.e.

$$w(r, \theta, t) = 0, \quad u(r, \theta, t) = 0 \quad (4)$$

and the equations of motion, equations (1), reduce to

$$(\lambda + 2G) \frac{1}{r^2} \frac{\partial^2 v}{\partial \theta^2} + G \frac{1}{r} \frac{\partial v}{\partial r} - G \frac{v}{r^2} + G \frac{\partial^2 v}{\partial r^2} = \rho \frac{\partial^2 v}{\partial t^2} \quad (5)$$

With the boundary condition along the circumference of the cylinder:

$$v(r_0, \theta, t) = r_0 \zeta_0 e^{i\omega t} \quad (6)$$

the solution to equation (5) can be sought in the form:

$$v = R(r) \Phi(\theta) e^{i\omega t} \quad (7)$$

Substitution of equation (7) into equation (5) yields

$$r^2 \frac{R''}{R} + r \frac{R'}{R} + \left(\frac{\rho \omega^2}{G} r^2 - 1 \right) = - \frac{\lambda + 2G}{G} \frac{\Phi''}{\Phi} \quad (8)$$

This equation can be split into two ordinary differential equations for $R(r)$ and $\Phi(\theta)$

$$r^2 \frac{R''}{R} + r \frac{R'}{R} + (k^2 r^2 - 1) = n^2 \quad (9)$$

$$-\frac{1}{\alpha^2} \frac{\Phi''}{\Phi} = n^2 \quad (10)$$

in which

$$k^2 = \frac{\rho \omega^2}{G}, \quad \alpha^2 = \frac{G}{\lambda + 2G} \quad (11)$$

Solution to equation (10) is

$$\Phi = A_n \cos n\alpha\theta + B_n \sin n\alpha\theta \quad (12)$$

Motion v is independent of angle θ which, with respect to equation (7), requires that in (12) $n = 0$ and thus $\Phi = A_n$.

Equation (9) now takes the form:

$$r^2 R'' + rR' + (\alpha^2 r^2 - 1)R = 0 \quad (13)$$

The solution to this equation is

$$R = CH_1^{(1)}(kr) + DH_1^{(2)}(kr) \quad (14)$$

in which $H_1^{(1)}, H_1^{(2)}$ = Hankel functions of the first order, first and second kind, respectively; C, D = constants to be determined.

From the asymptotic form of Hankel functions (see, e.g. Reference 5, p. 616) it can be seen that with excitation coming from the body (outward travelling waves) only the function $H_1^{(2)}$ comes into consideration and thus $C = 0$. From equations (7), (12) and (14) motion

$$v = AH_1^{(2)}(kr)e^{i\omega t} \quad (15)$$

in which A = a constant given by the boundary condition, equation (6). Comparison of equations (6) and (15) yields, with $r = r_0$ and $kr_0 = a_0$, the constant $A = \zeta_0 r_0 / H_1^{(2)}(a_0)$. Thus, motion at a distance r

$$v = \frac{\zeta_0 r_0}{H_1^{(2)}(a_0)} H_1^{(2)}(kr) e^{i\omega t} \quad (16)$$

in which the dimensionless frequency, $a_0 = r_0 \omega \sqrt{(\rho/G)}$.

The torsional stiffness of the layer is obtained from the stresses along the circumference of the cylinder. From general formulas, $\sigma_r = \sigma_\theta = \tau_{rz} = 0$ and circumferential shear

$$\tau_{r\theta} = G \left(\frac{\partial v}{\partial r} - \frac{v}{r} \right) \Big|_{r_0} \quad (17)$$

Integration of moment $r_0 \tau_{r\theta}$ along the circumference of the cylinder yields the relation between the total dynamic torsional reaction N_ζ of a layer of thickness l and cylinder motion $\zeta_0 e^{i\omega t}$:

$$N_\zeta(t) = -2\pi G \frac{r_0^2 l}{H_1^{(2)}(a_0)} [a_0 H_1^{(2)}(a_0) - 2H_2^{(2)}(a_0)] \zeta_0 e^{i\omega t} \quad (18)$$

or split into real and imaginary parts:

$$N_\zeta(t) = Gr_0^2 l (S_{\zeta 1} + iS_{\zeta 2}) \zeta_0 e^{i\omega t} \quad (19)$$

in which

$$S_{\zeta 1} = 2\pi \left(2 - a_0 \frac{J_0 J_1 + Y_0 Y_1}{J_1^2 + Y_1^2} \right) \quad (20)$$

and

$$S_{\zeta 2} = \frac{4}{J_1^2 + Y_1^2} \quad (21)$$

Here, $J_0(a_0)$, $J_1(a_0)$ are Bessel functions of the first kind of order zero and one respectively, and $Y_0(a_0)$, $Y_1(a_0)$ are Bessel functions of the second kind of order zero and one.

Function $S_{\zeta 1}$ has a meaning of a frequency dependent stiffness parameter while $S_{\zeta 2}$ represents a frequency dependent damping parameter. These parameters are shown as functions of a_0 in Figure 1. In Appendix I, approximate polynomial expressions are given which can facilitate the computations.

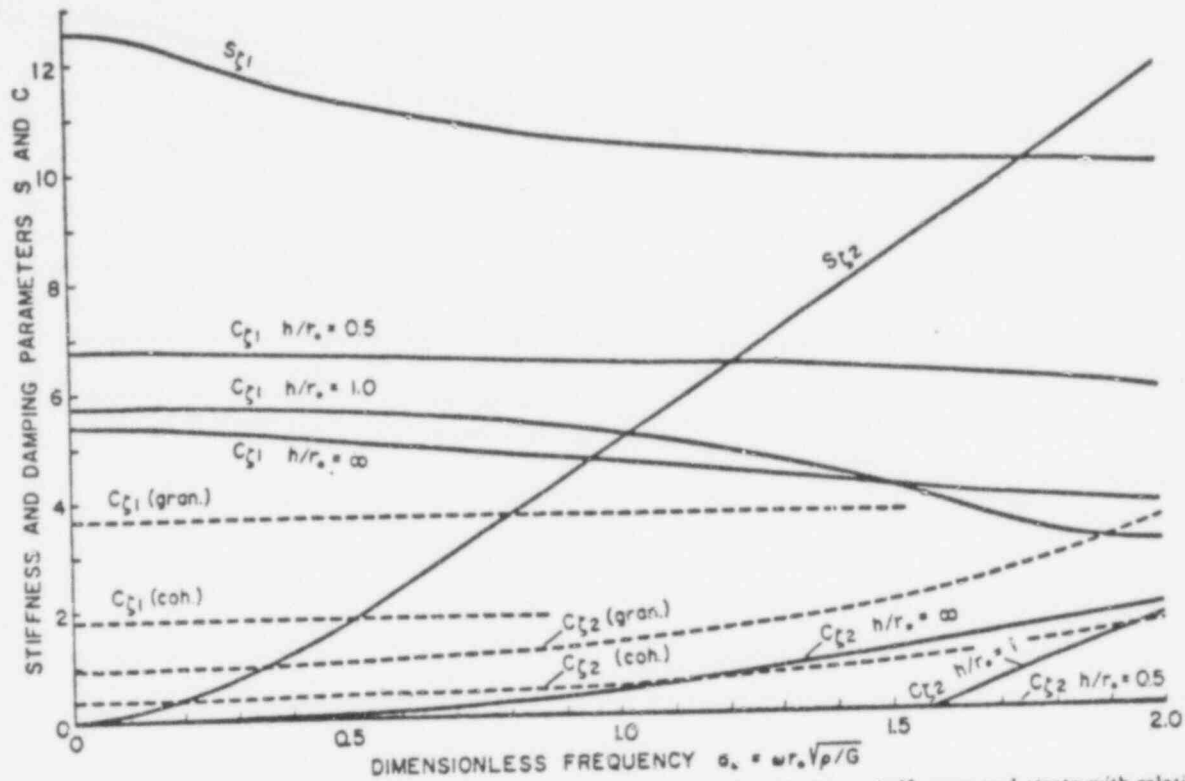


Figure 1. Stiffness parameters $S_{\zeta 1}$, $C_{\zeta 1}$ and damping parameters $S_{\zeta 2}$, $C_{\zeta 2}$ for side layer, half-space and strata with relative thickness $h/r = 0.5$ and 1 ($h/r = \infty$ denotes half space)

PURE TORSIONAL VIBRATIONS OF EMBEDDED FOOTINGS

The equation of torsional oscillations ζ of an embedded cylindrical footing about the vertical axis of symmetry is

$$I_{\zeta} \ddot{\zeta} = M_{\zeta}(t) - R_{\zeta}(t) - N_{\zeta}(t) \quad (22)$$

in which I_{ζ} = mass moment of inertia of footing about vertical axis Z , $M_{\zeta}(t)$ = moment of excitation, $R_{\zeta}(t)$ = torsional reaction of soil in footing base and $N_{\zeta}(t)$ = torsional reaction of layer adjacent to footing vertical sides.

The base reaction may be written in terms of displacement functions $f_{\zeta 1}$ and $f_{\zeta 2}$ (taken, e.g. from References 6 or 16):

$$R_{\zeta}(f) = -Gr_0^3 \frac{1}{f_{\zeta 1} + if_{\zeta 2}} \zeta(t) = Gr_0^3 (C_{\zeta 1} + iC_{\zeta 2}) \zeta(t) \quad (23)$$

in which stiffness parameter $C_{\zeta 1}$ and damping parameter $C_{\zeta 2}$ are

$$C_{\zeta 1} = \frac{-f_{\zeta 1}}{f_{\zeta 1}^2 + f_{\zeta 2}^2}, \quad C_{\zeta 2} = \frac{f_{\zeta 2}}{f_{\zeta 1}^2 + f_{\zeta 2}^2} \quad (24)$$

The side reaction is, according to equation (19),

$$N_{\zeta}(t) = G_s r_0^3 l (S_{\zeta 1} + iS_{\zeta 2}) \dot{\zeta}(t) \quad (25)$$

in which G_s = shear modulus of the side layer and $S_{c1,2}$ are given by equations (20) and (21). Substitution of equations (23) and (25) into equation (22) provides the differential equation of motion:

$$I_c \ddot{\zeta}(t) + Gr_0^3 \left[C_{c1} + \frac{G_s}{G} \frac{l}{r_0} S_{c1} + i \left(C_{c2} + \frac{G_s}{G} \frac{l}{r_0} S_{c2} \right) \right] \dot{\zeta}(t) = M_c(t) \quad (26)$$

With complex excitation:

$$M_c(t) = M_{c0} e^{i\omega t} = M_{c0} (\cos \omega t + i \sin \omega t) \quad (27)$$

in which M_{c0} = the real moment amplitude and ω = excitation frequency, the particular solution describing the steady-state motion is $\zeta(t) = \zeta_c e^{i\omega t}$ in which ζ_c = complex displacement amplitude.

The real part of the motion is

$$\zeta(t) = \zeta_0 \cos(\omega t + \phi) \quad (28)$$

With the notation of the frequency dependent stiffness (spring) constant:

$$k_c = Gr_0^3 \left(C_{c1} + \frac{G_s}{G} \frac{l}{r_0} S_{c1} \right) \quad (29)$$

and the frequency dependent damping constant:

$$c_c = \frac{Gr_0^3}{\omega} \left(C_{c2} + \frac{G_s}{G} \frac{l}{r_0} S_{c2} \right) \quad (30)$$

the real amplitude of torsional vibration

$$\zeta_0 = \frac{M_{c0}}{\sqrt{[(k_c - I_c \omega^2)^2 + (c_c \omega)^2]}} = \frac{M_{c0}}{k_c} \frac{1}{\sqrt{[1 - (\omega/\omega_0)^2]^2 + 4D_c^2(\omega/\omega_0)^2}} \quad (31)$$

and the phase shift:

$$\phi = -a \tan \frac{c_c \omega}{k_c - I_c \omega^2}$$

In equation (31) natural undamped frequency ω_0 and damping ratio D_c are

$$\omega_0 = \sqrt{(k_c/I_c)}, \quad D_c = c_c/2I_c \omega_0 \quad (32)$$

The natural undamped frequency of an embedded footing must be determined by a trial and error approach as it appears in k_c too. Equations (31) and (32) are formally equal to those of a single degree of freedom system (Voigt model). Often the dimensionless amplitude $A_c = \zeta_0 Gr_0^3/M_{c0}$ is useful. This dimensionless amplitude depends only on inertia ratio B_c and a_0 as can be seen.

In many practical problems the excitation is due to rotation of an unbalanced mass m_e with the eccentricity e_m acting at a distance r_c from the axis of the footing. The excitation moment amplitude is $M_{c0} = m_e e_m r_c \omega^2$ and a dimensionless rotation amplitude may be introduced, $A_c = \zeta_0 I_c / (m_e e_m r_c)$.

The predicted response depends on functions $C_{c1,2}$ substituted into the above formulas. Four typical cases can be considered: the footing can be embedded in the half-space or in a stratum and surrounded by undisturbed soil or backfill depending on the type of construction.

Embedment in the half-space

Stiffness parameter C_{c1} and damping parameter C_{c2} were computed from equations (24) with displacement functions $f_{c1,2}$ taken from Bycroft.⁸ These parameters are shown in Figure 1 in full lines and are given in Appendix I in a polynomial form to facilitate the computation.

The stiffness increase due to embedment was computed from equation (29) with frequencies $a_0 = 0$ and 1 and is compared with the static finite element solution by Kaldjian⁹ in Figure 2. The agreement is quite reasonable.

Examples of theoretical response curves computed from equation (31) with various relative embedments $\delta = l/r_0$ are shown in Figure 3.

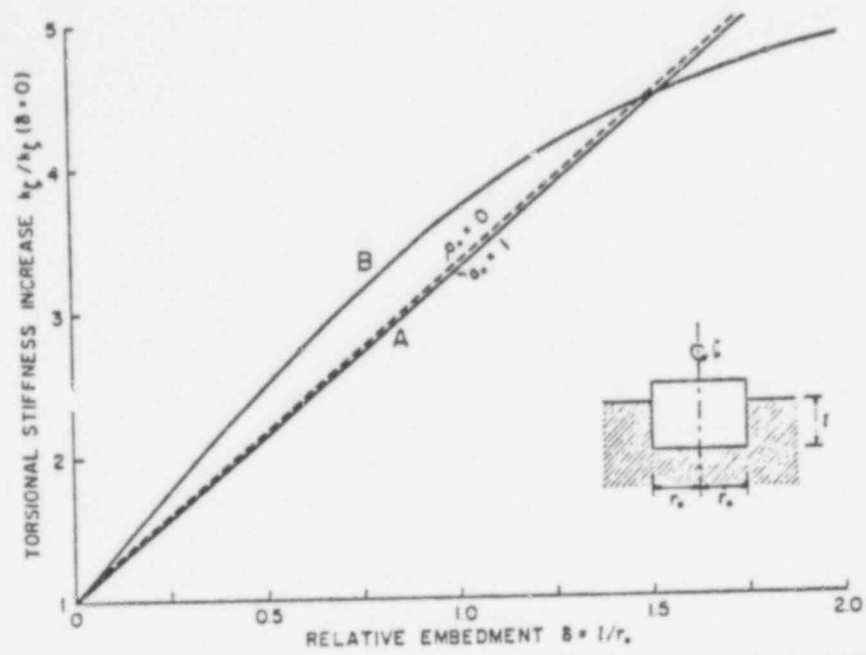


Figure 2. Torsional stiffness increase due to embedment: (A) approximate dynamic theory, (B) Kaldjian's⁸ static finite element solution

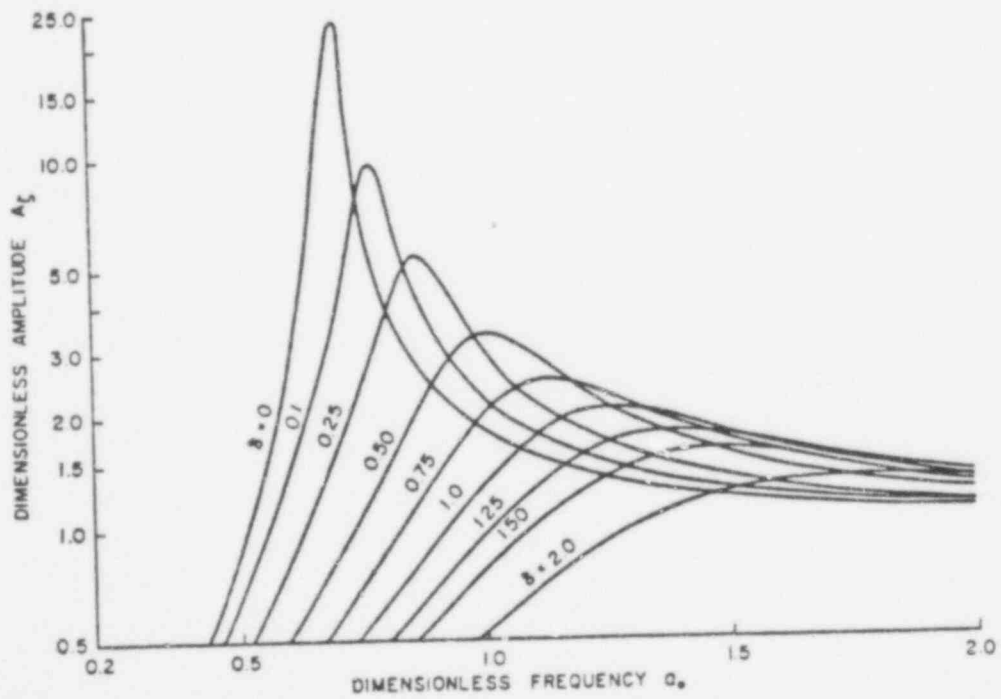


Figure 3. Theoretical response curves of torsional vibrations of footings embedded in elastic half-space (inertia ratio $B_t = 10$, $\rho_s/\rho = 1$, quadratic excitation)

649 275

It can be seen that the theory indicates a considerable increase in the resonant frequencies and reduction in the resonant amplitudes due to embedment.

Weissmann²¹ approximately considered slip in regions of high shear stress and included hysteretic damping of soil. Functions $C_{\Omega,2}$ derived from his solution are shown in Figure 1 in dashed lines for both granular and cohesive soils respectively. These functions considerably deviate from the strictly elastic solution, however, but may sometimes yield results closer to reality.

Embedment in a stratum

Embedment in a stratum can be considered with equal ease. The functions $C_{\Omega 1}$ and $C_{\Omega 2}$ for two strata featuring relative thicknesses $h/r_0 = 0.5$ and 1 are given in Appendix I and are shown in Figure 1. They were computed from Bycroft's functions $f_{1,3}$.

Base reactions for strata of any thickness can be obtained from Awojobi's solution.¹ The corresponding stiffness and damping parameters are also given in Table II (Appendix I).

Examples of response curves obtained from equation (31) with Awojobi's base reactions are shown in Figure 4 for sublayers having relative thicknesses $h/r_0 = 1, 2, 5$ and ∞ . In Figures 5 and 6 variations of

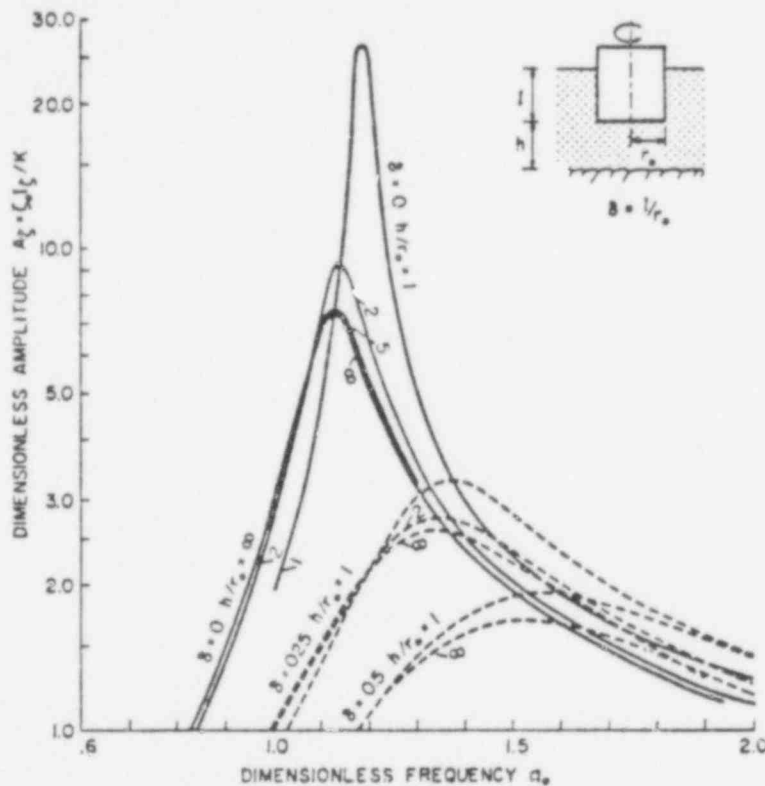


Figure 4. Theoretical response curves of torsional vibrations of footings embedded in strata with $h/r_0 = 1, 2, 5$ and ∞ . (Embedment ratios $\delta = 0, 0.25$ and $0.50, B_c = 3.5, \rho_s/\rho = 1$, quadratic excitation)

resonant (maximum) amplitudes and corresponding resonant frequencies with stratum thickness and embedment ratio are shown for inertia ratios $B_c = 2, 4$ and 10. These graphs were also calculated with Awojobi's base reactions. With $\delta = 0$ the solution corresponds to that for surface footings, i.e. to that of Awojobi or Bycroft according to the base reactions used. There is very little difference between Bycroft's and Awojobi's solutions with $h/r_0 = \infty$.

It can be seen from Figures 4-6 that the effect of embedment in a stratum is even more pronounced than with that of embedment in the half-space because of little or no geometric damping generated through the base. Figures 5 and 6 can be used to assess the effects of embedment, inertia ratio and layering.

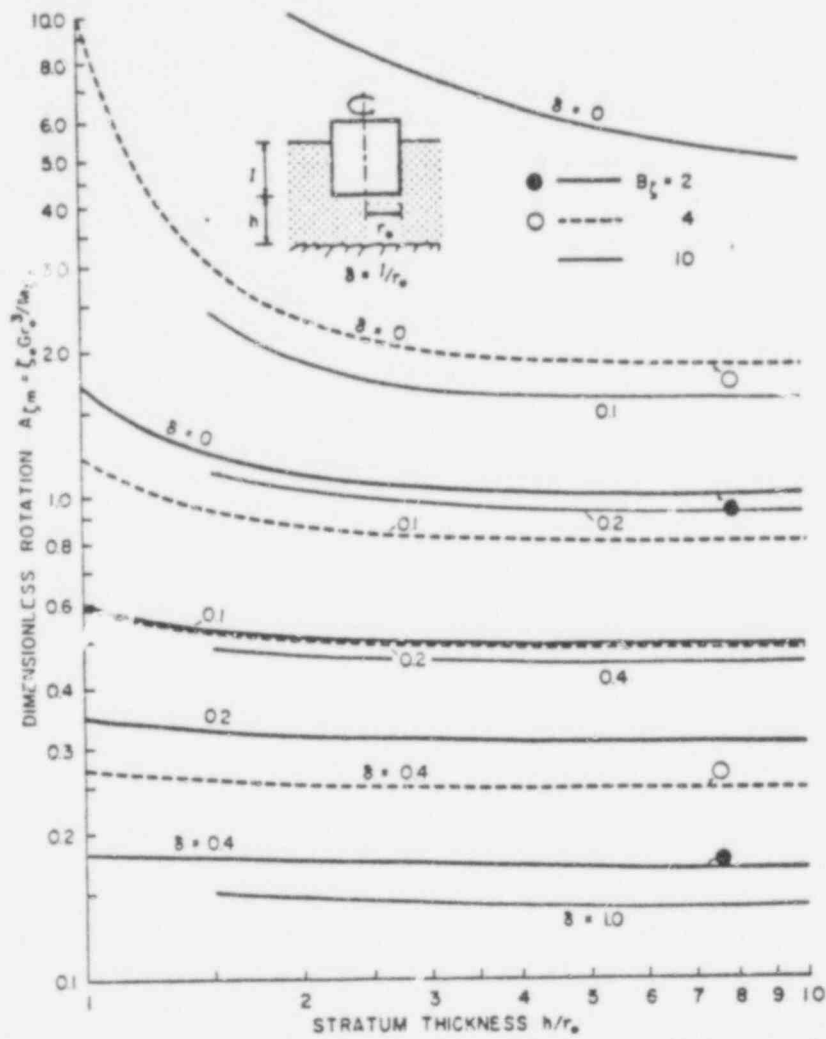


Figure 5. Dimensionless resonant amplitudes of torsional vibrations of footings embedded in strata for several embedment ratios and inertia ratios $B_\zeta = 2, 4$ and 10 . ($B_\zeta = I_c / r_0^2$; circles indicate finite element solution, Reference 20)

Fig

Lys
and
pol
of

The
cor
and
the
app
1
the
val
is o
P

in v
S
tor:

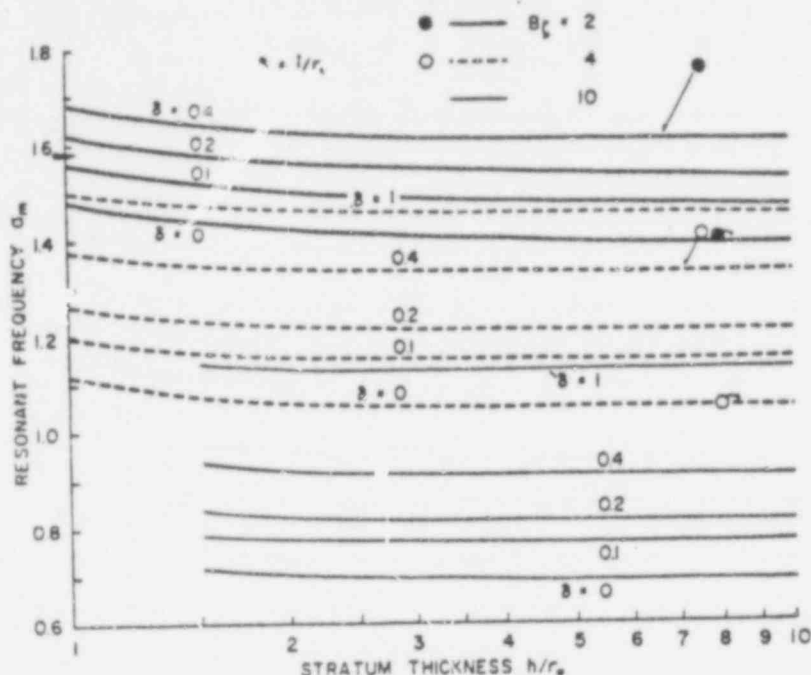


Figure 6. Dimensionless resonant frequencies of torsional vibrations of footings embedded in strata for several embedment ratios δ and inertia ratios $B_c = 2, 4$ and 10 . ($B_c = I_c / \rho r_0^4$; circles indicate finite element solution, Reference 20)

Also plotted in Figures 5 and 6 are resonant amplitudes and frequencies obtained for $h/r_0 = 8$ by Wass and Lysmer²⁰ using the finite element technique. Their results are shown as circles; arrows indicate with which analytical curve they compare. The agreement is quite good. (The finite element results shown were interpolated to match the parameters B_c used here. The differences in resonant frequencies with $\delta = 0.4$ are of little practical importance as the corresponding response curves are rather flat.)

SIMPLIFIED DESIGN ANALYSIS

The prediction of the response from the above formula is not difficult; however, the computation can be considerably simplified if stiffness factors C_{c1} and S_{c1} are considered as constant (frequency independent) and damping factors C_{c2} and S_{c2} as proportional to dimensional frequency a_0 . It can be seen from Figure 1 the degree to which these assumptions are acceptable. They seem reasonable and quite adequate for applications with respect to all the physical uncertainties involved.

Thus, stiffness parameters can be considered approximately constant, i.e. $C_{c1} = \bar{C}_{c1}$ and $S_{c1} = \bar{S}_{c1}$, where the constants denoted by bars can be readily obtained from Figure 1 or Appendix I in which some suitable values are given. With constant stiffness parameters \bar{C}_{c1} and \bar{S}_{c1} , the frequency independent stiffness constant is obtained from equation (29). Then, the natural frequency ω_0 can be directly calculated from equation (32). Proportionality of damping factors to frequency assumes:

$$C_{c2} = \bar{C}_{c2} a_0 \quad \text{and} \quad S_{c2} = \bar{S}_{c2} a_0 \tag{33}$$

in which \bar{C}_{c2} and \bar{S}_{c2} are constants whose values can be again established from Figure 1 or Appendix I.

Substitution of equations (33) into equation (30) yields the frequency independent damping constant for torsional vibrations of embedded footings:

$$c_c = r_0^4 \sqrt{(\rho G)} \left[\bar{C}_{c2} + \bar{S}_{c2} \frac{1}{r_0 \omega} \sqrt{\left(\frac{\rho_s G_s}{\rho G} \right)} \right] \tag{34}$$

The frequency independent damping ratio is from equations (32) and (29)

$$D_{\zeta} = \frac{1}{2\sqrt{B_{\zeta}}} \left[C_{\zeta 2} + S_{\zeta 2} \frac{I}{r_0 \sqrt{\left(\frac{\rho_s G_s}{\rho G}\right)}} \right] / \sqrt{\left(C_{\zeta 1} + \frac{G_s I}{G r_0} S_{\zeta 1} \right)} \quad (35)$$

in which inertia ratio $B_{\zeta} = I_{\zeta} / \rho r_0^2$. For surface footings, equation (35) yields $D_{\zeta} = 0.17 / \sqrt{B_{\zeta}}$ and numerical results close to those of Richart and co-workers (Reference 17, p. 226).

With D_{ζ} obtained, the 'resonant' amplitude at natural frequency ω_0 (slightly smaller than the maximum amplitude) is simply $\zeta_0(\omega_0) = M_{\zeta 0} / (k_{\zeta} 2D_{\zeta})$ or with quadratic excitation $\zeta_0(\omega_0) = m_s e_m r_c / (2D_{\zeta} I_{\zeta})$. The maximum amplitude is $1/\sqrt{(1-D_{\zeta}^2)}$ times larger.

An example of comparison of response curves computed with variable parameters and with constant parameters is shown in Figure 7. ($C_{\zeta} = 0.5$ was used for the half-space in this case because it yielded better agreement in the frequency range employed.) The agreement appears satisfactory for design purposes. As even better agreement can be obtained with a mass adjustment.

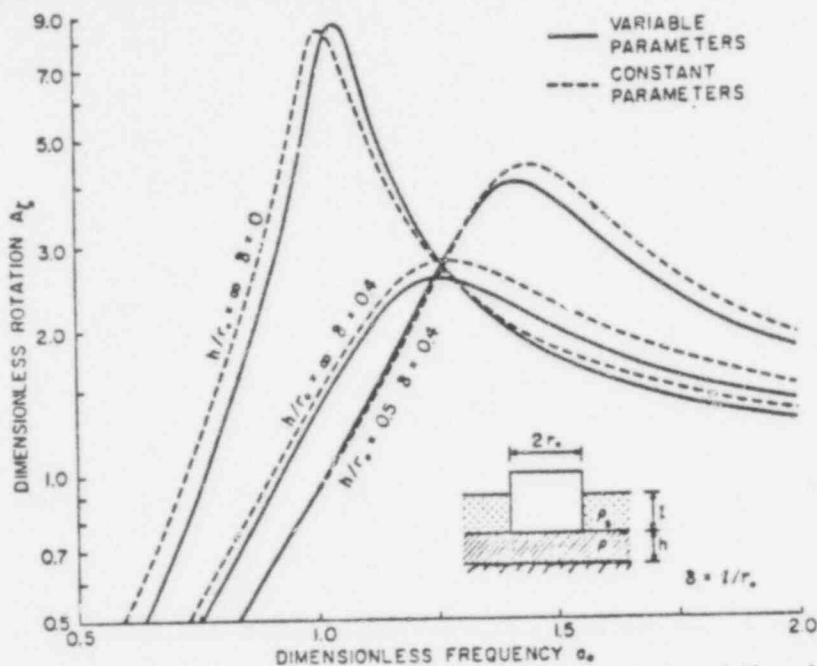


Figure 7. Comparison of response curves of torsional vibrations computed with both variable and constant parameters ($B_{\zeta} = 4.18$, backfill with $\rho_s/\rho = 0.8$, $G_s/G = 0.5$, quadratic excitation, Bycroft's base reactions)

In practical applications, the effect of embedment may be reduced due to backfill and an imperfect bond between the footing and the soil. The effect of backfill can be accounted for by considering $G_s < G$ and $\rho_s < \rho$ in equations (29) and (35). Possible lack of bond between the footing and the soil can be approximately taken into account by considering Weissmann's base reactions (dashed lines in Figure 1) and intuitively reduced values of $S_{\zeta 1,2}$.

COUPLED VIBRATION INVOLVING TORSIONAL, HORIZONTAL AND ROCKING COMPONENTS

If the centre of gravity of the footing does not lie on the vertical geometric axis of the footing, a coupled motion in three degrees of freedom is produced by a horizontal force Q , by a moment M_{ζ} in the horizontal plane and by a moment in the vertical plane M_{ψ} . The components of this motion are the horizontal translation $u(t)$, rotation in the horizontal plane $\zeta(t)$ and rotation in the vertical plane (rocking) $\psi(t)$. This motion can also be solved under the same assumptions as introduced for pure torsional vibration.

Consider the centre of gravity the origin of co-ordinates. With the notation according to Figure 8 and with the omission of product moments of inertia and of coupling between displacements and reactions in

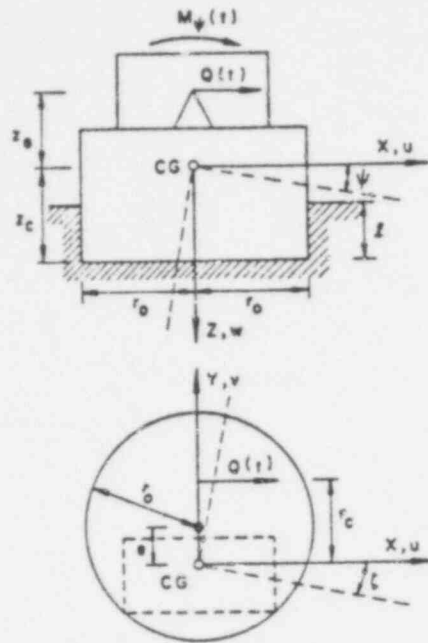


Figure 8. Notation for coupled vibration of footing in three degrees of freedom involving horizontal translation, rocking and torsion

the footing base,^{10, 19} the equations of the motion are

$$\begin{aligned}
 m\ddot{u}(t) + r_0[G(C_{u1} + iC_{u2}) + G_s \delta(S_{u1} + iS_{u2})]u(t) \\
 + er_0[G(C_{u1} + iC_{u2}) + G_s \delta(S_{u1} + iS_{u2})]\zeta(t) \\
 + r_0^2 \left\{ -G \frac{z_c}{r_0} (C_{u1} + iC_{u2}) + G_s \delta \left[\left(\frac{1}{2} \delta - \frac{z_c}{r_0} \right) (S_{u1} + iS_{u2}) \right] \right\} \psi(t) = Q(t) \quad (36a)
 \end{aligned}$$

$$\begin{aligned}
 I_\psi \ddot{\psi}(t) + r_0^2 \left[G_s \delta \left(\frac{\delta}{2} - \frac{z_c}{r_0} \right) (S_{u1} + iS_{u2}) - G \frac{z_c}{r_0} (C_{u1} + iC_{u2}) \right] u(t) \\
 + er_0^2 \left[G_s \delta \left(\frac{\delta}{2} - \frac{z_c}{r_0} \right) (S_{u1} + iS_{u2}) - G \frac{z_c}{r_0} (C_{u1} + iC_{u2}) \right] \zeta(t) \\
 + r_0^3 \left[G(C_{\psi1} + iC_{\psi2}) + G_s \delta \left[S_{\psi1} + iS_{\psi2} + \left(\frac{\delta^2}{3} - \delta \frac{z_c}{r_0} + \frac{z_c^2}{r_0^2} \right) (S_{u1} + iS_{u2}) \right] \right. \\
 \left. + G \frac{z_c^2}{r_0^2} (C_{u1} + iC_{u2}) \right] \psi(t) = M_\psi(t) \quad (36b)
 \end{aligned}$$

$$\begin{aligned}
 I_\zeta \ddot{\zeta}(t) + er_0[G(C_{u1} + iC_{u2}) + G_s \delta(S_{u1} + iS_{u2})]u(t) \\
 + (e^2 r_0[G(C_{u1} + iC_{u2}) + G_s \delta(S_{u1} + iS_{u2})] \\
 + [G_s r_0^3 \delta(S_{\zeta1} + iS_{\zeta2}) + Gr_0^2(C_{\zeta1} + iC_{\zeta2})])\zeta(t) \\
 + er_0^2 \left[-G \frac{z_c}{r_0} (C_{u1} + iC_{u2}) + G_s \delta \left(\frac{1}{2} \delta - \frac{z_c}{r_0} \right) (S_{u1} + iS_{u2}) \right] \psi(t) = M_\zeta(t) \quad (36c)
 \end{aligned}$$

In these equations, C_ζ and S_ζ are the parameters derived above. Parameters C_u , S_u and C_ψ , S_ψ are analogous functions related to horizontal translation u and rocking ψ and can be found in Reference 4.

With harmonic excitation in complex form

$$Q(t) = Q_0 e^{i\omega t}, \quad M_\psi(t) = M_{\psi 0} e^{i\omega t}, \quad M_\zeta(t) = M_{\zeta 0} e^{i\omega t} \quad (37)$$

the response is

$$u(t) = u_c e^{i\omega t}, \quad \psi(t) = \psi_c e^{i\omega t}, \quad \zeta(t) = \zeta_c e^{i\omega t} \quad (38)$$

in which subscript c denotes complex amplitudes. Substitution of equations (37) and (38) into equations (36) yields for the complex amplitudes of coupled motion:

$$\left. \begin{aligned} (k_{uu} - m\omega^2 + i\omega c_{uu}) u_c + (k_{u\psi} + i\omega c_{u\psi}) \psi_c + (k_{u\zeta} + i\omega c_{u\zeta}) \zeta_c &= Q_0 \\ (k_{\psi\psi} + i\omega c_{\psi\psi}) u_c + [(k_{\psi\psi} - I_\psi \omega^2) + i\omega c_{\psi\psi}] \psi_c + (k_{\psi\zeta} + i\omega c_{\psi\zeta}) \zeta_c &= M_{\psi 0} \\ (k_{\zeta\zeta} + i\omega c_{\zeta\zeta}) u_c + (k_{\psi\zeta} + i\omega c_{\psi\zeta}) \psi_c + [(k_{\zeta\zeta} - I_\zeta \omega^2) + i\omega c_{\zeta\zeta}] \zeta_c &= M_{\zeta 0} \end{aligned} \right\} \quad (39)$$

in which frequency dependent stiffness constants:

$$\left. \begin{aligned} k_{uu} &= Gr_0 \left(C_{u1} + \frac{G_s}{G} \delta S_{u1} \right) \\ k_{u\psi} &= -Gr_c \left[z_c C_{u1} + \frac{G_s}{G} \delta (z_c - \frac{1}{2} r_0 \delta) S_{u1} \right] \\ k_{u\zeta} &= ek_{uu} \\ k_{\psi\psi} &= Gr_0^3 \left[C_{\psi 1} + \left(\frac{z_c}{r_0} \right)^2 C_{u1} + \frac{G_s}{G} \delta S_{\psi 1} + \frac{G_s}{G} \delta \left(\frac{\delta^2}{3} + \frac{z_c^2}{r_0^2} - \delta \frac{z_c}{r_0} \right) S_{u1} \right] \\ k_{\psi\psi} &= k_{\psi\psi} \\ k_{\psi\zeta} &= -Ger_0 \left[z_c C_{u1} + \frac{G_s}{G} \delta (z_c - \frac{1}{2} r_0 \delta) S_{u1} \right] = ek_{u\psi} \\ k_{\zeta\zeta} &= Gr_0^3 \left(C_{\zeta 1} + \frac{G_s}{G} \delta S_{\zeta 1} + \frac{e^2}{r_0^2} C_{u1} + \frac{G_s}{G} \delta \frac{e^2}{r_0^2} S_{u1} \right) \\ k_{\zeta u} &= ek_{uu} = k_{u\zeta} \\ k_{\zeta\psi} &= k_{\psi\zeta} \end{aligned} \right\} \quad (40)$$

and frequency dependent damping constants:

$$\left. \begin{aligned} c_{uu} &= \frac{Gr_0}{\omega} \left(C_{u2} + \frac{G_s}{G} \delta S_{u2} \right) \\ c_{u\zeta} &= c_{uu} e \\ c_{\psi\psi} &= -\frac{Gr_0}{\omega} \left[z_c C_{u2} + \frac{G_s}{G} \delta (z_c - \frac{1}{2} r_0 \delta) S_{u2} \right] \\ c_{\psi\psi} &= \frac{Gr_0^3}{\omega} \left[C_{\psi 2} + \frac{z_c^2}{r_0^2} C_{u2} + \frac{G_s}{G} \delta S_{\psi 2} + \frac{G_s}{G} \delta \left(\frac{\delta^2}{3} + \frac{z_c^2}{r_0^2} - \delta \frac{z_c}{r_0} \right) C_{u2} \right] \\ c_{\psi u} &= c_{\psi\psi} \\ c_{\psi\zeta} &= -\frac{Ger_0}{\omega} \left[z_c C_{u2} + \frac{G_s}{G} \delta (z_c - \frac{1}{2} r_0 \delta) S_{u2} \right] \\ c_{\zeta u} &= c_{\psi\zeta} \\ c_{\zeta\psi} &= c_{\psi\zeta} \\ c_{\zeta\zeta} &= \frac{Gr_0^3}{\omega} \left(C_{\zeta 2} + \frac{G_s}{G} \delta S_{\zeta 2} + \frac{e^2}{r_0^2} C_{u2} + \frac{G_s}{G} \delta \frac{e^2}{r_0^2} S_{u2} \right) \end{aligned} \right\} \quad (41)$$

649 20

281

From equations (39), the complex amplitudes $u_c = u_1 + iu_2$, etc. can be obtained with any excitation frequency. The real and imaginary parts of the complex amplitudes yield the real amplitudes:

$$u_0 = \sqrt{(u_1^2 + u_2^2)}, \quad \psi_0 = \sqrt{(\psi_1^2 + \psi_2^2)}, \quad \zeta_0 = \sqrt{(\zeta_1^2 + \zeta_2^2)} \quad (42)$$

With quadratic excitation, these amplitudes can be made dimensionless according to the formulas:

$$A_x = \frac{m}{m_e e_m} u_0, \quad A_\psi = \frac{I_\psi}{m_e e_m z_e} \psi_0, \quad A_\zeta = \frac{I_\zeta}{m_e e_m r_e} \zeta_0 \quad (43)$$

The natural frequencies can be obtained from equation (39) by setting the right sides and the terms labelled by i equal to zero and solving the eigenvalue problem by trial and error.

The reciprocity relations in equations (40) and (41) hold in this approach but need not hold in general as shown in References 10 and 19.

An example of the response of embedded footings in three degrees of freedom is shown in Figure 9 for eccentricity $e = r_0/3$ and for various embedment depths. Dashed lines denoted $a_{1,2,3}$ indicate the first, second and third resonances of the surface footing ($\delta = 0$).

The first resonant peak shows clearly in all three components of the motion.

The second resonant region is dominated by torsion and can hardly be recognized in the translation component A_x .

The third resonant peak is completely suppressed in all three components.

These relations, of course, depend on the properties of the footing. Nevertheless, the example illustrates possible importance of the torsional component and the effect of embedment on the response in the three resonant regions. It can be seen that the response above the second resonance depends very little on the embedment. With small eccentricities (e) and medium or low mass ratios the third resonance usually appears suppressed.

The analysis of the coupled response can again be considerably simplified if constant parameters \bar{C} and \bar{S} are introduced as it was shown in the case of pure torsional vibration. The efficiency of such a simplified approach in two degrees of freedom was demonstrated in Reference 4. With constant parameters \bar{C} and \bar{S} introduced into equations (40) and (41), frequency independent stiffness and damping matrices are obtained that can be readily used in the analysis of any structure supported by embedded or surface footings, as discussed in Reference 23.

COMPARISON WITH EXPERIMENTS

To assess the applicability of the theory to circular footings and also to footings featuring square and rectangular bases (cross-sections), field experiments were conducted with three concrete blocks at The University of Western Ontario. The blocks were cast directly into neatly cut excavations. The embedment was changed by removing the soil in three steps. The effect of backfill was investigated by step-wise backfilling of the soil. Pure torsional vibrations were excited by means of a torsional mechanical oscillator with exchangeable eccentric masses.

The soil was a brown, silty clay underlain by a glacial till. The shear modulus and Poisson's ratio of the soil were obtained from wave velocities measured in the field. These measurements were complemented by laboratory investigations. The following properties of the soil were found:

Bulk density of undisturbed soil	= 110 lb/ft ³ (1760 kg/m ³)
Bulk density of backfill	= 100 lb/ft ³ (1602 kg/m ³)
Water content of soil	= 15 per cent
Void ratio of undisturbed soil	= 0.7
Shear modulus of undisturbed soil	= 1.13×10^6 lb/ft ² (549 kg/cm ²)

649 282

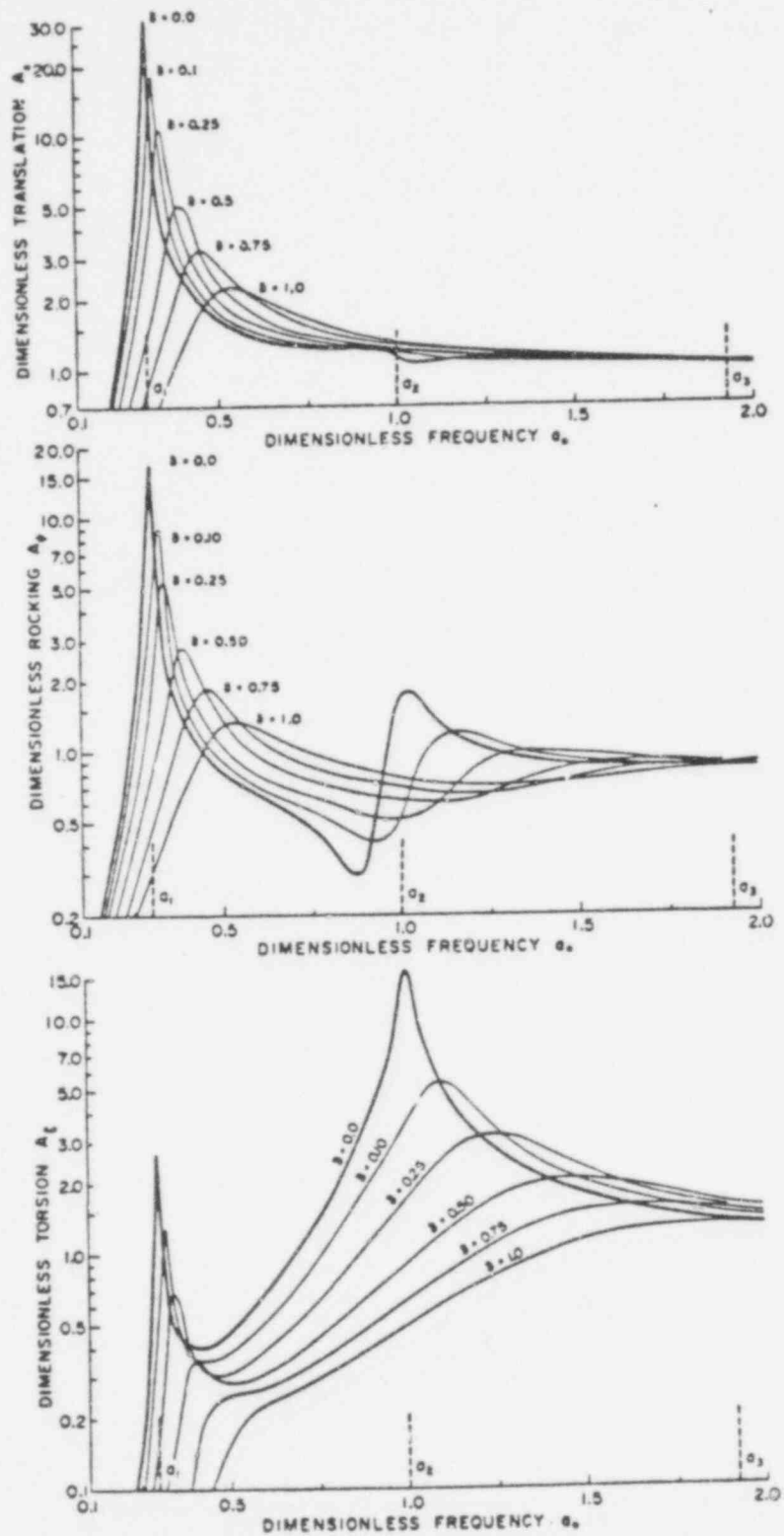


Figure 9. Example of coupled response of embedded footing in three degrees of freedom ($B_f = 4.56, e = r_0/3, G_1 = G_2$; translation, rocking and torsional components, quadratic excitation)

The main data on the test footings are given in Table I. The equivalent radii r_0 for square and rectangular footings were computed from the equality of polar moments of inertia of the base.

Table I

Shape of base	Base area ft ² (m ²)	J_c lb ft ² s ²	r_0 ft (m)	B_c
Circular	3.98 (0.369)	54.5 (7.54)	1.125 (0.343)	8.65
Square	5.06 (0.469)	77.6 (10.70)	1.284 (0.391)	6.50
Rectangular	5.01 (0.464)	93.2 (12.88)	1.330 (0.405)	6.55

A typical example of steady torsional response measured at various embedments is shown in Figure 10. The foundation base was circular in this case and the excitation intensity was the same for all embedments.

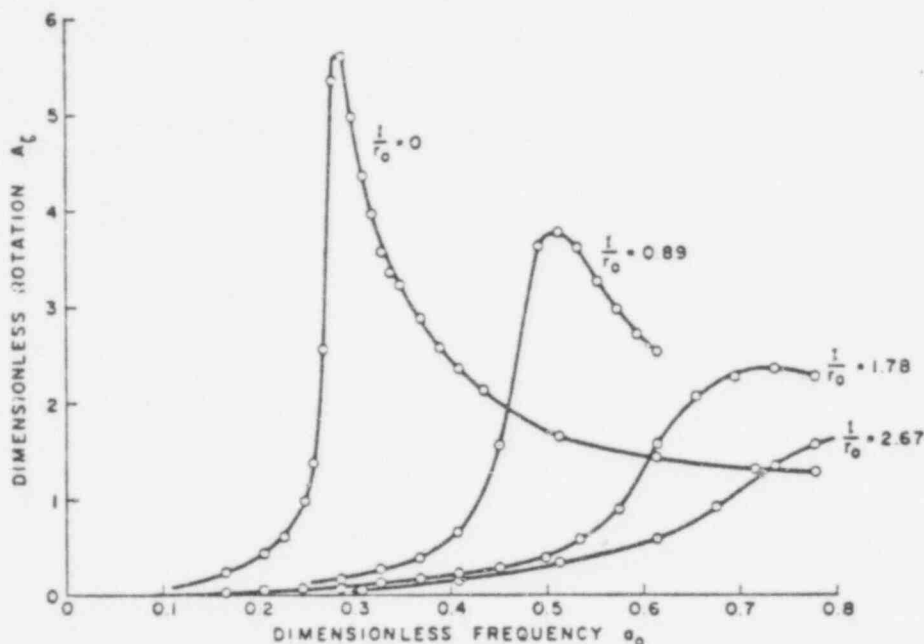


Figure 10. Measured response curves of cylindrical footing at various embedments ($m_e e_m r_c = 0.00326$ lb ft s², undisturbed soil, $B_c = 8.65$)

Comparison of Figure 10 with Figure 3 indicates a good qualitative agreement in the major effects of embedment manifested through drastic reduction in resonant amplitudes and large increase in resonant frequencies. The former effect is primarily due to increased geometric damping while the latter effect confirms an increase in stiffness.

With other foundation shapes the changes in response due to embedment were similar to those depicted in Figure 10. A comparison of response curves observed with various footings is shown in Figure 11 for surface footings and for an embedment of one foot. It can be seen that embedment was most efficient with the rectangular footing. This indicates the efficiency with which torque can be transmitted into the surrounding soil.

The quantitative comparison of theoretical and experimental resonant amplitudes and resonant frequencies is somewhat complicated by non-linearity of the response which renders the dimensionless resonant amplitudes and frequencies dependent on the excitation intensity as shown in Figures 12 and 13. In Figure 13, resonant rotations are shown in full lines, resonant frequencies in dashed lines and embedment is indicated as 0, 1 or 2 ft.

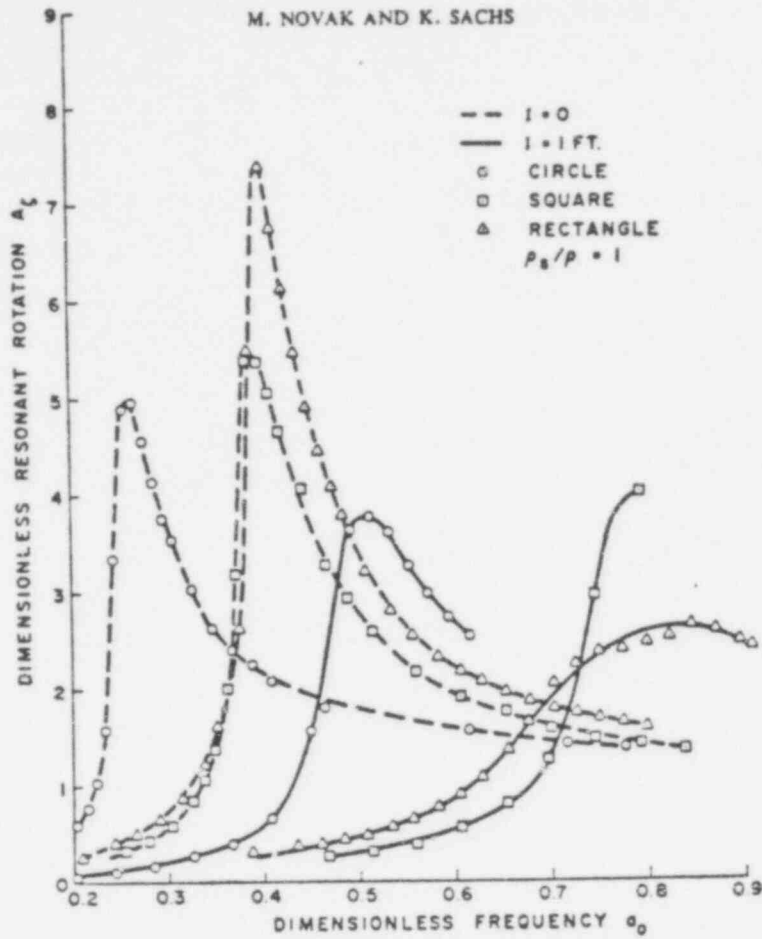


Figure 11. Measured response curves of cylindrical, square and rectangular footings with embedment 0 and 1 ft (undisturbed soil)

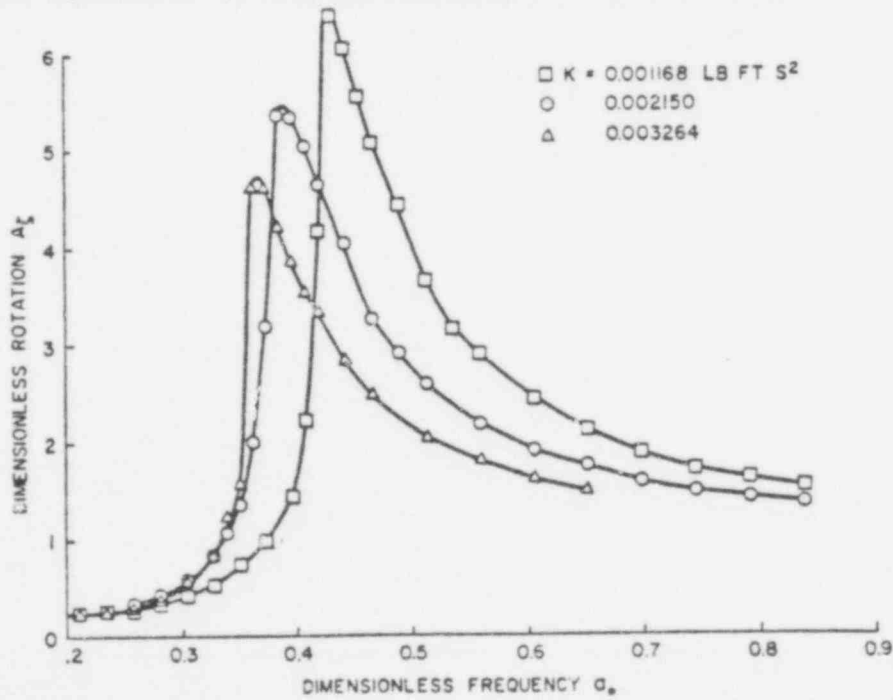


Figure 12. Dimensionless experimental response curves of torsional vibrations measured with three excitation intensities (square footing, embedment = 0, $B_c = 6.5$, quadratic excitation)

649 285

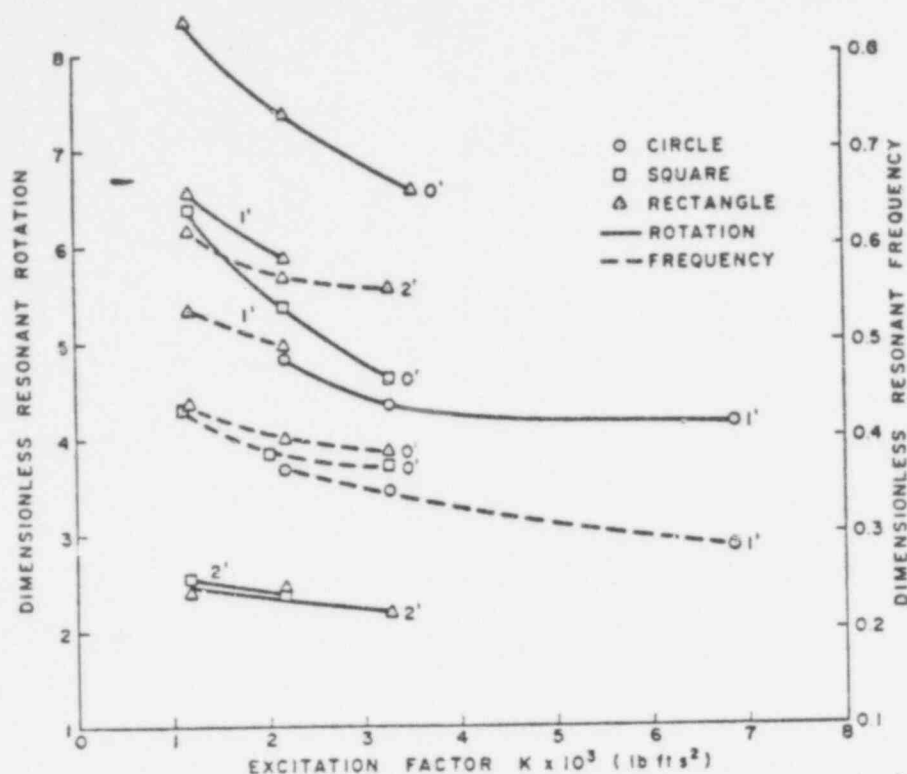


Figure 13. Measured dimensionless resonant rotations A_{ζ_m} and resonant frequencies a_m versus excitation factor $K = m_r e_m r_c$ (zero embedment or backfill 1 or 2 ft)

It appears that there is a trend for both the resonant amplitudes and resonant frequencies to decline with the increasing intensity of excitation. (The measurements were conducted with increasing intensity of excitation.) These changes seem to indicate a damping producing slip between the footing and the soil in regions of high shear stresses as suggested by Whitman²² for surface footings. The theory presented herein assumes a perfect bond between the footing and the soil; therefore, the measurements conducted with minimum excitation intensities are used, for the most part, in further comparisons shown in Figures 14 and 15.

In Figure 14 the theoretical and experimental resonant amplitudes are compared.

For surface footings, the experimental amplitudes are considerably smaller than the theoretical ones, in agreement with observations made by Whitman.²² For embedded footings the experimental amplitudes are larger than the theoretical values; however, the differences are smaller than with surface footings in the case of undisturbed soil and are quite small for the rectangular footing. For backfill the agreement is very poor. It can be seen from Figure 14 that there is a region of small embedments ($l/r_0 \approx 0.1-0.5$) in which the theoretical and experimental amplitudes must coincide.

The comparison of theoretical and experimental resonant frequencies is shown in Figure 15. The experimental resonant frequencies are consistently much lower than the theoretical predictions. The differences do not diminish with increasing embedment and appear largest for the circular footing. (Of course, there is a dependence on the rather inaccurate value of the shear modulus.) Nevertheless, it is clear that the torsional stiffness is much less than the elastic theory predicts.

The experimental frequencies and amplitudes of surface footings reported here are in reasonable agreement with Fry's experiments and with Weissmann's modified theory.²¹

It can be concluded that the quantitative agreement between the strictly elastic theory and the experiments is, in general, poor, particularly as far as resonant frequencies and the effect of backfill are concerned. These differences may be attributed to limited capacity of the soil to transmit the torque from the footing through shear. It is desirable for any theory to allow for a slip in the regions of high shear stresses. The presented

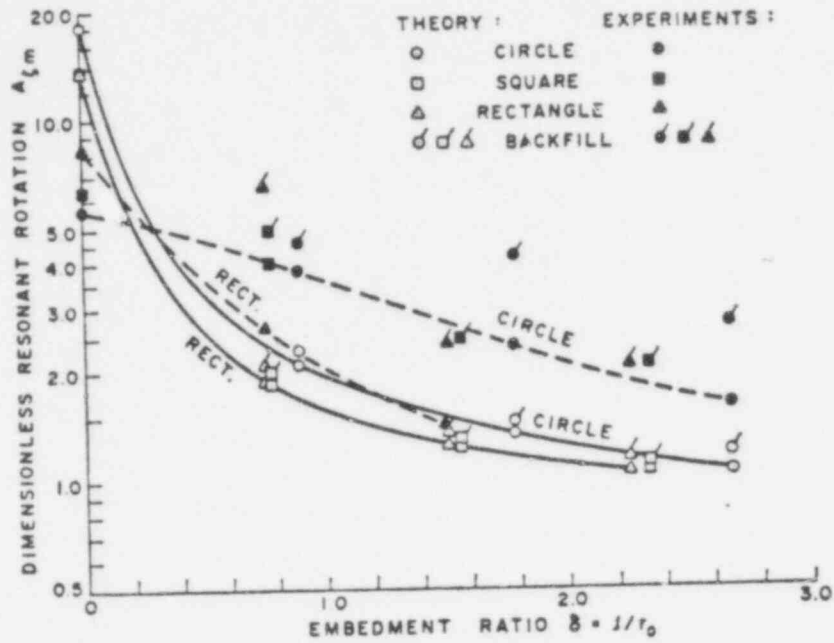


Figure 14. Comparison of theoretical and experimental resonant amplitudes of torsional vibrations (— theory; - - - - experiments)

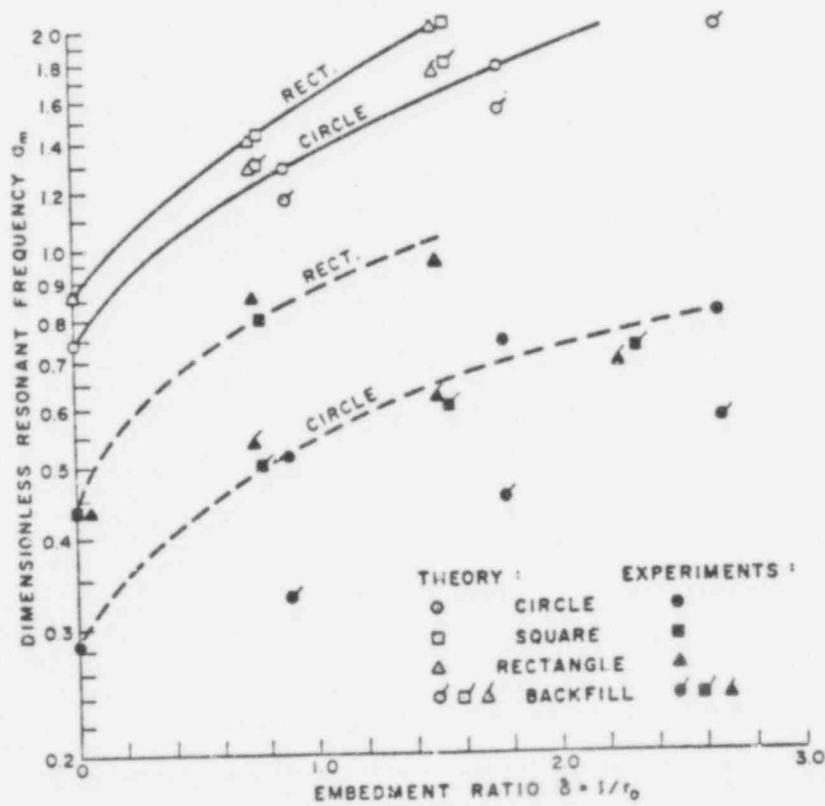


Figure 15. Comparison of theoretical and experimental resonant frequencies of torsional vibration (— theory; - - - - experiments)

649 287

theory makes it possible to include such modified soil reactions in the footing base. Such a modification would bring the theoretical predictions closer to experimental results.

CONCLUSIONS

Embedment produces a drastic decrease in resonant amplitudes and a marked increase in resonant frequencies of torsional vibrations. These effects are particularly pronounced for footings embedded in shallow strata with relative depth h/r_0 smaller than about 2 where the omission of embedment and internal damping can yield unrealistically large resonant amplitudes. With embedment taken into account, layering appears much less important.

The coupled response involving translation, rocking and torsion is strongly affected by embedment in the regions of the first and second resonances but depends very little on embedment in the region of the third resonance where there is usually no appreciable increase in amplitudes.

The approximate analytical solution agrees quite well with the available finite element solutions and requires very little computing time, and layers with any thickness can be readily considered.

The field experiments show a good qualitative agreement with the theory in the reduction of resonant amplitudes and in the increase in resonant frequencies due to embedment but the quantitative agreement in general is poor. Best agreement is found in resonant amplitudes for small embedments and rectangular footings, worst agreement appears for surface footings, and for circular footings in general.

The real resonant amplitudes are smaller than those theoretically predicted for surface footings and are larger than predicted for embedded footings. Only for small embedments fair agreement can be expected.

The resonant frequencies are considerably lower than the predicted values. Also the effect of backfill is in general much smaller than predicted.

The differences observed can be attributed to the slip in the regions of high shear. The inclusion of this effect appears necessary in order to improve the reliability of the theoretical predictions of the torsional response of footings no matter what kind of approach is used.

ACKNOWLEDGEMENTS

This study was supported by a grant-in-aid of research from the National Research Council of Canada. The assistance of Y. Beredugo is gratefully acknowledged, as well as the assistance of J. G. Lusk and J. Howell.

APPENDIX I

Stiffness and damping parameters

Stiffness and damping parameters are given in Table II, calculated from papers indicated. From Awojobi's solution,¹ the parameters can be obtained for any stratum thickness with $a_0 > r_0/h$ when the equivalent dimensionless frequency is introduced

$$a_e = \sqrt{[a_0^2 - r_0^2/h^2]} \quad (44)$$

Table II. Stiffness and damping parameters for torsional vibration

Stiffness and damping parameters	Constant parameters	Validity range
Side layer		
$S_{\zeta 1} = 12.58 - 1.01a_0 - 5.912a_0^2$	$\bar{S}_{\zeta 1} = 12.4$	$0 \leq a_0 \leq 0.2$
$S_{\zeta 1} = 12.59 - 1.855a_0 - 3.349a_0^2 + 5.335a_0^3 - 2.76a_0^4 + 0.495a_0^5$	$\bar{S}_{\zeta 1} = 10.2$	$0.2 \leq a_0 \leq 2.0$
$S_{\zeta 2} = 9.04a_0^2$	$\bar{S}_{\zeta 2} = 2.0$	$0 \leq a_0 \leq 0.2$
$S_{\zeta 2} = 7.5a_0 - \frac{3.726a_0}{0.455 + a_0}$	$\bar{S}_{\zeta 2} = 5.4$	$0.2 \leq a_0 \leq 2.0$
Half space*		
$C_{\zeta 1} = 5.333 + 0.032a_0 - 1.358a_0^2 + 0.7434a_0^3 - 0.1414a_0^4$	$\bar{C}_{\zeta 1} = 4.3$	$0 \leq a_0 \leq 2.0$
$C_{\zeta 2} = 0.486a_0^2$	$\bar{C}_{\zeta 2} = 0.7$	$0 \leq a_0 \leq 2.0$
Stratum $h/r_0 = 0.5^*$		
$C_{\zeta 1} = 6.78 - 0.5377a_0 + 0.4545a_0^2 - 0.2206a_0^3$	$\bar{C}_{\zeta 1} = 6.5$	$0 \leq a_0 \leq 2.5$
$C_{\zeta 2} = 0$	$\bar{C}_{\zeta 2} = 0$	$0 \leq a_0 \leq 3.14$
Stratum $h/r_0 = 1.0^*$		
$C_{\zeta 1} = 5.75 - 0.4191a_0 + 1.381a_0^2 - 2.115a_0^3 + 0.5927a_0^4$	$\bar{C}_{\zeta 1} = 5.2$	$0 \leq a_0 \leq 2.00$
$C_{\zeta 2} = 0$	$\bar{C}_{\zeta 2} = 0$	$0 \leq a_0 \leq 1.57$
$C_{\zeta 2} = -6.28 + 4.0a_0$	$\bar{C}_{\zeta 2} = 0.6$	$1.57 \leq a_0 \leq 2.00$
Any stratum thickness†		
$C_{\zeta 1} = 5.333 - 1.0678a_0^2 + 0.5607a_0^3 - 0.2715a_0^4 + 0.0739a_0^5 - 0.0109a_0^6$	Depends on h/r_0	$\left\{ \begin{array}{l} a_0 > r_0/h \\ a_0 \leq 2.0 \end{array} \right.$
$C_{\zeta 2} = 0.755a_0^2 - 0.4228a_0^3 + 0.1631a_0^4 - 0.0302a_0^5 + 0.00204a_0^6$		

* Derived from Bycroft.⁴† Derived from Awojobi.¹

APPENDIX II

Notation

- A = constant
 A_n = function
 $A_x = u_0 m / (m_e e_m)$ = dimensionless amplitude of horizontal component of coupled vibration
 $A_y = \psi_0 I_\psi / (m_e e_m z_e)$ = dimensionless amplitude of rocking component of coupled motion
 $A_\zeta = \zeta_0 I_\zeta / K$ = dimensionless amplitude of torsional vibration with quadratic excitation
 $A_\zeta = \zeta_0 G r_0^3 / M_{\zeta 0}$ = dimensionless amplitude of torsional vibration with constant force amplitude
 $A_{\zeta m} = \zeta_m I_\zeta / K$ = dimensionless resonant (maximum) amplitude of torsional vibration
 $a_e = [a_0^2 - (r_0/h)^2]^{1/2}$ = equivalent dimensionless frequency for strata
 a_m = dimensionless resonant frequency (at maximum amplitude)
 $a_0 = \omega r_0 \sqrt{(\rho/G)}$ (or $= \omega r_0 \sqrt{(\rho_s/G_s)}$) = dimensionless frequency of excitation
 B_m = function
 $B_\zeta = I_\zeta / (\rho r_0^4)$ = inertia ratio for torsional vibration
 C = integration constant
 C_{x1}, C_{x2} = elastic half space stiffness and damping parameters for horizontal translation
 C_{y1}, C_{y2} = elastic half space stiffness and damping parameters for rocking
 $C_{\zeta 1}, C_{\zeta 2}$ = elastic half space (stratum) stiffness and damping parameters for torsional vibration
 $\bar{C}_{\zeta 1}, \bar{C}_{\zeta 2}$ = frequency independent elastic half space (stratum) stiffness and damping parameters for torsional vibration

bi's
lent

(44)

- c_{ij} = constant of damping force acting in direction i due to displacement (velocity) in direction j
 c_{ζ} = equivalent damping constant for torsional vibration
 D = integration constant
 D_{ζ} = damping ratio for torsional vibration
 e = eccentricity of centre of gravity
 e_m = eccentricity of rotating mass
 $f_{\zeta 1}, f_{\zeta 2}$ = components of Reissner's displacement function for torsional vibration
 G = shear modulus of elastic medium (soil beneath footing)
 G_s = shear modulus of side layer (backfill)
 H = height of footing
 $H_1^{(1)}, H_1^{(2)}$ = Hankel functions of the first order, first or second kind respectively
 h = thickness of elastic stratum
 I_{ψ} = mass moment of inertia of footing about horizontal axis
 I_{ζ} = mass moment of inertia of footing about vertical axis
 $i = \sqrt{-1}$
 J_0, J_1 = Bessel functions of first kind of order 0 and 1 respectively
 $K = m_e e_m r_c$ = excitation factor with quadratic excitation
 k = constant
 k_{ij} = constant of elastic restoring force acting in direction i due to displacement in direction j
 k_{ζ} = stiffness (spring) constant for torsional vibration
 l = depth of embedment of footing
 M_{ψ} = excitation moment about horizontal axis
 M_{ζ} = excitation moment about vertical axis
 $M_{\psi 0}$ = amplitude of moment M_{ψ}
 $M_{\zeta 0}$ = amplitude of moment M_{ζ}
 m = mass of footing
 m_e = unbalanced rotating mass
 N_{ζ} = torsional reaction of layer adjacent to footing
 Q = horizontal excitation force
 Q_0 = amplitude of horizontal excitation force
 r = cylindrical co-ordinate
 r_c = lever arm of horizontal excitation
 r_0 = radius of footing base; equivalent radius of footing base
 R = function of r
 R_{ζ} = torsional reaction of soil in footing base
 S_{u1}, S_{u2} = side layer stiffness and damping parameters for horizontal translation
 $S_{\psi 1}, S_{\psi 2}$ = side layer stiffness and damping parameters for rocking
 $S_{\zeta 1}, S_{\zeta 2}$ = side layer stiffness and damping parameters for torsion
 $S_{\zeta 1}, S_{\zeta 2}$ = frequency independent side layer stiffness and damping parameters for torsion
 t = time
 u = complex horizontal displacement of footing; radial displacement of medium
 u_c = complex amplitude of horizontal displacement
 u_0 = real amplitude of horizontal displacement
 $u_{1,2}$ = real and imaginary parts of u_c
 v = horizontal displacement of medium perpendicular to r
 X = horizontal axis
 $Y_{0,1}$ = Bessel functions of second kind of order 0 and 1 respectively
 z = vertical co-ordinate
 z_c = height of centre of gravity above footing base
 z_e = height of horizontal excitation force above centre of gravity
 w = vertical displacement of medium

for

- α = constant
 Δ = relative volume change
 $\delta = l/r_0$ = embedment ratio
 ζ = torsional vibration
 $\zeta_c = \zeta_1 + i\zeta_2$ = complex amplitude of torsional component
 ζ_0 = real amplitude of torsional vibration
 ζ_1, ζ_2 = real and imaginary parts of ζ_c
 $\eta = \rho_s/\rho$ = density ratio
 θ = cylindrical co-ordinate
 λ = Lamé's constant
 ρ = mass density of elastic medium; mass density of undisturbed soil
 ρ_s = mass density of side layer; mass density of backfill
 σ = normal stress
 τ = shear stress
 Φ = function of θ
 ϕ = phase shift
 ψ = rocking component of vibration
 $\psi_c = \psi_1 + i\psi_2$ = complex amplitude of rocking component of vibration
 ψ_0 = real amplitude of rocking component
 $\psi_{1,2}$ = real and imaginary parts of complex amplitude of rocking ψ_c
 ω = circular excitation frequency
 ω_m = circular frequency at maximum amplitude
 ω_0 = natural circular frequency
 $\omega_{r,\theta,z}$ = components of rotational vector

REFERENCES

1. A. O. Awojobi, 'Torsional vibration of a rigid circular body on an infinite elastic stratum', *Int. J. Solids Structures*, **5**, 369-378 (1969).
2. V. A. Baranov, 'On the calculation of excited vibrations of an embedded foundation', (in Russian), *Vop. Dynamiki i Prochnosti*, No. 14, Polytech Inst. Riga, 195-209 (1967).
3. Y. Beredugo, 'Vibration of embedded symmetric footings', Thesis submitted in partial fulfillment of the requirements for the degree of Doctor of Philosophy, Faculty of Engineering Science, The University of Western Ontario, London, Canada, August 1971.
4. Y. Beredugo and M. Novak, 'Coupled horizontal and rocking vibration of embedded footings', *Can. Geotech. J.* Nov. (1972), **9**, 477-497.
5. E. Butkov, *Mathematical Physics*, Addison-Wesley, 1968.
6. G. N. Bycroft, 'Forced vibrations of a rigid circular plate on a semi infinite elastic space and on an elastic stratum', *Phil. Trans. Roy. Soc. London, Series A*, **248**, Math. Phys. Sci. 327-368 (1965).
7. G. M. L. Gladwell, 'The forced torsional vibration of an elastic stratum', *Int. J. Engng Sci.* **7**, 1011-1024 (1969).
8. M. J. Kildjian, 'Torsional stiffness of embedded footings', *J. Soil Mech. Found. Div., Proc. ASCE*, **97**, No. SM7, 969-980 (1971).
9. T. Kobori, R. Minai, Suzuki and K. Kusakabe, 'Dynamical ground compliance of rectangular foundation on a semi-infinite elastic medium (Part 1)', *Disaster Prevent. Res. Inst., Kyoto Univ. Kyoto, Japan, Bulletin No. 10*, 283-314 (1967). (In Japanese with English captions.)
10. Y. E. Luco, and R. A. Westmann, 'Dynamic response of circular footings', *J. Engng Mech. Div., Proc. ASCE*, **97**, No. EM5, 1971, 1381-1395.
11. J. Lysmer and R. L. Kuhlemeyer, 'Finite dynamic model for infinite media', *J. Engng Mech. Div., Proc. ASCE*, **95**, No. EM4, 959-977 (1969); Closure to Discussions in February 1971, 129-131.
12. M. Novak, 'Prediction of footing vibrations', *J. Soil Mech. Found. Div., Proc. ASCE*, **96**, No. SM3, 837-861 (1970).
13. M. Novak and Y. Beredugo, 'The effect of embedment on footing vibrations', *Proc. 1st Can. Conf. Earthquake Engng Res.*, Univ. of British Columbia, Vancouver, B.C., Paper No. 7, 111-125 (1971).
14. M. Novak and Y. Beredugo, 'Vertical vibration of embedded footings', *J. Soil Mech. Found. Div., Proc. ASCE*, **98**, 1291-1310 (1972).
15. E. Reissner, 'Freie und erzwungene Torsionsschwingungen des elastischen Halbraumes', *Ingenieur-Archiv. Berlin, Germany*, **8**, No. 4, 229-245 (1937).
16. E. Reissner and H. F. Sagoci, 'Forced torsional oscillations of an elastic half-space', *J. Appl. Phys.* **15**, 652-662 (1944).
17. F. E. Richart, J. A. Hall and R. D. Woods, *Vibrations of Soils and Foundations*, Prentice-Hall, 1970.
18. F. E. Richart, Jr. and R. V. Whitman, 'Comparison of footing vibration tests with theory', *J. Soil Mech. Found. Div., Proc. ASCE*, **93**, No. SM6, Proc. Paper 5568, 143-168 (1967).

19. A. S. Veletsos and Y. T. Wei, 'Lateral and rocking vibrations of footings', *J. Soil Mech. Found. Div., Proc. ASCE*, 97, No. SM9, 1227-1248 (1971).
20. G. Waas and J. Lysmer, 'Vibrations of footings embedded in layered media', *Proc. WES Symp. Appl. Finite Element Meth. Geotech. Engng*, U.S. Army Engineer Waterways Experiment Station, Vicksburg, Miss., 1972.
21. G. F. Weissmann, 'Torsional vibrations of circular foundations', *J. Soil Mech. Found. Div., Proc. ASCE*, 97, No. SM9, Proc. Paper 8402, 1293-1316 (1971). (Also private communication.)
22. R. V. Whitman, 'Analysis of foundation vibrations', *Proc. Symp. Vibration in Civil Engng*, Imperial College, London, April 1965, Butterworths, London, 159-179, 1966.
23. M. Novak, 'Vibrations of embedded footings and structures', paper presented to the ASCE National Meeting, No. 10, Soil and Rock Dynamics, San Francisco, 1973.

es, 5,
niki i
ments
ndon,
ch. J.
tum",
-980
semi-
3-314
, No.
E, 95,
(1970).
Engng
E, 98,
berlin,
(1944).
Div.,

Coupled Horizontal and Rocking Vibration of Embedded Footings

Y. O. BEREDUGO

Shell-B.P. Nigeria Limited, Lagos, Nigeria

AND

M. NOVAK

Faculty of Engineering Science, The University of Western Ontario, London, Ontario

Received April 26, 1972

Accepted June 1, 1972

The prediction of the coupled response to horizontal forces is of major importance for the design of footings exposed to dynamic effects. The theory of surface footings greatly overestimates the real response and neglects the fact that the footings are founded beneath the surface of the ground, i.e. partly embedded. This latter factor considerably affects the footing vibrations in that it reduces the resonant amplitudes and increases the resonant frequencies.

An approximate analytical solution was developed in this paper and the theoretical response curves were compared with field experiments. Closed form formulas were obtained that are simple enough to be directly used in design. The approximate analytical solution is better able to predict the coupled response of embedded footings than that of surface footings. The response is usually dominated by the first resonant peak with the second resonant peak entirely suppressed. The derived formulas for equivalent stiffnesses and damping coefficients due to soil can be introduced into the solution of any structure.

La prédiction de la réponse combinée à des forces horizontales est d'importance majeure pour le calcul des emplacements soumis à des efforts dynamiques. La théorie des emplacements de surface surestime la réponse réelle et néglige le fait que les emplacements sont placés sous la surface du sol, i.e. ils sont partiellement enfouis. Ce dernier facteur affecte considérablement les vibrations de l'emplacement en réduisant les amplitudes de résonance et en augmentant leurs fréquences.

Une solution analytique approximative est développée dans cet article et les courbes théoriques de réponse sont comparées avec des mesures effectuées sur le terrain. On obtient des formules finies qui sont assez simples pour être utilisées directement dans le calcul des fondations. Cette solution analytique approximative est meilleure pour prédire la réponse combinée des emplacements enfouis que celle des emplacements de surface. Le comportement est habituellement gouverné par la première pointe de résonance alors que la seconde pointe disparaît complètement. Pour tenir compte du sol autour de la fondation, on propose des formules avec des coefficients de rigidité et d'amortissement équivalents, formules qui peuvent servir à la solution des calculs pour n'importe quelle structure.

Introduction

It has been recognized for many years that the vibrations of footings can be greatly affected by their partial embedment into the soil. Nevertheless, very little quantitative information is available because of the difficulties associated with a rigorous theoretical solution and with the generalization of experimental findings. *Uncoupled vibration* of embedded footings was solved by Lysmer and Kuhlemeyer (1969, 1971), who investigated vertical motion using the finite element method. Novak and Beredugo (1971) have presented approximate formulas for vertical, horizontal, and rocking vibrations. *Coupled horizontal and rocking vibration* of embedded footings, most important in design of machine foundations, nuclear power plants, etc., was

first investigated by Baranov (1967), who formulated an approximate analytical solution; however, he presented numerical results only for pure rocking. Tajimi (1969) analyzed the response of a structure partially embedded in an elastic stratum and attached at its base to a rigid half space underlying the elastic stratum.

In this paper, an approximate theory is used based on the assumption that the dynamic reactions in the footing base are equal to those of an elastic half space and that the reactions acting on the footing sides are equal to those of an overlying independent elastic layer. This approach, employed first by Baranov (1967), is extended here to yield closed form formulas and graphs that can be directly used for design purposes. Also, the

effect of backfill is incorporated. The major advantages of this approach are its relative simplicity and great versatility. The known solutions for coupled motion of surface footings (Richart *et al.* 1970; Ratay 1971) are a special case of the more general approach presented herein.

To provide more experimental data, field tests were conducted with concrete blocks subjected to horizontal excitation. The block bases were either square or rectangular in accordance with shapes most often used in practice. The reported test results are compared with the theoretical solution in order to assess the validity of the theory.

Equations of Motion

With the notation given in Fig. 1, the equations of vibration of a footing in coupled horizontal translation $u(t)$ and rotation $\psi(t)$ about a horizontal axis passing through the center of gravity are:

$$[1] \quad \begin{cases} m\ddot{u}(t) = Q(t) - R_x(t) - N_x(t) \\ I\ddot{\psi}(t) = M(t) - R_\psi(t) - N_\psi(t) \end{cases}$$

in which m = total mass of footing, I = mass moment of inertia about a horizontal axis passing through the center of gravity, $R_x(t)$ = horizontal reaction at the footing base, $N_x(t)$ = resultant horizontal reaction acting on embedded surfaces (sides) of footing, $R_\psi(t)$ = reactive moment of forces acting at footing base about center of gravity, $N_\psi(t)$ = reactive moment of forces acting on footing sides about center of gravity and t = time. The dots represent differentiation with respect to time. $Q(t)$ = horizontal exciting force acting at height z_c . If $M_c(t)$ = exciting moment, the total moment of excitation is:

$$[2] \quad M(t) = Q(t)z_c + M_c(t)$$

No rigorous expressions for reactions R and N are known; however, they can be ap-

proximately described if the following assumptions are adopted:

(i) the footing is of cylindrical shape,
(ii) the reactions in the base are the same as those of a surface footing and thus can be taken from the solutions of the elastic half-space or stratum, and

(iii) the side reactions are produced by an independent layer lying above the level of the footing base.

For this layer, various assumptions can be made. If it is assumed that the layer is composed of independent infinitesimally thin layers, then the side reactions derived by Baranov (1967) can be used. Baranov's original solution can be extended to yield formulas, directly applicable in foundation design and analysis, and to involve the effect of soil layering, backfill, and various stress distributions.

In accepting the assumptions (ii) and (iii), the compatibility condition is satisfied only at the footing and far from it. Despite this, the comparison with experiments and with finite element solutions for vertical motion (Novak and Beredugo 1972) and torsion indicates that the approximate theory yields quite reasonable results.

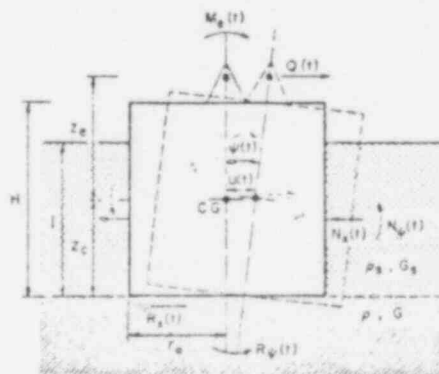


FIG. 1. Mathematical model of embedded footing in coupled motion.

With the above assumptions, the soil reactions can be formulated as follows. The horizontal and moment reactions in the footing base are:

$$[3] \quad \begin{cases} R_x(t) = Gr_o(C_{u1} + iC_{u2}) [u(t) - z_c \psi(t)] \\ R_\psi(t) = Gr_o^2 (C_{\psi 1} + iC_{\psi 2}) \psi(t) - Gr_o(C_{u1} + iC_{u2}) [u(t)z_c - z_c^2 \psi(t)] \end{cases}$$

in which

$$[4] \quad \begin{cases} C_{u1} = \frac{-f_{u1}}{f_{u1}^2 + f_{u2}^2} \\ C_{u2} = \frac{f_{u2}}{f_{u1}^2 + f_{u2}^2} \\ C_{\psi1} = \frac{-f_{\psi1}}{f_{\psi1}^2 + f_{\psi2}^2} \\ C_{\psi2} = \frac{f_{\psi2}}{f_{\psi1}^2 + f_{\psi2}^2} \end{cases}$$

Here, G = shear modulus, r_o = base radius, $i = \sqrt{-1}$, f_{ij} = displacement functions of dimensionless frequency $a_n = \omega r_o \sqrt{\rho/G}$ and Poisson's ratio ν , ω = frequency of excitation and ρ = mass density of the medium below the base. Functions f_{ij} can be found, e.g. in Bycroft (1956) or Luco and Westmann (1971) and are used here with the original signs.

The horizontal and moment side reactions can be written as

$$[5] \quad \begin{cases} N_x(t) = G_s r_o \delta (S_{u1} + i S_{u2}) \left[u(t) + \left(\frac{l}{2} - z_c \right) \psi(t) \right] \\ N_\psi(t) = G_s r_o^3 \delta \left\{ (S_{\psi1} + i S_{\psi2}) + \left(\frac{\delta^2}{3} - \delta \frac{z_c}{r_o} + \frac{z_c^2}{r_o^2} \right) (S_{u1} + i S_{u2}) \right\} \psi(t) \\ \quad + \frac{1}{r_o} \left(\frac{\delta}{2} - \frac{z_c}{r_o} \right) (S_{u1} + i S_{u2}) u(t) \end{cases}$$

in which G_s = shear modulus of the overlying layer, $\delta = l/r_o$ = relative embedment and l = embedment depth.

Functions S_{ij} are independent of ν and are

$$[6] \quad \begin{cases} S_{\psi1} = \pi \left[1 - a_o \frac{J_o(a_o) J_1(a_o) + Y_o(a_o) Y_1(a_o)}{J_1^2(a_o) + Y_1^2(a_o)} \right] \\ S_{\psi2} = \frac{2}{J_1^2(a_o) + Y_1^2(a_o)} \end{cases}$$

In Eq. [6] $J_n(a_o)$ and $Y_n(a_o)$ are Bessel functions of the first and second kinds, respectively, of order n .

Functions S_{u1} and S_{u2} depend on Poisson's ratio ν and are the real and imaginary parts of the complex function:

$$[7] \quad \begin{aligned} S_u(a_o, \nu) &= G_s [S_{u1}(a_o, \nu) + i S_{u2}(a_o, \nu)] \\ &= 2\pi G_s a_o \frac{\frac{1}{\sqrt{q}} H_2^{(2)}(a_o) H_1^{(2)}(x_o) + H_1^{(2)}(x_o) H_2^{(2)}(a_o)}{H_o^{(2)}(a_o) H_1^{(2)}(x_o) + H_o^{(2)}(x_o) H_2^{(2)}(a_o)} \end{aligned}$$

Here, $q = (1 - 2\nu)/2(1 - \nu)$, $x_o = a_o \sqrt{q}$ and $H_n^{(2)}$ = Hankel functions of the second kind of order n . Baranov evaluated functions S_{u1} and S_{u2} only for Poisson's ratio $\nu = 0.5$ with which Eq. [7] simplifies. For several other values of ν these parameters were computed from Eq. [7]

and approximated by polynomials. The results are given in Appendix I together with polynomial descriptions of other parameters C and S to facilitate the computation. The parameters are shown in Fig. 2.

Substitution of Eqs. [3] and [5] into Eq. [1] yields the differential equations of coupled vibration of embedded footings:

$$[8] \quad \begin{cases} m\ddot{u}(t) + r_o[G(C_{u1} + iC_{u2}) + G_s\delta(S_{u1} + iS_{u2})]u(t) \\ \quad + r_o\left[-Gz_c(C_{u1} + iC_{u2}) + G_s\delta\left(\frac{1}{2}l - z_c\right)(S_{u1} + iS_{u2})\right]\psi(t) = Q(t) \\ I\ddot{\psi}(t) + r_o^2\left[G_s\delta\left(\frac{1}{2}\delta - \frac{z_c}{r_o}\right)(S_{u1} + iS_{u2}) - G\frac{z_c}{r_o}(C_{u1} + iC_{u2})\right]u(t) \\ \quad + r_o^2\left\{G(C_{\psi 1} + iC_{\psi 2}) + G_s\delta\left[(S_{\psi 1} + iS_{\psi 2}) + \left(\frac{\delta^2}{3} - \delta\frac{z_c}{r_o} + \frac{z_c^2}{r_o^2}\right)\right.\right. \\ \quad \left.\left.(S_{u1} + iS_{u2})\right] + G\frac{z_c^2}{r_o^2}(C_{u1} + iC_{u2})\right\}\psi(t) = M(t) \end{cases}$$

With complex excitation

$$[9] \quad \begin{cases} Q(t) = Q_o \exp(i\omega t) = Q_o(\cos \omega t + i \sin \omega t) \\ M(t) = M_o \exp(i\omega t) = M_o(\cos \omega t + i \sin \omega t) \end{cases}$$

in which Q_o and M_o are real excitation amplitudes, the particular solutions describing the steady state motions are:

$$[10] \quad \begin{cases} u(t) = u_c \exp(i\omega t) \\ \psi(t) = \psi_c \exp(i\omega t) \end{cases}$$

where u_c and ψ_c are complex displacement amplitudes. Substitution of Eqs. [10] into Eqs. [8] provides the following equations for the complex amplitudes of coupled motion:

$$[11] \quad \begin{cases} [(k_{xx} - m\omega^2) + i\omega c_{xx}]u_c + (i\omega c_{x\psi} + k_{x\psi})\psi_c = Q_o \\ [(k_{\psi\psi} - I\omega^2) + i\omega c_{\psi\psi}]\psi_c + (i\omega c_{\psi x} + k_{\psi x})u_c = M_o \end{cases}$$

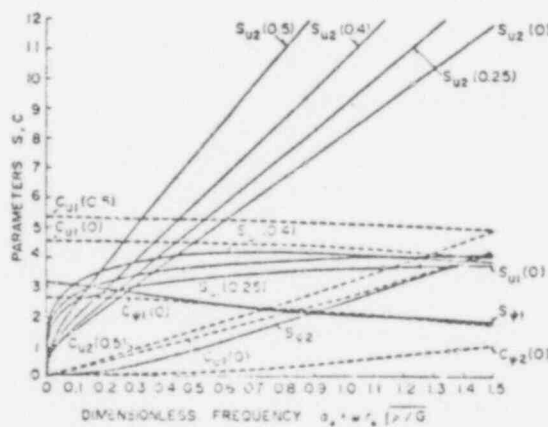


FIG. 2. Half-space stiffness and damping parameters $C_{1,2}$ (dashed lines) and Baranov's layer stiffness and damping parameters $S_{1,2}$ (full lines). (Poisson's ratio shown in parenthesis).

in which frequency dependent stiffness constants

$$[12] \begin{cases} k_{xx} = Gr_o \left(C_{u1} + \frac{G_s}{G} \delta S_{u1} \right) \\ k_{\psi\psi} = Gr_o^3 \left[C_{\psi1} + \left(\frac{z_c}{r_o} \right)^2 C_{u1} + \frac{G_s}{G} \delta S_{\psi1} + \frac{G_s}{G} \delta \left(\frac{\delta^2}{3} + \frac{z_c^2}{r_o^2} - \delta \frac{z_c}{r_o} \right) S_{u1} \right] \\ k_{x\psi} = -Gr_o \left[z_c C_{u1} + \frac{G_s}{G} \delta \left(z_c - \frac{1}{2} l \right) S_{u1} \right] \end{cases}$$

and frequency dependent damping constants

$$[13] \begin{cases} c_{xx} = \frac{Gr_o}{\omega} \left(C_{u2} + \frac{G_s}{G} \delta S_{u2} \right) \\ c_{\psi\psi} = \frac{Gr_o^3}{\omega} \left[C_{\psi2} + \left(\frac{z_c}{r_o} \right)^2 C_{u2} + \frac{G_s}{G} \delta S_{\psi2} + \frac{G_s}{G} \delta \left(\frac{\delta^2}{3} + \frac{z_c^2}{r_o^2} - \delta \frac{z_c}{r_o} \right) S_{u2} \right] \\ c_{x\psi} = -\frac{Gr_o^2}{\omega} \left[z_c C_{u2} + \frac{G_s}{G} \delta \left(z_c - \frac{1}{2} l \right) S_{u2} \right] \end{cases}$$

Eqs. [11] are formally equal to the equations of motion of a two-degrees-of-freedom system and therefore, k_{xx} , $k_{\psi\psi}$, and $k_{x\psi}$ are the frequency dependent spring constants, and c_{xx} , $c_{\psi\psi}$, and $c_{x\psi}$ are the frequency dependent damping coefficients. Thus, further solution does not represent any difficulties.

Calculation of Vibration Amplitudes

Forced Vibration

Constant force excitation is considered first. Note

$$[14] \begin{cases} \alpha_1 = k_{\psi\psi} - I\omega^2 - \frac{M_o}{Q_o} k_{x\psi} \\ \alpha_2 = (c_{\psi\psi} - \frac{M_o}{Q_o} c_{x\psi}) \omega \\ \beta_1 = k_{xx} - m\omega^2 - \frac{Q_o}{M_o} k_{x\psi} \\ \beta_2 = (c_{xx} - \frac{Q_o}{M_o} c_{x\psi}) \omega \\ \epsilon_1 = m\omega^4 - (v.k_{\psi\psi} + Ik_{xx} + c_{xx}c_{\psi\psi} - c_{\psi\psi}^2)\omega^2 + (k_{xx}k_{\psi\psi} - k_{x\psi}^2) \\ \epsilon_2 = -(mc_{\psi\psi} + Ic_{xx})\omega^3 + (c_{xx}k_{\psi\psi} + c_{\psi\psi}k_{xx} - 2c_{x\psi}k_{x\psi})\omega \end{cases}$$

Then, the complex vibration amplitudes are from Eqs. [11],

$$[15] \quad \begin{cases} u_c = Q_0 \frac{\alpha_1 + i\alpha_2}{\varepsilon_1 + i\varepsilon_2} \\ \psi_c = M_0 \frac{\beta_1 + i\beta_2}{\varepsilon_1 + i\varepsilon_2} \end{cases}$$

or

$$[16] \quad \begin{cases} u_c = u_1 + iu_2 = Q_0 \frac{\alpha_1\varepsilon_1 + \alpha_2\varepsilon_2}{\varepsilon_1^2 + \varepsilon_2^2} + iQ_0 \frac{\alpha_2\varepsilon_1 - \alpha_1\varepsilon_2}{\varepsilon_1^2 + \varepsilon_2^2} \\ \psi_c = \psi_1 + i\psi_2 = M_0 \frac{\beta_1\varepsilon_1 + \beta_2\varepsilon_2}{\varepsilon_1^2 + \varepsilon_2^2} + iM_0 \frac{\beta_2\varepsilon_1 - \beta_1\varepsilon_2}{\varepsilon_1^2 + \varepsilon_2^2} \end{cases}$$

The real vibration amplitudes u_o and ψ_o from Eqs. [16] are

$$[17] \quad \begin{cases} u_o = \sqrt{u_1^2 + u_2^2} = Q_0 \sqrt{\frac{\alpha_1^2 + \alpha_2^2}{\varepsilon_1^2 + \varepsilon_2^2}} \\ \psi_o = \sqrt{\psi_1^2 + \psi_2^2} = M_0 \sqrt{\frac{\beta_1^2 + \beta_2^2}{\varepsilon_1^2 + \varepsilon_2^2}} \end{cases}$$

When the motion is excited by a moment alone, $Q_0 = 0$ and Eqs. [17] simplify to:

$$[18] \quad \begin{cases} u_o = M_0 \sqrt{\frac{k_{xx}^2 + c_{xx}^2\omega^2}{\varepsilon_1^2 + \varepsilon_2^2}} \\ \psi_o = M_0 \sqrt{\frac{(k_{xx} - m\omega^2)^2 + c_{xx}^2\omega^2}{\varepsilon_1^2 + \varepsilon_2^2}} \end{cases}$$

The phase angles are:

$$[19] \quad \begin{cases} \phi_u = \text{Arc tan } \frac{u_2}{u_1} = -\text{Arc tan } \left(\frac{\alpha_2\varepsilon_1 - \alpha_1\varepsilon_2}{\alpha_1\varepsilon_1 + \alpha_2\varepsilon_2} \right) \\ \phi_\psi = \text{Arc tan } \frac{\psi_2}{\psi_1} = -\text{Arc tan } \left(\frac{\beta_2\varepsilon_1 - \beta_1\varepsilon_2}{\beta_1\varepsilon_1 + \beta_2\varepsilon_2} \right) \end{cases}$$

and the real motion of the center of gravity is:

$$[20] \quad \begin{cases} u(t) = u_o \cos(\omega t + \phi_u) \\ \psi(t) = \psi_o \cos(\omega t + \phi_\psi) \end{cases}$$

As in the case of uncoupled modes, dimensionless amplitudes $A_u = u_o Gr_o / Q_0$ and $A_\psi = \psi_o Gr_o^2 / M_0$ may be introduced to facilitate the presentation and analysis of the results.

Frequency variable excitation, often encountered in practical cases, can be easily introduced into the above formulae. Assume a frequency variable horizontal excitation, caused by an unbalanced rotating mass m_e , acting at a height z_e above the center of gravity. Then, in Eqs. [14]-[20]:

$$[21] \quad Q_0 = m_e e \omega^2, \quad M_0 = m_e e \omega^2 z_e, \quad \text{and} \quad \frac{M_0}{Q_0} = z_e$$

in which e = rotating mass eccentricity.

The dimensionless vibration amplitudes are, in the case of frequency variable excitation $u_0/m_e e$ and $A_\psi = \psi_0 I/m_e e z_e$.

From Eqs. [17] and [18], the complete response of embedded footings in coupled motion can be computed directly and relatively easily. With the use of approximate expressions for the side reactions S given in Appendix 1, the computation becomes even simpler.

The uncoupled modes of vibration (Novak and Beredugo 1971) and the known solutions of surface footings (Richart *et al.* 1970; Ratay 1971) are special cases of the solution described.

It may be noted that an alternative direct calculation may be used in which the complex amplitudes u_e and ψ_e are separated into their real and imaginary parts beforehand. This approach leads to four simultaneous equations with real coefficients; however, the computing requires more time.

From the motion of the center of gravity, the horizontal and vertical components of the motion experienced by the surface (edges) of the footing can be computed. The upper edge of the footing experiences vertical amplitude w_e and horizontal amplitude u_e that are:

$$[22] \quad \begin{cases} w_e = r_0 \psi_0 \\ u_e = u_0 + (H - z_e) \psi_0 \end{cases}$$

(In the last formula, the phase difference is neglected between u and ψ .)

Natural Frequencies and Modes

In addition to the computation of the complete response, the natural undamped frequencies and modes of free vibrations can be of interest and are useful in the direct resonant amplitude calculation described later herein.

The equations for the natural frequencies and modes follow from Eqs. [11] by putting the damping coefficients c_{xx} , $c_{\psi\psi}$, and $c_{x\psi}$ as well as Q_0 and M_0 equal to zero, which yields, in terms of real amplitudes,

$$[23] \quad \begin{bmatrix} k_{xx} - m\omega^2 & k_{x\psi} \\ k_{x\psi} & k_{\psi\psi} - I\omega^2 \end{bmatrix} \begin{Bmatrix} u_0 \\ \psi_0 \end{Bmatrix} = 0$$

The two natural undamped frequencies ω_1 and ω_2 are found from the condition that the determinant of the coefficients must be equal to zero, which yields:

$$[24] \quad \omega_{1,2}^2 = \frac{1}{2} \left(\frac{k_{xx}}{m} + \frac{k_{\psi\psi}}{I} \right) \mp \sqrt{\frac{1}{4} \left(\frac{k_{xx}}{m} - \frac{k_{\psi\psi}}{I} \right)^2 + \frac{k_{x\psi}^2}{mI}}$$

From this equation, two natural undamped frequencies can be found by a trial and error procedure because coefficients k are frequency dependent according to Eqs. [12]. With these two natural frequencies ω_j ($j = 1, 2$) the two vibration modes (eigenvectors) are, from Eqs. [23]:

$$[25] \quad \left(\frac{u_0}{\psi_0} \right)_j = \frac{-k_{x\psi}(\omega_j)}{k_{xx}(\omega_j) - m\omega_j^2} = \frac{k_{\psi\psi}(\omega_j) - I\omega_j^2}{-k_{x\psi}(\omega_j)}$$

with $j = 1$ or 2 . (These equations provide a quick check of ω_j . With correct values of $\omega_{1,2}$ both equations give the same results).

The first mode represents rotation about a center lying under the footing base. In the second mode the rotation takes place about a point lying above the center of gravity (Fig. 3). The modes actually have a meaning of radii of rotation.

Examples of Theoretical Response Curves

Several examples of theoretical response curves computed from Eqs. [17] with quadratic excitation according to Eqs. [21] are plotted in Figs. 4-6.

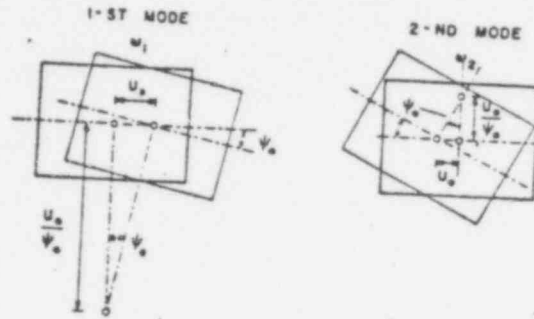


FIG. 3. Modes of free vibrations.

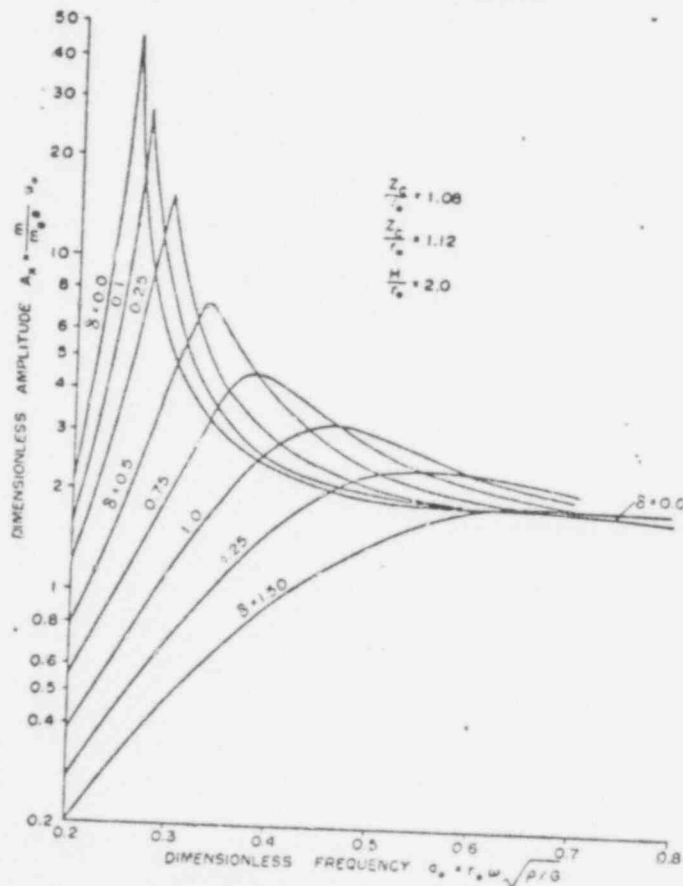


FIG. 4. Theoretical response curves for horizontal translation of footing in coupled motion ($\eta = 1.0$, $\nu = 0$, $B_x = 4.0$, $D_y = 4.35$, various embedments).

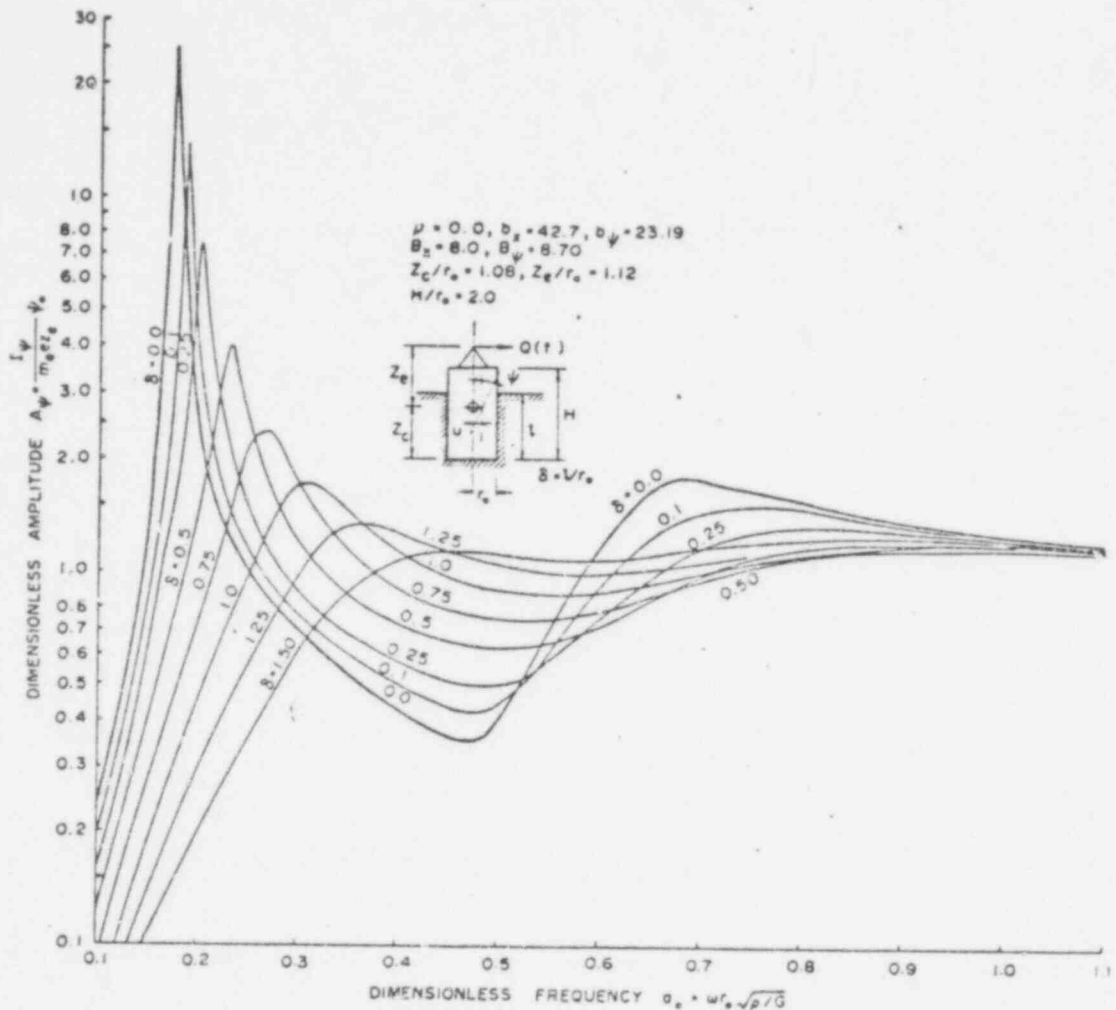


FIG. 5. Theoretical response curves for rocking component of coupled motion ($\eta = 1.0$, $B_{\psi} = 8.0$, $b_{\psi} = 8.70$, various embedments):

In these figures the horizontal translation and rocking components are plotted for various relative embedments $\delta = l/r_e$. The mass parameters used are shown in both the standard b_{ψ} and modified B_{ψ} shapes (Richart *et al.* 1970). The modified mass parameters are shown here to reduce the dependence of the results on Poisson's ratio. Two sets of mass parameters were used to indicate their effects on the character of the response. Figures 4 and 5 illustrate the steady response of footings embedded in undisturbed soil. Figure 6 illustrates the effects of backfill. The properties of backfill G_b , ρ_b were introduced using an approximate expression (Beredugo 1971) $G_b/G \approx (\rho_b/\rho)^4$. Thus, ratio $\eta = \rho_b/\rho = 1$ denotes embedment in undisturbed soil.

Several conclusions can be drawn from Figs. 4-6¹. The response of embedded footings is dominated by the first resonance peak, which is thus of major importance. (For surface footings this was also observed by Ratay (1971). The response in the region of the second resonance is, in general, much less pronounced and does not vary too much with embedment.

¹See also Fig. 9.

In most practical cases, the second resonant peak is entirely suppressed: it can only be recognized in the rocking components with very high mass ratios (Fig. 5).

The increase in the first resonant frequency and the decrease in the corresponding resonant amplitude due to embedment are quite drastic. Both of these effects are smaller in the case of backfill.

The variations of the resonant amplitudes and resonant frequencies with relative embedment and mass ratios are further illustrated in Figs. 7 and 8. Resonant amplitude ratio R_1 and resonant frequency ratio R_f represent the relative variations of resonant amplitudes and frequencies due to embedment related to amplitudes and frequencies of a surface footing. These figures apply exactly just for the parameters used in the computing; however, they indicate the trends to be expected in any particular case. Further parameter studies revealed that the resonant amplitude ratio is practically independent of the relative height of horizontal excitation z/H and only weakly dependent on the modified mass ratio with any particular embedment. Comparison with pure rocking and horizontal translation (uncoupled motions) indicates that coupling increases the resonant horizontal amplitudes and decreases the rocking amplitudes and resonant frequencies. (Similar observations were made with surface footings by Ratay 1971).

Simplified Design Analysis

The calculation of natural frequencies, vibration modes and amplitudes of forced oscillations from the above formulas can be considerably simplified if the stiffness parameters C_1 and S_1 are assumed to be constant and if the damping parameters C_2 , S_2 are assumed to be proportional

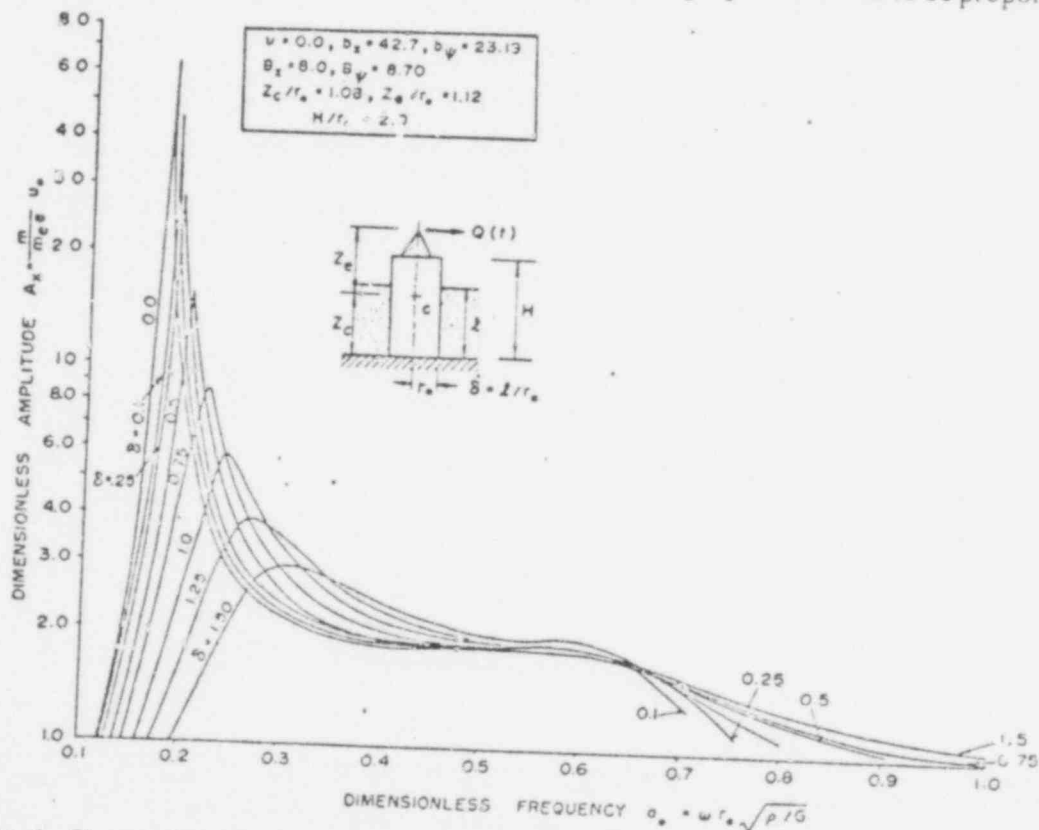


FIG. 6. Theoretical response curves for horizontal translation in coupled motion of footing (backfill with $\eta = 0.75$, $B_x = 8.0$, $B_p = 8.70$).

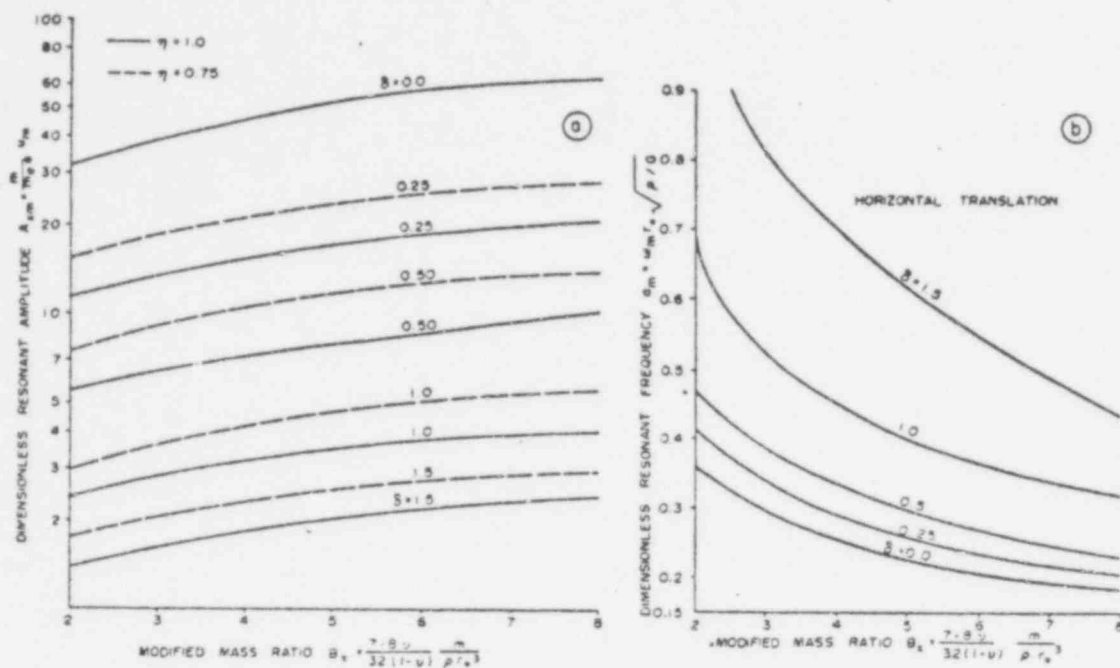


FIG. 7a. Effect of mass ratio on theoretical resonant amplitude for horizontal translation in coupled motion.
 FIG. 7b. Effect of mass ratio on theoretical resonant frequency of footing in coupled motion ($\eta = 1.0$).

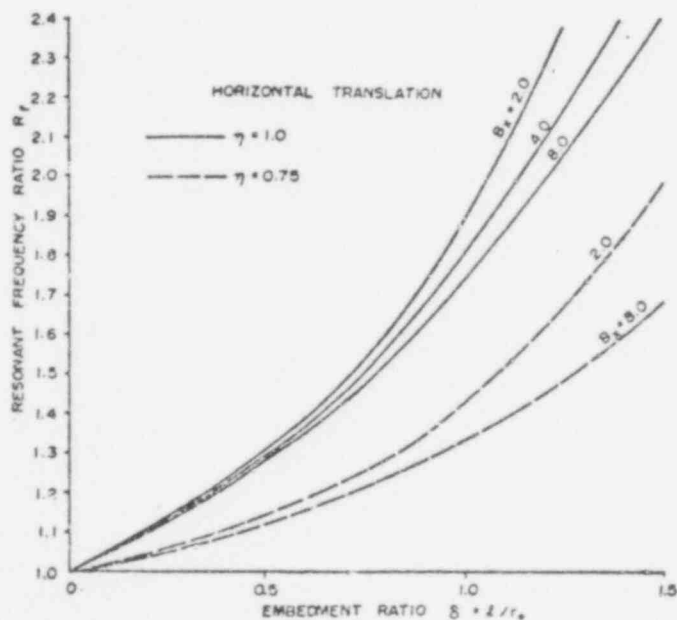


FIG. 8. Theoretical resonant frequency ratio vs. embedment for footing in coupled motion.

to dimensionless frequency a_m . It can be seen from Fig. 2 that these assumptions are quite acceptable for practical applications except for some side reactions at very low frequencies. Thus, stiffness parameters can be considered approximately constant:

$$[26] \quad C_{u1} = \bar{C}_{u1}, \quad C_{\psi1} = \bar{C}_{\psi1}, \quad S_{u1} = \bar{S}_{u1}, \quad S_{\psi1} = \bar{S}_{\psi1}$$

and with these values the stiffness constants, given by Eqs. [12], become frequency independent. The damping parameters in Eqs. [13] can be approximately taken as:

$$[27] \quad C_{u2} = \bar{C}_{u2} a_0, \quad C_{\psi2} = \bar{C}_{\psi2} a_0, \quad S_{u2} = \bar{S}_{u2} a_0, \quad S_{\psi2} = \bar{S}_{\psi2} a_0$$

The parameters denoted by bars are constants. Their suitable values are given in Tables 1 and 2 in Appendix I.

Substitution of Eqs. [27] into Eqs. [13] yields the frequency independent damping constants for embedded footings:

$$[28] \quad \begin{cases} c_{xx} = \sqrt{\rho G} r_0^2 \left(\bar{C}_{u2} + \delta \sqrt{\frac{\rho_s}{\rho} \frac{G_s}{G}} \bar{S}_{u2} \right) \\ c_{\psi\psi} = \sqrt{\rho G} r_0^2 \left\{ \bar{C}_{\psi2} + \left(\frac{z_c}{r_0} \right)^2 \bar{C}_{u2} + \delta \sqrt{\frac{\rho_s}{\rho} \frac{G_s}{G}} \left[\bar{S}_{\psi2} + \left(\frac{\delta^2}{3} + \frac{z_c^2}{r_0^2} - \delta \frac{z_c}{r_0} \right) \bar{S}_{u2} \right] \right\} \\ c_{x\psi} = -\sqrt{\rho G} r_0^2 \left[z_c \bar{C}_{u2} + \delta \sqrt{\frac{\rho_s}{\rho} \frac{G_s}{G}} \left(z_c - \frac{1}{2} l \right) \bar{S}_{u2} \right] \end{cases}$$

With frequency independent stiffness and damping parameters, the calculation of vibration amplitudes is as follows: (i) with values of \bar{C}_1 and \bar{S}_1 taken from Tables 1 and 2 (or read from Fig. 2) stiffness constants are obtained from Eqs. [12] and the two natural frequencies from Eq. [24]; (ii) damping coefficients are computed from Eqs. [28] with \bar{C}_2 and \bar{S}_2 taken from Tables 1 and 2, and α, β , and c obtained from Eqs. [14] for any excitation frequency of interest. Substitution of these values into Eqs. [17] yields the amplitudes of horizontal translation and rotation at the center of gravity. Eqs. [22] give the motions of footing edges.

Very often only the amplitudes at the first resonance with ω_1 need to be found because these resonant vibrations cause frequent difficulties. (The amplitudes at ω_1 are slightly smaller than the maximum).

Examples of response curves computed with constant parameters are shown in Fig. 9. The agreement with the results obtained with variable parameters is satisfactory for em-

bedded footings. For surface footings, the constant parameters given in Tables 1 and 2 yield smaller resonant amplitudes. This is desirable for reasons discussed in the next section. (If desired, a perfect fit can also be obtained for surface footings by the proper choice of constant parameters).

The effect of embedment may be reduced by an imperfect bond between the footing and the soil and by backfill. These effects can be accounted for by considering $G_s < G$ and $\rho_s < \rho$ in Eqs. [12] and [28].

The choice of equivalent radius r_0 for rectangular footings is rather uncertain. Some indications of the possible differences are mentioned in the next paragraph.

Comparison with Experiments

Relatively few experiments have been conducted with embedded footings subjected to horizontal excitation despite the fact that this is the case of major practical importance. To provide more data, a series of field tests has been carried out at The University of

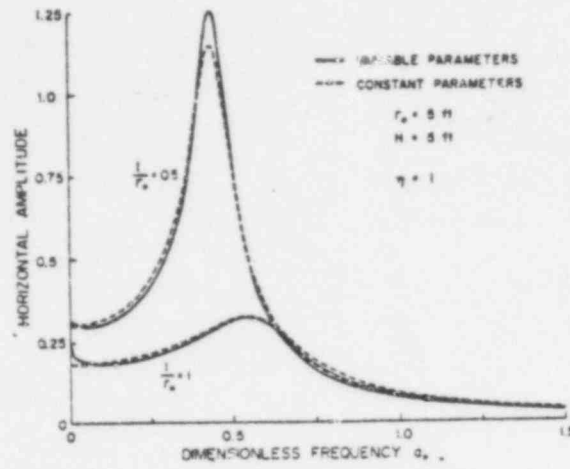


FIG. 9. Comparison of response curves computed with variable and constant parameters ($\nu = 0, \eta = 1$).

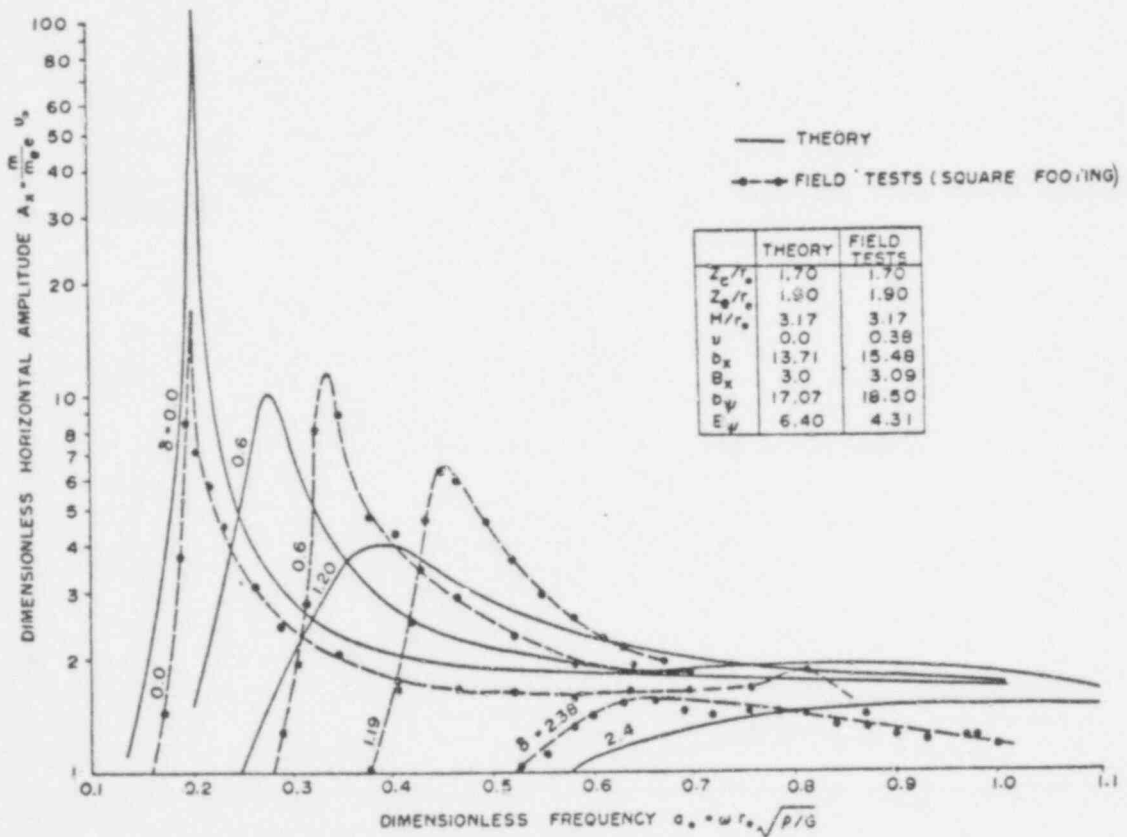


FIG. 10. Comparison of theoretical and measured response curves for horizontal translation in coupled motion of square footing (undisturbed soil, $eg_0 = 1.71$ lb-in.).

Western Ontario with two concrete blocks, one having a square base, the other featuring a rectangular base with a side ratio of 2/1. The base area was $5 \text{ ft}^2 (0.465 \text{ m}^2)$ in both cases. The blocks were cast directly into neatly cut excavations. The embedment depth was changed by removing the soil in several steps. The effect of embedment into backfill was investigated by stepwise backfilling of the soil and by tamping to two different densities. The subsoil was composed of about 5 ft (1.5 m) of brown, silty clay underlain by a glacial till of considerable thickness. Shear modulus of undisturbed soil was found to be $6.6 \times 10^5 \text{ lb/ft}^2 (320 \text{ kg/cm}^2)$ and Poisson's ratio was 0.38. Further details can be found in Beredugo (1971) and Novak and Beredugo (1971).

The comparison of the theory with the experiments is complicated by distinct non-

linearities. This effect is accepted as a scatter in resonant frequencies and amplitudes in this paper. (Some other ways of dealing with nonlinearities observed in experiments are described in Novak (1971). Another difficulty is to choose an equivalent radius r_e for rectangular embedded footings vibrating in a coupled mode.

Figures 10-15 indicate the suitability of the theory and the differences in response of the rectangular footings in the two major directions.

Figure 10 shows the comparison of theoretical and measured response curves of a square footing. The equivalent radius $r_e = 1.26 \text{ ft} (0.38 \text{ m})$ was derived from the equality of footing bases. In Figs. 11 and 12 the first resonant amplitudes and frequencies are compared. It can be seen that the resonant amplitudes are predicted much better for

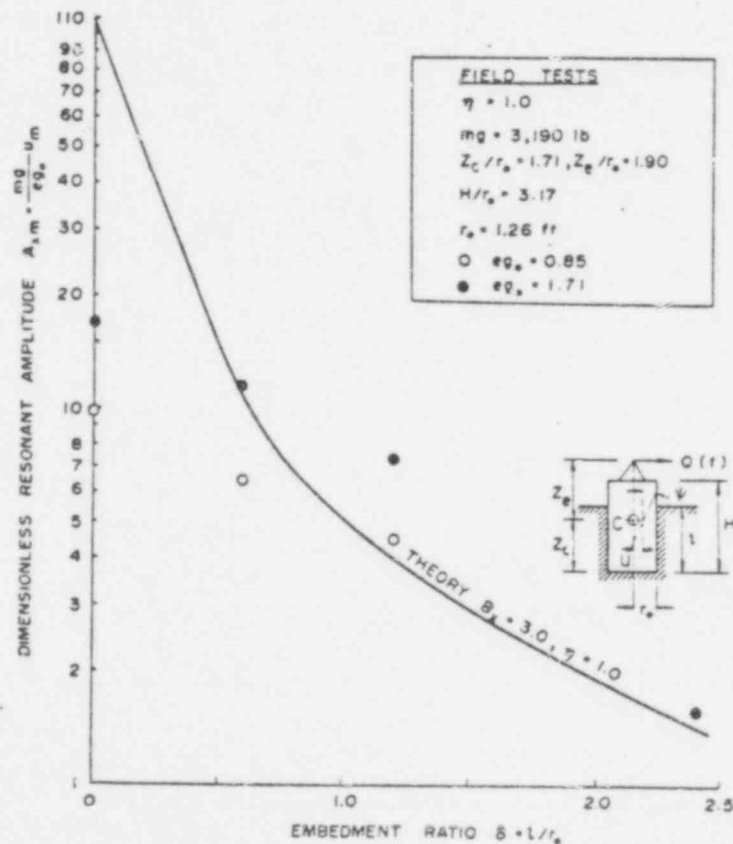


FIG. 11. Comparison of theoretical and measured resonant amplitudes for horizontal translation in coupled motion (undisturbed soil, square footing, $\nu = 0.38$, $b_v = 15.48$, $b_\psi = 18.50$).

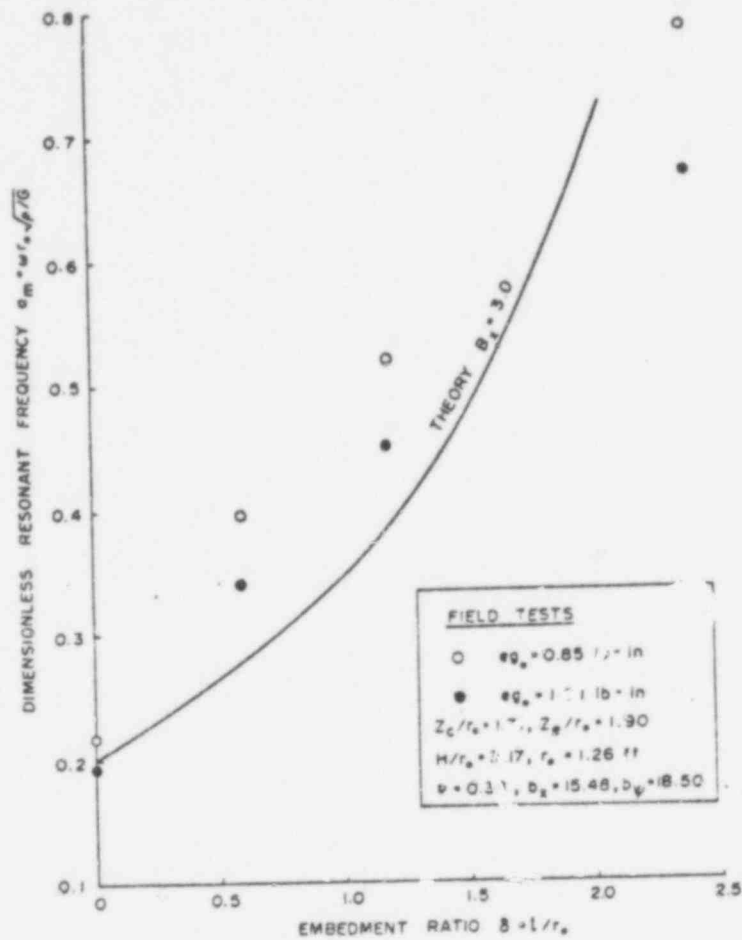


FIG. 12. Comparison of theoretical and measured resonant frequencies in coupled motion ($\eta = 1.0$, square footing, $\nu = 0.38$, $b_x = 15.48$, $b_y = 18.50$).

the embedded footings than for the surface ones. This important observation probably can be attributed to the overwhelming effect of geometric damping with embedded footings. The first resonant amplitudes of surface footings seem considerably overestimated because the geometric damping is very small and the hysteretic damping is omitted in the theory. The prediction of resonant frequencies appears quite reasonable too. *Rectangular footings* also show a better agreement in resonant amplitudes in the case of embedment (Fig. 13). The choice of equivalent radii for embedded rectangular footings is, of course, questionable. Figures 14 and 15

give some idea about the differences in response in both major directions. Smaller amplitudes in the direction of the longer axis can be recognized despite the scatter due to nonlinearity (Fig. 14), while a somewhat smaller relative increase in stiffness due to embedment can be seen in the same direction (Fig. 15).

Until better guidelines are found it seems that the equivalent ratios for rectangular footings can be derived from equality of base areas for translation constants k_{xz} and c_{xz} in Eqs. [12] and [13], and from equality of base moments of inertia for the other constants. Useful data on rectangular surface

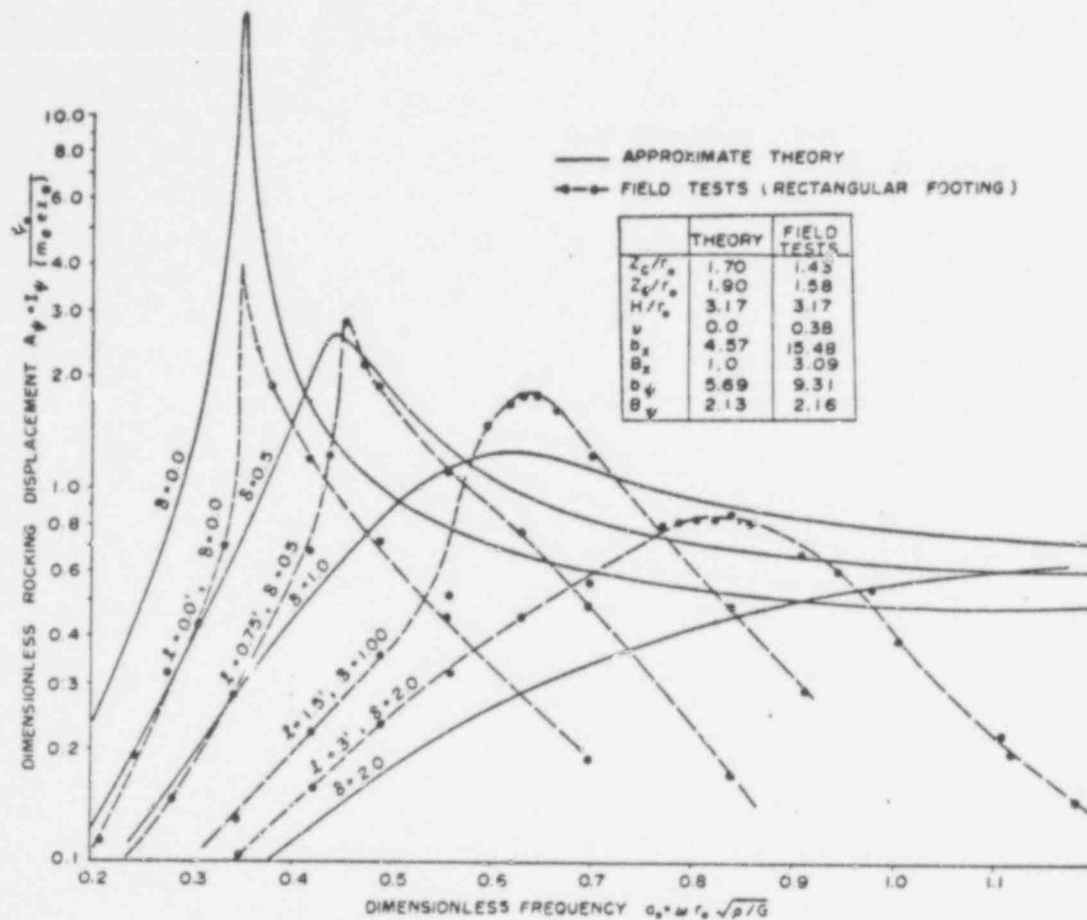


FIG. 13. Comparison of theoretical and measured response curves for rocking in coupled motion of rectangular footing (in disturbed soil, $c_g = 1.71$ lb-in.).

footings were derived by Kobori *et al.* (1971) and may be helpful together with the intuition of the designer. Equivalent base radii for surface footings can be found in Richart *et al.* (1970).

Summary and Conclusions

Coupled forced vibration in horizontal translation and rocking of partially embedded rigid footings was investigated both theoretically and experimentally.

An approximate analytical solution was used to derive directly usable formulas and graphs, information about embedment into backfill and relations between uncoupled and coupled motions. The major advantages of

this approach are its simplicity, the ease with which parameters can be changed and the ability to consider layering and to introduce the soil reactions into the solution of any structure.

Field experiments were carried out with concrete embedded footings subjected to horizontal excitation. The theoretical and experimental results were compared.

The major findings can be summarized as follows:

(1) The response is usually dominated by the first resonant peak and the second resonant peak is entirely suppressed. Despite this, the omission of coupling leads to considerable errors in both resonant frequencies and amplitudes.

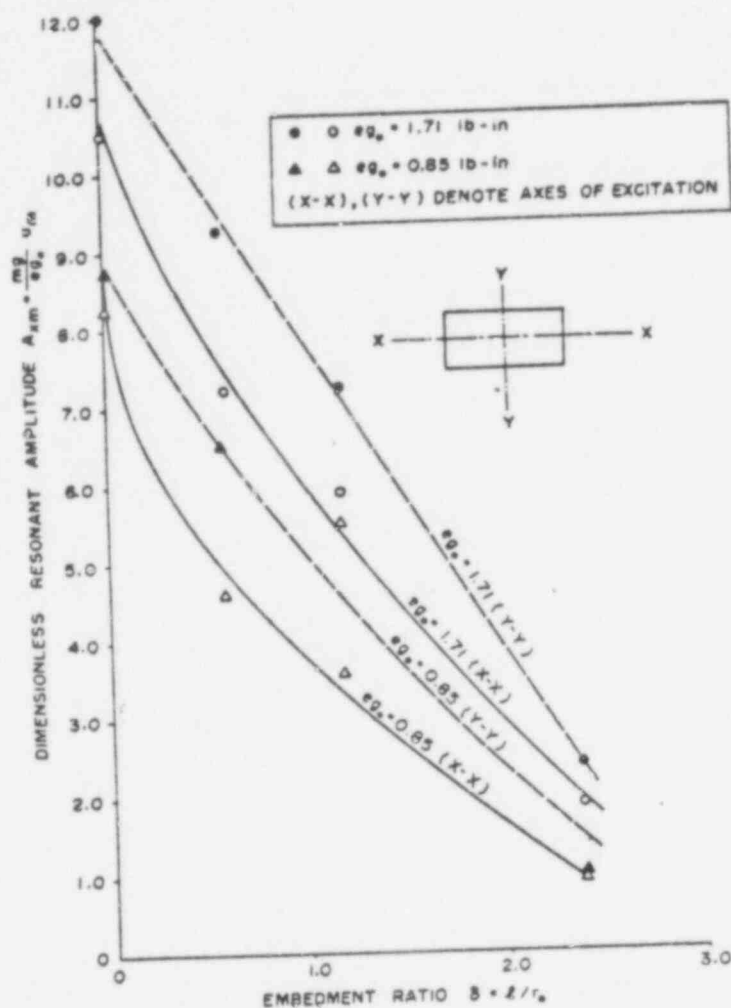


FIG. 14. Variation of measured horizontal resonant amplitude with embedment for rectangular footing in coupled motion (undisturbed soil, $e g_0 = 0.85$ and 1.71 lb-in.)

(2) Embedment substantially affects the response in that it increases the resonant frequencies and reduces the resonant amplitudes. This effect is much more pronounced in coupled motion than in vertical translation.

(3) Backfill reduces the effect of embedment. This can be accounted for in the theory.

(4) The approximate theory is better able to predict the coupled response of embedded footings than of surface footings. The theory of surface footings considerably overestimates the resonant amplitudes.

(5) Equivalent frequency independent damping and stiffnesses were derived for design purposes. They facilitate the prediction of resonant frequencies and amplitudes from closed form formulas.

Acknowledgments

The study was carried out as a part of a broader research program at The University of Western Ontario and supported by a grant-in-aid of research from the National Research Council of Canada to the senior author and by the award of a Commonwealth Scholarship from the Canadian Federal Go-

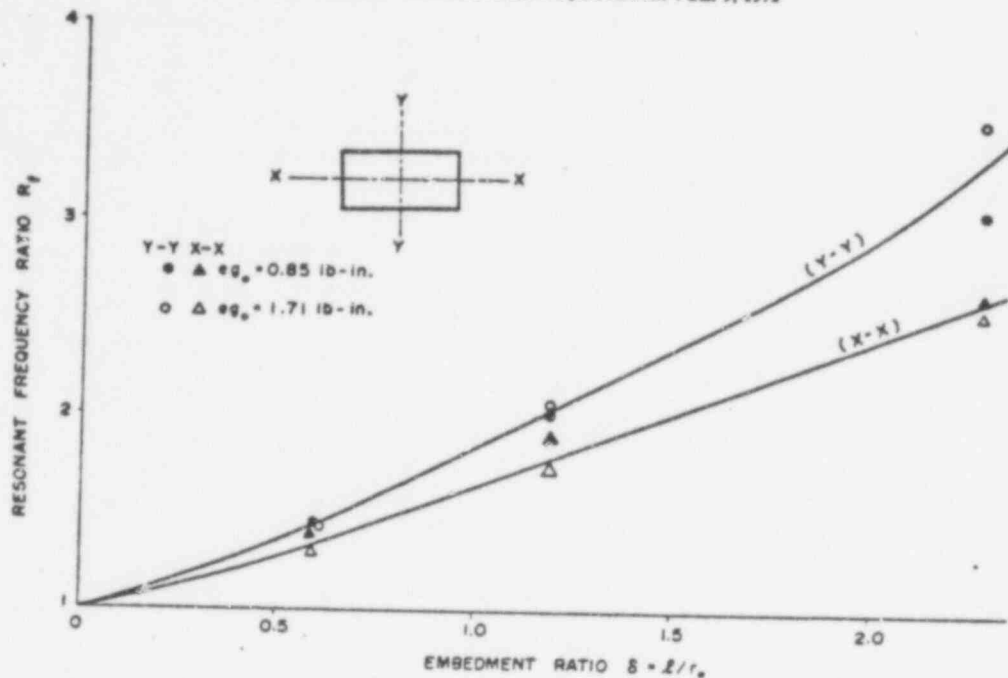


FIG. 15. Variation of measured resonant frequency ratio with embedment for rectangular footing in coupled motion ($\eta = 1.0$).

vernment to the junior author. The assistance of K. Sachs is gratefully acknowledged.

- BARANOV, V. A. 1967. On the calculation of excited vibrations of an embedded foundation. *in Russian*, *Voprosy Dynamiki i Prochnosti*, Polytechnical Institute of Riga. No. 14, pp. 195-209.
- BREDUGO, Y. 1971. Vibration of embedded symmetric footings. Ph.D. thesis, Faculty of Engineering Science, The University of Western Ontario, London, Canada.
- BYCROFT, G. N. 1956. Forced vibrations of a rigid circular plate on a semi-infinite elastic half space and on an elastic stratum. *Philos. Trans. Royal Soc., Lond., Ser. A*, 248, No. 948, pp. 327-368.
- KOBORI, T., MINAI, R., and SUZUKI, T. 1971. The dynamical ground compliance of a rectangular foundation on a viscoelastic stratum. *Bull. Disaster Prev. Res. Inst., Kyoto Univ.* 20, Part 4, No. 183, pp. 289-329.
- LUCO, Y. E., and WESTMANN, R. A. 1971. Dynamic response of circular footings. *J. Eng. Mech. Div., Proc. A.S.C.E.* 97, No. EM5, pp. 1381-1395.
- LYSMER, J., and KUHLEMEYER, R. L. 1969. Finite dynamic model for infinite media. *J. Eng. Mech. Div., Proc. A.S.C.E.* 95, No. EM4, pp. 859-877.
- 1971. Finite dynamic model for infinite media: Closure to discussions. *J. Eng. Mech. Div., Proc. A.S.C.E.* 97, No. EM1, pp. 129-131.
- NOVAK, M. 1971. Data reduction from nonlinear response curves. *J. Eng. Mech. Div., Proc. A.S.C.E.* 97, No. EM4, pp. 1187-1204.
- NOVAK, M., and BEREDUGO, Y. 1971. The effect of embedment on footing vibrations. *Proc. First Can. Conf. Earthquake Eng. Res.*, May, University of British Columbia, Vancouver, B.C., pp. 111-125.
- 1972. Vertical vibration of embedded footings. *J. Soil Mech. Found. Div., Proc. A.S.C.E.* Dec. 1972.
- RATAY, R. T. 1971. Sliding-rocking vibration of body on elastic medium. *J. Soil Mech. Found. Div., Proc. A.S.C.E.* 97, No. SMI, pp. 177-192.
- RICHART, F. E., HALL, J. R., and WOODS, R. D. 1970. *Vibrations of soils and foundations*. Prentice-Hall Inc., Englewood Cliffs, U.S.A.
- TAJIMI, H. 1969. Dynamic analysis of a structure embedded in an elastic stratum. *Proc. 4th World Conf. Earthquake Eng.* Santiago, Chile, Session A-6, pp. 53-69.

Appendix I. - Stiffness and Damping Parameters C and S

To facilitate the computation, the stiffness and damping functions C and S were approximated by the expressions given below. Their accuracy is sufficient for practical applications. The elastic half space formulas for C were computed with Bycroft's (1956) functions $f_{1,2}$. Functions S for the layer were calculated from general equations derived by Baranov (1967).

In all formulas dimensionless frequency $a_0 = \omega r_0 \sqrt{\rho/G}$. Constant parameters \bar{C} and \bar{S} can be used in frequency range $0 < a_0 < 2$. The parameter S_{n1} exhibits pronounced variations with a_0 for Poisson's ratio $\nu \approx 0.43$.

TABLE 1

ν	Half space functions	Validity range	Constant parameters
<i>Horizontal translation</i>			
0.0	$C_{n1} = 4.571 - 4.653a_0 + \frac{89.09a_0}{a_0 + 19.14}$	$0 \leq a_0 \leq 2.0$	$\bar{C}_{n1} = 4.30$
	$C_{n2} = 2.536a_0 - \frac{0.1345a_0}{a_0 + 1.923}$		$\bar{C}_{n2} = 2.70$
0.5	$C_{n1} = 5.333 - 1.584a_0 + \frac{10.39a_0}{a_0 + 6.552}$	$0 \leq a_0 \leq 2.0$	$\bar{C}_{n1} = 5.10$
	$C_{n2} = 2.923a_0 - \frac{0.1745a_0}{a_0 + 1.927}$		$\bar{C}_{n2} = 3.15$
<i>Rotation about horizontal axis (rocking)</i>			
0.0	$C_{\psi_1} = 2.654 + 0.1962a_0 - 1.729a_0^2 - 1.485a_0^3 - 0.4881a_0^4 - 0.03498a_0^5$	$0 \leq a_0 \leq 1.5$	$\bar{C}_{\psi_1} = 2.50$
	$C_{\psi_2} = 0.008025a_0 + 0.01583a_0^2 - 0.2035a_0^3 - 1.202a_0^4 - 1.448a_0^5 + 0.4491a_0^6$		$\bar{C}_{\psi_2} = 0.43$

TABLE 2

ν	Side layer functions	Validity range	Constant parameters
<i>Horizontal translation</i>			
0.0	$S_{n1} = 0.2328a_0 - \frac{3.609a_0}{a_0 + 0.06159}$	$0.2 \leq a_0 \leq 1.5$	$\bar{S}_{n1} = 3.60$
	$S_{n1} = 150.7a_0 - 3630a_0^2 - 3948a_0^3 - 1934a_0^4 + 3488a_0^5$	$0 \leq a_0 \leq 0.2$	
0.25	$S_{p2} = 7.334a_0 - \frac{0.8652a_0}{a_0 + 0.00874}$	$0 \leq a_0 \leq 1.5$	$\bar{S}_{n2} = 8.20$
	$S_{n1} = 2.474 - 4.119a_0 - 4.320a_0^2 - 2.057a_0^3 - 0.362a_0^4$	$0.2 \leq a_0 \leq 2.0$	$\bar{S}_{n1} = 4.00$
0.4	$S_{n1} = -1.468\sqrt{a_0} + 5.662\sqrt[4]{a_0}$	$0 \leq a_0 \leq 0.2$	$\bar{S}_{n2} = 9.10$
	$S_{n2} = 0.83a_0 + \frac{41.59a_0}{3.90 + a_0}$	$0 \leq a_0 \leq 1.5$	
0.4	$S_{n1} = 2.824 + 4.776a_0 - 5.539a_0^2 - 2.445a_0^3 - 0.394a_0^4$	$0.2 \leq a_0 \leq 2.0$	$\bar{S}_{n1} = 4.10$
	$S_{n1} = -1.796\sqrt{a_0} - 6.539\sqrt[4]{a_0}$	$0 \leq a_0 \leq 0.2$	$\bar{S}_{n2} = 10.60$
$S_{n2} = 0.96a_0 - \frac{56.55a_0}{4.68 + a_0}$	$0 \leq a_0 \leq 1.5$		
<i>Rotation about a horizontal axis (rocking)</i>			
any value	$S_{\psi_1} = 3.142 - 0.4215a_0 - 4.209a_0^2 - 7.165a_0^3 - 4.667a_0^4 - 1.093a_0^5$	$0 \leq a_0 \leq 1.5$	$\bar{S}_{\psi_1} = 2.50$
	$S_{\psi_2} = 0.0144a_0 - 5.263a_0^2 - 4.177a_0^3 - 1.643a_0^4 - 0.2542a_0^5$		$\bar{S}_{\psi_2} = 1.80$

Appendix II. - Notation

- $A_x = \frac{m}{m_c e} u_o =$ dimensionless amplitude of horizontal vibration
 $A_{xm} = \frac{m}{m_c e} u_m =$ dimensionless resonant (maximum) amplitude of horizontal vibration
 $A_\psi = \frac{I}{m_c e z_c} \psi_o =$ dimensionless angular amplitude of rocking
 $A_{\psi m} = \frac{I}{m_c e z_c} \psi_m =$ dimensionless resonant (maximum) amplitude of rocking
 $a_o = \omega r_o \sqrt{\rho/G} =$ dimensionless excitation frequency
 $a_m =$ dimensionless resonant frequency (at maximum amplitude)
 $B_x = b_x(7-8\nu)/32(1-\nu) =$ modified mass ratio for horizontal vibration
 $B_\psi = 3b_\psi(1-\nu)/8 =$ modified mass ratio for rocking motion
 $b_x = m/\rho r_o^3 =$ mass ratio for horizontal vibration
 $b_\psi = I/\rho r_o^5 =$ mass ratio for rocking motion
 $C_{u1}, C_{u2} =$ elastic half space stiffness and damping parameters for horizontal translation
 $\bar{C}_{u1}, \bar{C}_{u2} =$ frequency independent half space stiffness and damping parameters for horizontal translation
 $C_{\psi1}, C_{\psi2} =$ elastic half space stiffness and damping parameters for rocking
 $\bar{C}_{\psi1}, \bar{C}_{\psi2} =$ frequency independent half space stiffness and damping parameters for rocking
 $c_{xx} =$ equivalent damping constant for horizontal component of coupled motion
 $c_{x\psi} =$ equivalent "cross" damping constant for coupled motion
 $c_{\psi\psi} =$ equivalent damping constant for rocking in coupled motion
 $e =$ eccentricity of rotating mass
 $f_{u1}, f_{u2} =$ components of Reissner's displacement function for horizontal vibration
 $f_{\psi1}, f_{\psi2} =$ components of Reissner's displacement function for rocking
 $G =$ shear modulus of elastic half space; shear modulus of undisturbed soil beneath footing
 $G_s =$ shear modulus of side layers; shear modulus of backfill
 $g =$ acceleration of gravity
 $g_o = m_c g =$ weight of rotating mass
 $H =$ height of footing
 $H_n^{(2)} =$ Hankel function of the second kind of order $n = J_n - iY_n$
 $h =$ thickness of elastic stratum
 $I =$ mass moment of inertia about horizontal axis passing through center of gravity
 $i = \sqrt{-1}$
 $J_0, J_1, J_2 =$ Bessel functions of first kind of orders 0, 1, and 2 respectively
 $k_{xx} =$ equivalent spring constant for horizontal component of coupled motion
 $k_{x\psi} =$ equivalent "cross" spring constants for coupled motion
 $k_{\psi\psi} =$ equivalent spring constant for rocking component of coupled motion
 $L =$ length of footing
 $l =$ depth of embedment of footing
 $M_o =$ amplitude of excitation moment
 $M(t) =$ excitation moment about horizontal axis
 $m =$ mass of footing; mass of footing and oscillator
 $m_c =$ unbalanced rotating mass
 $N_x(t) =$ horizontal side reaction due to embedment in coupled motion

- $N_{\psi}(t)$ = reactive torque due to embedment in coupled motion
 Q_0 = amplitude of horizontal excitation force
 $Q(t)$ = horizontal excitation force
 q = $(1 - 2\nu)/2(1 - \nu)$ = function of Poisson's ratio
 R_a = resonant amplitude ratio (relative decrease in resonant amplitude)
 R_f = resonant frequency ratio (relative increase in resonant frequency)
 $R_x(t)$ = horizontal reaction in the footing base
 $R_{\psi}(t)$ = half space reactive torque in coupled motion
 r_0 = radius of cylindrical footing; equivalent radius of rectangular footing
 S_u, S_{ψ} = Baranov's rigidity parameters
 S_{n1}, S_{n2} = side layer stiffness and damping parameters for horizontal translation
 $S_{\psi 1}, S_{\psi 2}$ = side layer stiffness and damping parameters for rocking
 $\bar{S}_{n1}, \bar{S}_{n2}$ = frequency independent side layer stiffness and damping parameters for translation
 $\bar{S}_{\psi 1}, \bar{S}_{\psi 2}$ = frequency independent side layer stiffness and damping parameters for rocking
 t = time
 u_r = $u_1 + iu_2$ = complex amplitude of horizontal displacement
 u_m = resonant (maximum) amplitude of horizontal displacement
 u_0 = real amplitude of horizontal displacement
 u_1, u_2 = real and imaginary parts of complex amplitude u_r
 $u(t)$ = horizontal displacement
 x_0 = $a_0 \sqrt{q}$ parameter depending on ω and ν
 z_b = height of horizontal excitation force above base of footing
 z_c = height of center of gravity above footing base
 Y_n = Bessel functions of the second kind of order n
 z_e = height of horizontal exciting force above center of gravity
 δ = l/r_0 = embedment ratio
 η = ρ_1/ρ = density ratio
 ν = Poisson's ratio
 ω = circular excitation frequency
 ω_m = frequency at maximum amplitude
 ω_j = j^{th} undamped natural frequency
 $\omega_{1,2}$ = first and second undamped natural frequency
 ϕ_u, ϕ_{ψ} = phase angles
 ψ_r = $\psi_1 + i\psi_2$ = complex amplitude of angular (rocking) displacement
 ψ_m = resonant amplitude of angular displacement
 ψ_0 = real amplitude of angular displacement
 ψ_1, ψ_2 = real and imaginary parts of ψ_r
 $\psi(t)$ = angular displacement
 ρ = mass density of elastic half space; mass density of undisturbed soil
 ρ_1 = mass density of side layer; mass density of backfill